CIVIL ENGINEERING STUDIES
Illinois Center for Transportation Series No. 10-074
UILU-ENG-2010-2015
ISSN: 0197-9191

PIER AND CONTRACTION SCOUR PREDICTION IN COHESIVE SOILS AT SELECTED BRIDGES IN ILLINOIS

Prepared By
T. D. Straub
T. M. Over
U.S. Geological Survey

Research Report ICT-10-074

A report of the findings of
ICT-R27-19
Pier and Contraction Scour Prediction in Cohesive Soils

Illinois Center for Transportation

August 2010

Technical Report Documentation Page

1. Report No.	2. Government Accession No.	3. Recipient's Catalog No.
FHWA-ICT-10-074		

4. Title and Subtitle	5. Report Date
Pier and Contraction Scour Prediction in Cohesive Soils at Selected Bridges in Illinois	August 2010
	6. Performing Organization Code
7. Author(s)	8. Performing Organization Report N o.
Straub, T.D., Over, T.M.	ICT-10-074 UILU-ENG-2010-2015
9. Performing Organization Name and Address	10. Work Unit (TRAIS)
U.S. Geological Survey 1201 West University Avenue Urbana, IL 61801	11. Contract or Grant No. ICT-R27-19
	13. Type of Report and Period Covered
12. Sponsoring Agency Name and Address	
Illinois Department of Transportation Bureau of Materials and Physical Research 126 E. Ash Street Springfield, IL 62704	14. Sponsoring Agency Code

15. Supplementary Notes

16. Abstract

This report presents the results of testing the Scour Rate In Cohesive Soils-Erosion Function Apparatus (SRICOS-EFA) method for estimating scour depth of cohesive soils at 15 bridges in Illinois. The SRICOS-EFA method for complex pier and contraction scour in cohesive soils has two primary components. The first component includes the calculation of the maximum contraction and pier scour (Z_{max}). The second component is an integrated approach that considers a time factor, soil properties, and continued interaction between the contraction and pier scour (SRICOS runs).

The SRICOS-EFA results were compared to scour prediction results for non-cohesive soils based on Hydraulic Engineering Circular No. 18 (HEC-18). On average, the HEC-18 method predicted higher scour depths than the SRICOS-EFA method. A reduction factor was determined for each HEC-18 result to make it match the maximum of three types of SRICOS run results. The unconfined compressive strength (Q_u) for the soil was then matched with the reduction factor and the results were ranked in order of increasing Q_u. Reduction factors were then grouped by Q_u and applied to each bridge site and soil. These results, and comparison with the SRICOS Z_{max} calculation, show that less than half of the reduction-factor method values were the lowest estimate of scour; whereas, the Z_{max} method values were the lowest estimate for over half.

A tiered approach to predicting pier and contraction scour was developed. There are four levels to this approach numbered in order of complexity, with the fourth level being a full SRICOS-EFA analysis. Levels 1 and 2 involve the reduction factors and Z_{max} calculation, and can be completed without EFA data. Level 3 requires some surrogate EFA data. Levels 3 and 4 require streamflow for input into SRICOS. Estimation techniques for both EFA surrogate data and streamflow data were developed.

17. Key Words	18. Distribution Statement
Bridge, Pier, Contraction, Scour, Cohesive, Soil, Illinois, SRICOS, HEC-18	No restrictions. This document is available to the public through the National Technical Information Service, Springfield, Virginia 22161.

19. Security Classif. (of this report)	20. Security Classif. (of this page)	21. No. of Pages	22. Price
Unclassified	Unclassified		

EXECUTIVE SUMMARY

This report presents the results of testing the Scour Rate In Cohesive Soils-Erosion Function Apparatus (SRICOS-EFA) method for estimating scour depth of cohesive soils at selected bridges in Illinois. EFA tests were run on soil samples from 15 bridge sites so that SRICOS-scour predictions could be completed. Additionally, soil properties were determined for each soil so that the development of relations between soil properties and erosion potential, as determined by the EFA, could be studied.

Streamflow data needed in the SRICOS modeling were retrieved either from historic data records or they were estimated. Historic daily data were disaggregated from daily to hourly using methods outlined in this report. Hourly streamflow data were needed at most sites to provide an accurate description of flood events for the purpose of scour estimation. Bridge and channel geometry were retrieved either from historic data files or collected in this study. A streamflow, velocity, and depth rating (needed for SRICOS modeling) was computed for each site by use of the Hydrologic Engineering Center River Analysis System (HEC-RAS) models. Various flow values and recurrence-interval floods were used, including the 100- and 500-year flood values.

The SRICOS-EFA method for complex pier scour and contraction scour in cohesive soils has two primary components. The first component includes the calculation of the maximum contraction and pier scour (Z_{max}). The second component is an integrated approach that considers a time factor, soil properties, and continued interaction between the contraction and pier scour (SRICOS runs). Hydraulic Engineering Circular No. 18 (HEC-18) scour-prediction methods for non-cohesive soils also were used to predict scour at each site.

To compare with the HEC-18 100-year storm-analysis method, both Z_{max} calculations and three types of SRICOS runs were completed. The three types of SRICOS runs were (1) the risk-based analysis where the 100-year and 500-year flood values are input, (2) the 500-year flood for 5 days, and (3) a 40-50-year hydrograph.

On average, the HEC-18 method predicted the highest amount of scour, followed by the SRICOS Z_{max} method, and the average of three types of SRICOS runs (with a safety factor) predicted the lowest scour. When compared to observed data, the SRICOS runs (with a safety factor) give a reasonable best-fit approach, while the SRICOS Z_{max} and HEC-18 estimates are always higher than observed.

A reduction factor was determined for each HEC-18 result to make it match the maximum of the three types of SRICOS run results (with a safety factor) for each bridge site and soil. The unconfined compressive strength (Q_u) expressed in tons per square foot (TSF) for the soil was then matched with the reduction factor and the results were ranked in order of increasing Q_u. The results were grouped by Q_u and a potential percent reduction was assigned to each group using an envelope approach based primarily on the minimum reduction factor in each group. The reduction factors were applied to each bridge site and soil. These results, and comparison with the SRICOS Z_{max} calculation, show that less than half of the reduction-factor method values were the lowest estimate of scour; whereas, the Z_{max} method values were the lowest estimate for over half. These results show that the reduction-factor method (using a single soil property) may not always give the lowest estimate and that computing Z_{max} (using a single soil property and hydraulic properties) may give an even lower estimate of scour. Eighty-three percent of the Z_{max} predictions show a 45- to 77-percent reduction in the HEC-18 predictions that are over 10 feet. The Z_{max} is the equilibrium maximum contraction and pier scour of cohesive soils for a bridge site over time as determined by the SRICOS method. This “upper limit” of scour prediction can then be used for sites where the reduction-factor method result is higher than Z_{max}.

Development of a tiered approach to predicting pier and contraction scour was completed using the results from this study. The approach includes four levels that are numbered in order of complexity, with the fourth level consisting of a full SRICOS-EFA analysis. Levels 1 and 2 can be completed without EFA data, but level 3 requires some surrogate EFA data. Levels 3 and 4 require streamflow data for input into SRICOS. Level 4 also includes analysis of Shelby tube samples taken at the site and run in the EFA.

In this study, equations based on soil properties were developed to obtain critical-shear values and erosion rates. These equations can be used where EFA soil-test results are not available. A best-fit and upper-limit approach to estimating critical shear and erosion rates were developed based on Q_u of the soil only. Lastly, streamflow-estimation techniques developed in this study are useful for ungaged sites and sites where historic hourly data are needed, but not available.

ACKNOWLEDGMENT

This publication is based on the results of ICT-R27-19, Pier and Contraction Scour Prediction in Cohesive Soils. ICT-R27-19 was conducted in cooperation with the Illinois Center for Transportation; the Illinois Department of Transportation, Division of Highways; and the U.S. Department of Transportation, Federal Highway Administration.

Matthew O'Connor served as the technical review panel chairperson for the current study. William Kramer, Riyad Wahab, Neil Vanbebber, Mark Gawedzinski, Marshall Metcalf, Francis Opfer, and Ronald Wagoner were the members of the technical review panel. They supported the use of advanced methodologies, facilitated correspondence with IDOT districts, and provided technical suggestions throughout the study.

Technical assistance also was provided by the following U.S. Geological Survey Illinois Water Science Center employees: Robert Holmes, Audrey Ishii, and Douglas Yeskis for overall project oversight; P. Ryan Jackson for hydraulic modeling development; Kevin Johnson, Patrick Mills, Charles Bohall, and Eric White for field use of advanced technologies; and Jennifer Sharpe for illustrations development.

DISCLAIMER

The contents of this report reflect the view of the authors, who are responsible for the facts and the accuracy of the data presented herein. The contents do not necessarily reflect the official views or policies of the Illinois Center for Transportation, the Illinois Department of Transportation, or the Federal Highway Administration. This report does not constitute a standard, specification, or regulation.

Trademark, product, firm names, or manufacturers' names appear in this report only because they are considered essential to the object of this document and do not constitute an endorsement by the Federal Highway Administration, Illinois Department of Transportation, Illinois Center for Transportation, U.S. Geological Survey, or other agencies of the U.S. Government.

TABLE OF CONTENTS

TABLES

FIGURES

CONVERSION FACTORS

U.S. Customary to International System (SI)

Multiply	By	To obtain
	Length	
inch (in.)	25.4	millimeter (mm)
foot (ft)	0.3048	meter (m)
	Area	
square mile (mi^2)	2.590	square kilometer (km^2)
	Flow rate	
foot per second (ft/s)	0.3048	meter per second (m/s)
cubic foot per second (ft^3/s)	0.02832	cubic meter per second (m^3/s)
inch per hour (in/h)	25.4	millimeter per hour (mm/h)
	Pressure	
pound per square foot (lb/ft^2)	47.88	pascal (Pa)
tons(short) per square foot ($tons/ft^2$)	95.76	kilopascal (kPa)
	Density	
pound per cubic foot (lb/ft^3)	16.02	kilogram per cubic meter (kg/m^3)

Vertical coordinate information is referenced to the North American Vertical Datum of 1988 (NAVD 88) or the National Geodetic Vertical Datum of 1929 (NGVD 29). Vertical datum is specified in the text. Horizontal coordinate information is referenced to the World Geodetic System of 1984 (WGS 84).

ABBREVIATIONS, ACRONYMS, AND SYMBOLS

a	coefficient
α	attack angle of the flow on the pier
AASHTO	American Association of State Highway and Transportation Officials
ADAPS	Automated Data Processing System
b	exponent
B_1	approach channel width
B_2	contracted channel width minus the total width of the piers
B	individual pier width
B'	pier projected width
c	coefficient
CSU	Colorado State University
Cl	percent clay
d	exponent
D	pipe diameter
D_{50}	median grain size for the soil
e	coefficient
EFA	Erosion Function Apparatus
ε	average height of the surface roughness
ε / D	pipe relative roughness
f	friction factor
FEQ	Full Equations model for one-dimensional unsteady flow in open channels
g	acceleration due to gravity
GPR	ground penetrating radar
GPS	global positioning system
h	exponent
H	water depth which includes the contraction scour depth
HEC-1	Hydrologic Engineering Center watershed hydrology model
HEC-2	Hydrologic Engineering Center river hydraulics model
HEC-18	Hydraulic Engineering Circular No. 18
HEC-RAS	Hydrologic Engineering Center River Analysis System
h_{rf}	height of the rectangular flume
IDA	instantaneous data archive
IDOT	Illinois Department of Transportation
j	coefficient
k	exponent
K	constant
K_θ	factor for influence of the transition angle
K_L	factor for the influence of the length of the contracted channel
K_{sh}	correction factor for pier shape effect on pier scour

K_{sp}	correction factor for pier spacing effect on the pier scour depth
K_w	correction factor for pier scour water depth
l	length of soil sample
L	pier length
LL	liquid limit
MC	Moisture Content
n	Manning's coefficient
NWIS	National Water Information System
Q_u	unconfined compressive strength
PI	plasticity index
PL	plastic limit
R^2	coefficient of determination
Re	Reynold's number
ρ	mass density of water
Sa	percent sand
Si	percent silt
S_i	soil property i
SRICOS	Scour Rate In Cohesive Soils
SRICOS-EFA	Scour Rate In Cohesive Soils-Erosion Function Apparatus
τ	shear stress
τ_c	critical shear stress
t	time elapsed
USGS	U.S. Geological Survey
V_1	mean velocity in the approach section
V_2	mean velocity in the contraction section (sometimes referred to as V_{hec} in Briaud et al. (2003))
V_c	critical velocity
v	mean flow velocity
ν	kinematic viscosity of water (approximately 1.0×10^{-6} m^2/s at 20^oC)
WD	wet density
WSPRO	a computer model for Water-Surface Profile computations
w_{rf}	width of the rectangular flume
$\dot{Z}_i$	erosion rate
$Z(t)$	scour depth for a given streamflow and duration
$Z_{max}(Cont)$	maximum contraction scour
$Z_{max}(Pier)$	maximum pier scour depth
Z_{max}	maximum contraction and pier scour

CHAPTER 1 INTRODUCTION

Most methods for predicting pier and contraction scour use erodability estimates from non-cohesive soils data. These erodability estimates generally overestimate the scour of cohesive soils, which can result in increased pier depth and cost to design and build bridges. These estimates also do not include a time-dependent estimate of scour, which is important for assessing scour in cohesive soils. The Scour Rate In Cohesive Soils-Erosion Function Apparatus (SRICOS-EFA) methodology outlined in the National Cooperative Highway Research Program Report 24-15 (Briaud et al. 2003) provides a potentially useful methodology for assessing scour in cohesive soils. Field-validation data are limited in testing the SRICOS-EFA method in addressing the issue of scour in cohesive soils. To further test the SRICOS-EFA method in Illinois, the U.S. Geological Survey (USGS), in cooperation with the Illinois Center for Transportation and the Illinois Department of Transportation (IDOT), began a study in 2006 at 15 selected bridge sites throughout the State.

1.1 PURPOSE AND SCOPE

The purpose of this report is to present the results of testing the SRICOS-EFA method for estimating scour depth of cohesive soils in Illinois streams. Fifteen sites were chosen for testing. Streamflow data were retrieved from historic data records or estimated, then disaggregated to hourly time step, if needed, using methods outlined in this report. Channel geometry (including measurement of historic scour) and bridge information were retrieved from historic data files or collected in this study. EFA tests were run on soil samples from each site so that SRICOS scour prediction could be completed. Also, at each site, scour prediction methods for non-cohesive soils outlined in Hydraulic Engineering Circular No. 18 (HEC-18) (Richardson and Davis, 2001) were used to predict scour. A reduction factor approach is presented in this report to adjust the scour estimates from HEC-18 based on SRICOS and observed scour. Also, soil properties were determined for each sample, so the development of relations between soil properties and the erosion potential as determined by the EFA could be completed.

1.2 PREVIOUS STUDIES

The National Cooperative Highway Research Program Report 24-15 (Briaud et al. 2003) documents the development and validation of the SRICOS-EFA methodology with laboratory testing, numerical modeling, and field data from eight bridges (with cohesive soils) in Texas (Briaud et al. 2003). The method is evaluated by comparing predicted scour depths and measured scour depths for 10 piers at 8 bridges. Briaud has collaborated on a number of additional papers involving the SRICOS-EFA methodology including Briaud et al. 2004; Briaud and Chen, 2005; and Brandimarte et al. 2006. Long-term bridge scour in cohesive soils in Maryland was estimated using the SRICOS-EFA methodology (Ghelardi, 2004). The SRICOS-EFA method is currently (2010) being evaluated in cohesive soils in South Dakota (http://rip.trb.org/browse/dproject.asp?n=15126).

1.3 SITE SELECTION

This study required 15 sites, with a variety of soils, throughout Illinois. Over 200 sites with a nearby streamgage were submitted from the nine IDOT Districts for consideration in the study. The sites were identified by a two-number system (e.g. 1-1). The first number represents the IDOT district and the second number is the order in which they were submitted

for selection. The final criteria for the selection of 15 bridge sites (Figure 1.1 and Table 1.1) for testing were based on the proximity to a USGS streamflow-gaging station and availability of design plans and historic soil-boring data. Also, access to the floodplain was critical because Shelby-tube sampling was completed in the dry floodplain as close to the channel and pier as possible to collect soil as similar as possible to soil that was eroded (method similar to Briaud et al. 2003).

The IDOT technical review panel reviewed the soil-boring data. They decided whether or not to accept or reject a site based on a Q_u (unconfined compressive strength, expressed in tons per square foot of a given soil) equal to or greater than 1 ton/ft^2 and by reviewing the visual description of the historic boring log for cohesive soil characteristics. It was important for site selection that the soil at and below the interface of the streambed and pier be considered cohesive. Most sites had fine-grained materials in both transport and on the banks, although Illinois streams (including ones in this study) can have sand and gravel in transport with the underlying local streambed being cohesive. The unconsolidated surficial sediments throughout most of Illinois can include fine-grained material, but even at a local scale soils can vary, so a detailed look at historic soil borings would need to be completed before applying the SRICOS-EFA method or results from this study.

1.4 APPROACH

Shelby tubes containing representative soils from a given site at an elevation near the scour zone were used for EFA testing conducted by IDOT personnel to determine erosion rates for input into SRICOS. Also, the following soil properties were determined from material in the Shelby tube: liquid limit, plastic limit, plasticity index, water content, unconfined compressive strength, wet density, and particle-size distribution. The results of the laboratory testing also were used to determine relations between soil properties and erosion potential as determined by the EFA method.

Shelby-tube sampling was completed in the dry floodplain as close to the channel and pier as possible to collect soil as similar as possible to soil that was eroded. This method was similar to the original SRICOS-EFA study by Briaud et al. (2003) and was considered acceptable in the current study given that the material near the pier and in the contraction cross section may have been scoured. Careful attention was paid to historic soil-boring data to ensure that the sampling location contained representative soils at an elevation near the scour zone. Samples were visually examined in the field to verify that the material collected matched the description in the historic borings.

Data collected at each of the 15 sites included the following: channel bathymetry and scour using echo sounder, ground penetrating radar (GPR), digital level, manual probing, and (or) a survey-grade global positioning system (GPS). Advanced technologies were used because scour holes may be filled on the recession limb of hydrographs or during low-flow conditions causing the elevation of the streambed not to reflect the actual historic scour elevation. Additional data about the bridge structure (e.g. pier skew angle, widths, lengths, and shapes) and channel characteristics (Manning's coefficient and channel slope) also were collected if not available from historic data reviewed during the site-selection process.

Data from the USGS streamflow-gaging station closest to each bridge was obtained for the period of record. If the closest gage was not at the bridge or the length of the record did not extend back at least 40 years, the streamflow was estimated using methods outlined in Chapter 2. Also, disaggregation of historic streamflow data from daily to hourly time steps was completed at all sites.

Pre-existing models obtained from the IDOT districts were converted to Hydrologic Engineering Center River Analysis System (HEC-RAS) models (U.S. Army Corps of Engineers 2008). Using the HEC-RAS models, a streamflow to velocity rating was computed for each site.

With this rating, the hydrograph could be transformed into a velocity hydrograph in the SRICOS-EFA model. HEC-RAS also was used to perform HEC-18 bridge-scour analysis. At 12 of the 15 sites, at least 1 pier was in the water at low flow in the main channel, and the pier in the main channel with the maximum scour was chosen for analysis. At the remaining three sites, the piers were perched in the overbank out of the low flow, and the pier with the maximum scour was chosen for analysis.

Using the data and analysis mentioned in the above paragraphs, the SRICOS-EFA model was used to predict scour depths. The results of the scour-depth prediction were then compared to the measured scour result and the HEC-18 estimates. A tiered approach to predicting pier and contraction scour was developed from the results.

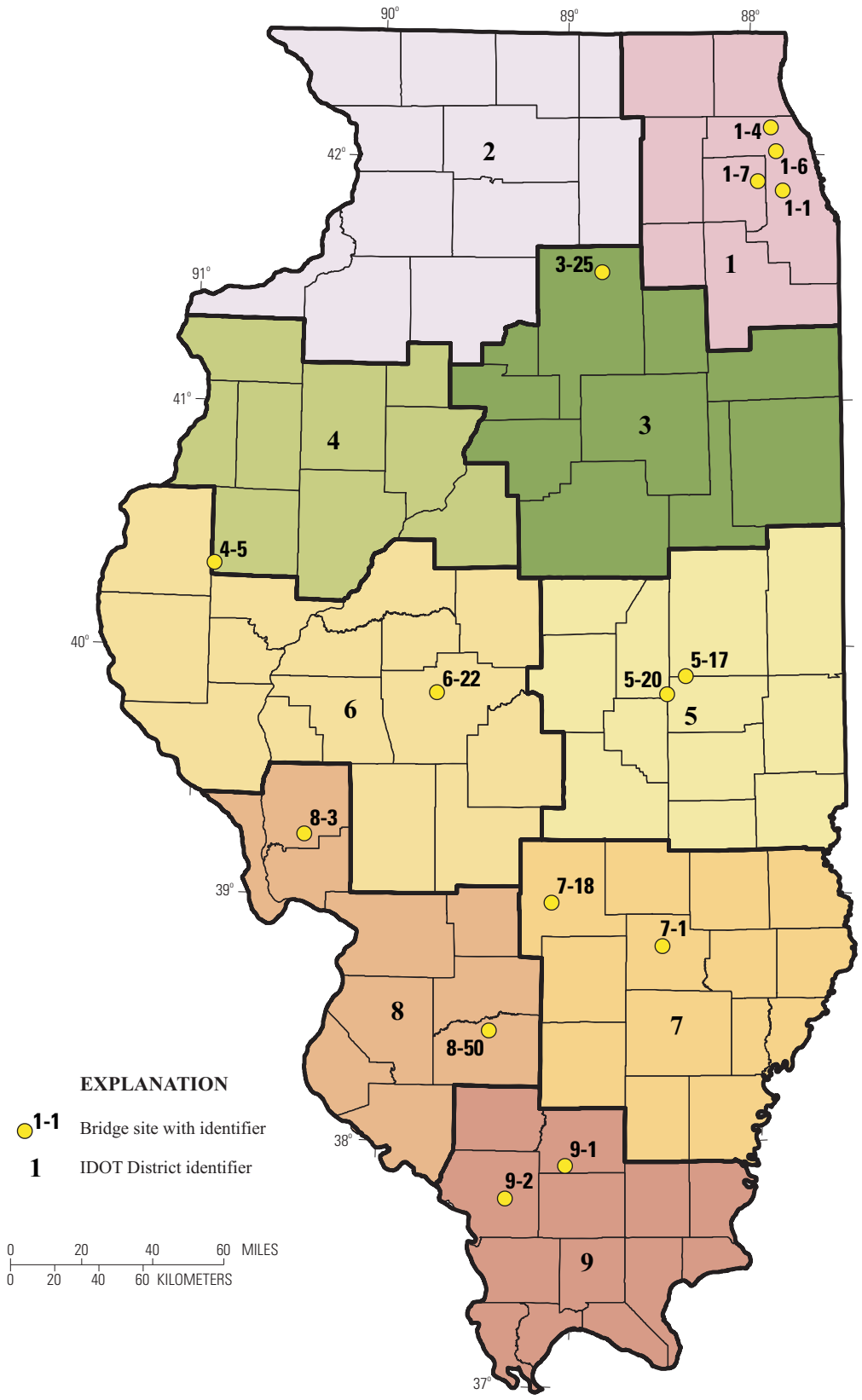

Figure 1.1. Location of the 15 bridge sites selected for scour-prediction analysis in Illinois.

Table 1.1. Structure Number, Drainage Area, and Location Information for the 15 Bridge Sites Selected for Scour-prediction Analysis
[Latitude and longitude are referenced to WGS84]

Bridge Site Identifier (Figure 1.1)	IDOT Structure Number	Location	County	Feature Crossed	Latitude	Longitude	Drainage Area (mi^2)
1-1	016-0634	Cermak Road	Cook	Des Plaines River	41°50'59.17"N	87°49'38.95"W	484
1-4	016-0273	Palatine Road	Cook	Des Plaines River	42° 6'31.11"N	87°53'15.12"W	359
1-6	016-0829	Touhy Avenue	Cook	Des Plaines River	42° 0'37.08"N	87°51'40.50"W	416
1-7	022-0045	IL 83	Du Page	Salt Creek	41°53'21.01"N	87°57'42.79"W	90.7
3-25	050-0159	IL 23	La Salle	Indian Creek	41°31'23.39"N	88°48'58.28"W	135
4-5	055-0010	IL 61	McDonough	Lamoine River	40°19'50.96"N	90°53'46.20"W	655
5-17	021-4022	CR 1550N	Douglas	Kaskaskia River	39°52'45.45"N	88°22'35.21"W	109
5-20	074-0034	CR 100N	Piatt	Lake Fork	39°48'22.97"N	88°28'34.96"W	149
6-22	084-0180	IL 97	Sangamon	Spring Creek	39°48'53.69"N	89°41'58.98"W	107
7-1	013-0010	US 45	Clay	Little Wabash River	38°47'01.18"N	88°30'28.90"W	711
7-18	026-0034	US 51	Fayette	Kaskaskia River	38°57'37.43"N	89°05'17.31"W	1,940
8-3	031-0022	US 67	Greene	Macoupin Creek	39°14'03.78"N	90°23'40.58"W	868
8-50	095-0066	IL 177	Washington	Little Crooked Creek	38°26'30.05"N	89°25'00.00"W	84.3
9-1	028-0037	IL 149	Franklin	Big Muddy River	37°53'29.56"N	89°01'10.46"W	795
9-2	039-0036	IL 127	Jackson	Big Muddy River	37°45'28.78"N	89°19'39.44"W	2,162

CHAPTER 2 STREAMFLOW

2.1 RETRIEVAL AND PROCESSING

Published daily mean and annual instantaneous peak streamflow data were retrieved from the USGS National Water Information System (NWIS) using the NWISweb website, http://waterdata.usgs.gov/il/nwis/sw/. Unpublished instantaneous hourly streamflow data were retrieved from the NWIS using the USGS Automated Data Processing System (ADAPS) (U.S. Geological Survey 2003) program outwat. If there was no data value on the hour, the outwat program performed linear interpolation between observed "unit" values treated as instantaneous observations, though usually there was a value on the hour so that no interpolation was necessary. The observed unit values retrieved and processed by outwat are similar to those posted publicly on the USGS instantaneous data archive (IDA) site (http://ida.water.usgs.gov/ida/); the only differences would be any updates that may have occurred since the data were last posted on the IDA site. The list of streamflow-gaging stations and periods of record used are presented in Section 2.2.

The hourly streamflow data were used in this project for two purposes. First, as described in Section 2.2, they were used in an unadjusted form to test whether the daily mean streamflow values were sufficient to characterize the high-flow periods to which scour processes are most sensitive. Second, once it was determined that hourly data would be sufficient while daily data would not, they were used to test and calibrate a disaggregation scheme for obtaining hourly streamflow estimates from published daily data (see Appendix A.1). For this second purpose, the hourly streamflow data obtained using outwat were checked, filled, and normalized using the corresponding daily streamflow data as a standard. The following steps were used in this process: (1) if the hourly value was negative or greater than 10,000,000.0, the value was considered as missing; (2) if the corresponding daily value was zero, all hourly values during the day were set to zero; (3) if the corresponding daily value was positive but all the hourly values were zero, the hourly values for that day were considered as missing; (4) short periods of missing hourly values were filled with the corresponding daily value; and (5) the hourly values on each day were normalized to match the corresponding published daily value by multiplying each hourly value by the ratio of the daily mean to the average of the hourly values on that day.

2.2 ESTIMATION

The streamflow-gaging stations and relevant characteristics used either directly or indirectly in the estimation of scour are presented in Table 2.1. As described below, it was determined that hourly streamflow data were needed at most sites to provide an accurate description of flood events for the purpose of scour estimation. Continuous streamflow records are published by the USGS at a daily time scale, though unit-value data with a shorter time step are available for recent years. Instantaneous hourly values based on the unit-value data, when available, were retrieved for use in this study, checked, and adjusted to provide the same daily total flow volume as the daily data as described in Section 2.1. None of the gaging stations have unit-value data for the full period needed for scour estimation, so a daily-to-hourly disaggregation scheme (Appendix A.1) was developed and applied to estimate *average* hourly discharges (not instantaneous hourly values as provided by our retrieval process). In addition, the scour modeling methodology assumes its streamflow input consists of average values, regardless of the time step. Although the unit-value discharges, when available, could have been used to create hourly average values, for sake of consistency between periods preceding and during the period when unit value data are available, disaggregated average hourly values were used in the scour modeling throughout the entire period. The retrieved hourly

instantaneous values were only used to establish the need for hourly as opposed to daily data and to calibrate the daily-to-hourly disaggregation procedure.

The application of the daily-to-hourly disaggregation scheme was the only manipulation of the streamflow data required at the sites at or near a gaging station having a published daily record covering the period of interest (sites 1-4, 4-5, 6-22, 7-18, 8-3, 8-50, 9-1, and 9-2). At sites 5-17 and 5-20, there is or was a gaging station, but the daily record does not cover the period of interest for scour estimation. In this case, record-extension techniques (Appendix A.3) were applied to extend the existing daily record to cover the period of interest. At the other sites (sites 1-1, 1-6, 1-7, 3-25, and 7-1), record-transfer techniques (Appendix A.4) were applied to transfer (with appropriate modification) streamflow records from other gaging stations to the site of interest. Sites 1-1 and 1-6 both have gaging stations within a short distance (measured in terms of drainage area ratio) upstream and downstream on the same stream; for these sites, record transfer by drainage area-based interpolation (Appendix A.4.2) was used. At sites 1-7 and 7-1, there are pairs of nearby gaging stations on the same stream with records covering the period of interest, both of which are downstream of the scour-estimation site. For these sites, record transfer by drainage area-based extrapolation constrained by the properties of these nearby gages on the same stream (Appendix A.4.3) was used. At the remaining site (3-25), no gaging station on the same stream was ever established. In this case, a simple drainage area ratio-adjustment technique (Appendix A.4.4) was used to estimate a record at the site.

The scour processes investigated in this study are most sensitive to the highest flows, so the observed daily mean and unadjusted instantaneous hourly values were checked for how well they represented the annual peak flow values. As would be expected, at most stations, the daily values consistently under-estimated the peak flow values on the same day, while the maximum hourly values usually were close in magnitude to the instantaneous peak, though slight under-estimation also occasionally occurred (Figure 2.1). Therefore, it was decided that 1 day is generally too coarse a time step to accurately represent the major flood hydrographs at the stations of interest, while 1 hour is sufficient. A procedure to disaggregate or “downscale” daily flow values to an hourly time step was thus determined to be needed (Appendix A.1).

Table 2.1. Streamflow-gaging Stations and Relevant Characteristics Used either Directly or Indirectly in the Estimation of Scour

Bridge Site Identifier	Drainage Area (mi^2)	Gaging Stations	Gaged Watershed DA (mi^2)	Site DA / Gaged DA (%)	Period simulated using SRICOS	Gage Records - Daily	Gage Records - Unit Value	Period of Daily Record Estima-tion	Period of Daily-Hourly Disaggre-gation	Hydrologic Data Summary	Streamflow Estimation Method Used	Calibration Period	Disag-gregation Exponent *pow*	Station(s) tested to determine *pow*
1-1	484	**05532500** 05529000	**630** 360	**76.8** 134.4	10/1957 - 9/2007	**10/1943 - Current** 10/1940 - Current	**8/1987 - Current** 4/1989 - Current	10/1957 - 9/2007	10/1957 - 9/2007	Site is between two gages. Synthesize record by interpolation.	Interpolation (Method IIIA) using 05532500 and 05529000	N/A	1.0	05532500 and 05529000
1-4	359	**05529000**	**360**	**99.7**	10/1957 - 9/2007	10/1940 - Current	4/1989 - Current	None	10/1957 - 3/1989	Hydrologically, the site is essentially at the gage. Only downscaling is needed.	I	N/A	1.0	05529000
1-6	416	**05529000** 05532500	**360** 630	**115.6** 66.0	10/1957 - 9/2007	10/**1940 - Current** 10/1943 - Current	**4/1989 - Current** 8/1987 - Current	10/1957 - 9/2007	10/1957 - 9/2007	Site is between two gages. Synthesize record by interpolation.	Interpolation (Method IIIA) using 05529000 and 05532500	N/A	1.0	05529000 and 05532500
1-7	90.7	**05531300** 05530990 05531500	**91.5** 30.5 115	**99.1** 297 78.9	10/1957 - 9/2007	**6/1989 - Current** 7/1973 - Current 10/1945 - Current	**6/1989 - Current** N/A N/A	10/1957 - 5/1989	10/1957 - 5/1989	Gage almost at the bridge, but not for the full life of the bridge. Extend record and extrapolate to site location.	(1) Extension: QPPQ (Method IIA) using 05531500; (2) Transfer: Extrapolation (Method IIIB) using 05531300 and 05531500	Extension of 05531300: WY1990-2007	0.50	05531300
3-25	134.6	**05552190** 05551700 05556500 05439000 05557500	**125.9** 70.2 196 77.1 99.0	**106.9** 192 68.7 175 136	10/1960 - 9/2007	**one day in 2000** 10/1960 - Current 3/1936 - Current 10/1979 - Current 4/1936 - 9/1966	**None** 10/1993 - Current 10/1993 - Current 10/1993 - Current None	10/1960 - 9/2007	10/1960 - 9/2007	No gage at bridge, one low flow measurement on stream near bridge (05552190).	Extrapolation by drainage-area ratio (Method IIIC) using 05551700	N/A	1.0	05551700
4-5	655	**05584500**	655	100.0	10/1957 - 9/2007	**10/1944- Current**	**10/87 - Current**	None	10/1957 - 9/1987	Gage on stream at bridge with record beginning before all piers were moved. Only downscaling needed.	I	N/A	1.0	05584500
5-17	109	**05590400** 05590800 05591200	**109** 149 473	**100.0** 77.9 23.0	10/1964 - 9/2007	**10/1964 - 9/1979** 10/1972 - Current 10/1970 - Current	**None** 3/1990 - Current 10/1987 - Current	10/1964 - 9/2007	10/1964 - 9/2007	Gage at the bridge, but not for the full life of the bridge.	Extension: QPPQ (Method IIA) using 05590800	WY1972-1979	1.0	05590800

Bridge Site Identifier	Drainage Area (mi^2)	Gaging Stations	Gaged Watershed DA (mi^2)	Site DA / Gaged DA (%)	Period simulated using SRICOS	Gage Records - Daily	Gage Records - Unit Value	Period of Daily Record Estima-tion	Period of Daily-Hourly Disaggre-gation	Hydrologic Data Summary	Streamflow Estimation Method Used	Calibration Period	Disag-gregation Exponent *pow*	Station(s) tested to determine *pow*
5-20	149	**05590800**	**149**	**100.0**	10/1957 - 9/2007	**10/1972 - Current**	**3/1990 - Current**	10/1957 - 9/1972	10/1957 - 2/1990	Gage at the bridge, but not for the full life of the bridge.	Extension: QPPQ-CPI (Method IIB) using Monticello precip data with K = 0.85	WY1972-2007	1.0	05590800
6-22	107	**05577500**	**107**	**100.0**	10/1957 - 9/2007	**1/1949 - Current**	**10/1989 - Current**	None	10/1957 - 9/1989	Good - downscaling only.	I	N/A	0.15	05577500
7-1	711	**03378900** 03378635 03379500	**745** 240 1131	**95.4** 296. 62.9	10/1965 - 9/2007	**8/1965 - 9/1982** 10/1966 - Current 8/1914 - Current	**None** 10/1993 - Current 10/1990 - Current	Site: 10/1965 - Current; 03378900 : 10/1982 - Current	10/1965 - 9/2007	Gage on stream, but not at bridge (though DA's differ by only 5%). Partial record (1966-82; need 1966-Current).	Extension of 03378900: QPPQ (Method IIA) using 03379500; Transfer: Extrapolation (Method IIIB) using 03378900 and 03379500	Extension of 03378900: WY1966-1982	1.0	03379500
7-18	1940	**05592500**	**1940**	**100.0**	10/1957 - 9/2007	**3/1908 - Current** (except missing data during 1913-14)	**10/1988 - Current**	None	10/1957 - 9/1988	Good - downscaling only	I	N/A	1.0	05592500
8-3	867.6	**05587000**	**868**	**100.0**	10/1957 - 9/2007	**3/1921 - Current** (except missing data 1933-40)	**8/1991 - Current**	None	10/1957 - 8/1991	Good - downscaling only	I	N/A	0.25	05587000
8-50	84.3	**05593575**	**84.3**	**100.0**	10/1967 - 9/2007	**10/1967 - Current**	**10/1989 - Current**	None	10/1967 - 9/1989	Good - downscaling only	I	N/A	0.10	05593575
9-1	795	**05597000**	**794**	**100.1**	10/1957 - 9/2007	**6/1908 - Current** (except missing data during 1910-14)	**8/1993 - Current**	None	10/1957 - 8/1993	Good - downscaling only	I	N/A	0.50	05597000
9-2	2162	**05599500** 05599490	**2169** 2100	**99.7** 103	10/1957 - 9/2007	**12/1916 - Current** 96-05 stage only	**10/1987 - Current** None	None	10/1957 - 9/1987	Primary gage is hydrologically essentially at the site; only downscaling needed. Alternate record at bridge is stage only.	I	N/A	0.50	05599500

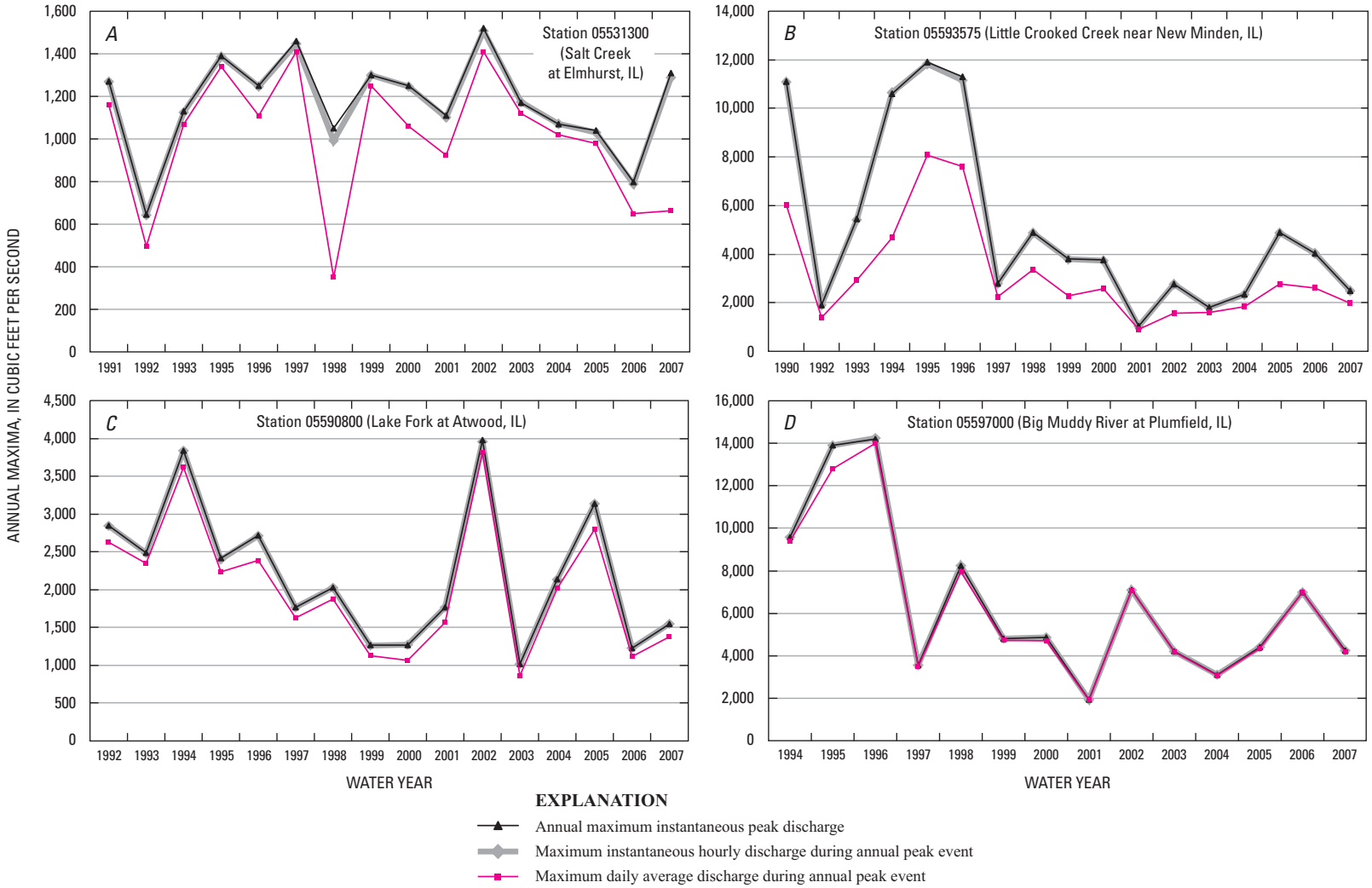

Figure 2.1. Comparisons among annual maximum instantaneous peak discharges and maximum instantaneous hourly and average daily discharges during annual peak event: (a) station 05531300 (Salt Creek at Elmhurst, Illinois), near scour investigation site 1-7; (b) station 05593575 (Little Crooked Creek near New Minden, Illinois), at scour investigation site 8-50; (c) station 05590800 (Lake Fork at Atwood, Illinois), at scour investigation site 5-20; and (d) station 05597000 (Big Muddy River at Plumfield, Illinois), at scour investigation site 9-1. Water years with missing hourly data during the annual peak event are not shown.

CHAPTER 3 HYDRAULICS

3.1 BRIDGE AND CHANNEL GEOMETRY DATA

As part of the site selection process, the IDOT districts submitted any available pre-existing hydraulic models and plan data. The pre-existing hydraulic model types and formats are listed in Table 3.1. Additional data about the bridge structure (e.g. widths, lengths and shapes, skew angle, Manning's coefficient, and channel slope) also were collected if data were not available from the pre-existing hydraulic models or plans. USGS personnel collected data by use of echosounder, ground penetrating radar (GPR), digital level, manual probing, and (or) a survey-grade global positioning system (GPS) to document current channel conditions at the 15 sites.

Table 3.1. Structure Number, Location, and Pre-existing Hydraulic Model Information for the 15 Bridge Sites Selected for Scour-prediction Analysis [---, no pre-existing model]

Bridge Site Identifier	Structure Number	Location	County	Feature Crossed	Pre-Existing Hydraulic Model
1-1	016-0634	Cermak Road	Cook	Des Plaines River	HEC-2 - Digital
1-4	016-0273	Palatine Road	Cook	Des Plaines River	HEC-2 - Digital
1-6	016-0829	Touhy Avenue	Cook	Des Plaines River	HEC-2 - Digital
1-7	022-0045	IL 83	Du Page	Salt Creek	FEQ - Digital
3-25	050-0159	IL 23	La Salle	Indian Creek	WSPRO - Paper
4-5	055-0010	IL 61	McDonough	Lamoine River	HEC-RAS - Digital
5-17	021-4022	CR 1550N	Douglas	Kaskaskia River	---
5-20	074-0034	CR 100N	Piatt	Lake Fork	---
6-22	084-0180	IL 97	Sangamon	Spring Creek	WSPRO - Paper
7-1	013-0010	US 45	Clay	Little Wabash River	---
7-18	026-0034	US 51	Fayette	Kaskaskia River	WSPRO - Digital
8-3	031-0022	US 67	Greene	Macoupin Creek	HEC-2 - Digital
8-50	095-0066	IL 177	Washington	Little Crooked Creek	HEC-2 - Digital
9-1	028-0037	IL 149	Franklin	Big Muddy River	WSPRO - Paper
9-2	039-0036	IL 127	Jackson	Big Muddy River	WSPRO - Paper

3.2 MODELING

Pre-existing models obtained from the IDOT districts (Table 3.1) were converted to HEC-RAS models (U.S. Army Corps of Engineers 2008). The models were calibrated to streamflow-gaging data, where available (Table 2.1). The gaging records used in the calibration were subsampled by date of measurement, type of measurement (wading or bridge), and flow conditions (levee breaks, backwater, etc.). For the sites not near a gage, extensions to the model and (or) comparisons to previous models were made to ensure consistency.

Using the HEC-RAS models, a streamflow, velocity, and depth rating (needed for SRICOS-EFA modeling) was computed for each site (Appendix C). Various flow values and recurrence interval floods were used, including the 100- and 500-year flood values, and are presented in Appendixes C and D. The 100- and 500-year floods used were obtained from Soong et al. (2004), except for sites 3-25, 1-1, 1-4, and 1-6. At site 3-25, a long-term gage was not available and StreamStats (http://water.usgs.gov/osw/streamstats/), which uses equations developed in Soong et al. (2004), was used. For the sites along the Des Plaines River (1-1, 1-4, and 1-6) the 100- and 500-year flood predictions from a hydrologic model (HEC-1) were used (written communication, Rick Gosch, Illinois Department of Natural Resources, 2008). The HEC-RAS models also were used to perform HEC-18 bridge scour analysis as described in Chapter 5.

CHAPTER 4 SOILS

Laboratory tests were performed on undisturbed cohesive sediment samples to test erosive response to increasing velocity and shear stress. The samples were collected with standard Shelby tubes with a 3-in. (76.2-mm) outside diameter, and all were tested by the Illinois Department of Transportation (IDOT) in their Erosion Function Apparatus (Figure 4.1). For consistency, a single lab technician performed the testing. Also, soil properties were determined from samples in the Shelby tubes by IDOT. The results of the laboratory testing also were used to determine relations between soil properties and erosion potential as measured by the EFA. These relations can be used as surrogates in SRICOS-EFA modeling if EFA data are not available.

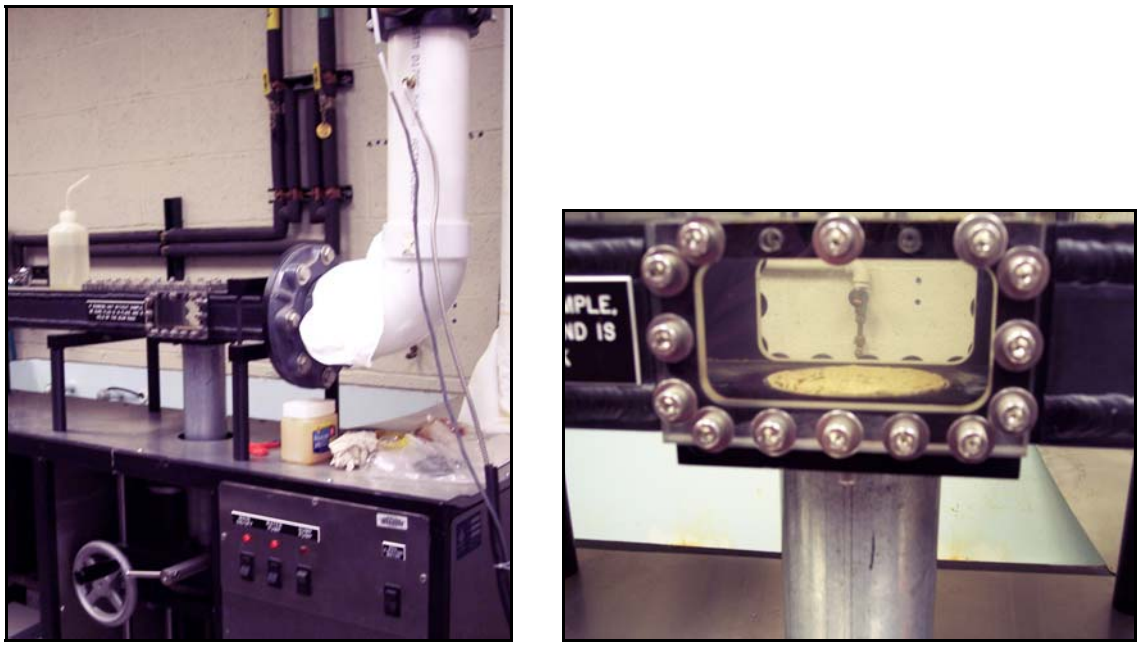

(a) (b)

Figure 4.1. Erosion Function Apparatus owned and operated by the Illinois Department of Transportation.

4.1 EROSION FUNCTION APPARATUS

Methods, description, and studies for the EFA are fully explained in Briaud et al. (1999, 2002, 2003, 2004, 2005), Kwak et al. (2001) and Brandimarte et al. (2006), and the methods are summarized in the following paragraphs (including some direct excerpts from Briaud et al. 2003). The results of EFA testing from this study are presented in Appendix B. Before the start of the study, difficulties had been reported in operation of the EFA with respect to observing the soil sample exposure into the flume through the murky water and judging the effective time to advance the soil sample. One IDOT lab technician experienced with using the EFA and the existing EFA capabilities was used to be as consistent and accurate as possible with the best available technology at the start of the study.

A Shelby tube is placed through a circular opening in the bottom of a rectangular conduit (1.22-m long by 101.6-mm wide by 50.8-mm high) (Figure 4.1). The samples were placed in the EFA and saturated before EFA testing started. A piston, controlled by the operator by use of a computer, pushes the soil until it protrudes 0.5 to 1.0 mm into the rectangular conduit to be eroded by the flowing water (Figure 4.2). The erosion rate ($\dot{Z}_i$) for each flow velocity is determined by:

$$\dot{Z}_i = \frac{l}{t} \quad (4.1)$$

where

l = the length of soil sample eroded (mm)

t = time elapsed (s)

After several attempts at measuring the shear stress (τ) in the apparatus, the developers found that the best way to obtain τ was by using the Moody Chart (Moody 1944) for pipe flows given as:

$$\tau = \frac{1}{8} f \rho v^2 \quad (4.2)$$

where

τ = shear stress on the sample (Pa);

f = friction factor obtained from the Moody Chart (dimensionless);

ρ = mass density of water (1,000 kg/m^3); and

v = mean flow velocity (m/s).

The friction factor (f) is a function of the pipe Reynold's number (Re) and the pipe relative roughness (ε / D) (where ε is the surface roughness (m) and D is the pipe diameter (m)).

$$\mathrm{Re} = \frac{vD}{\nu} \quad (4.3)$$

where

ν = kinematic viscosity of water (approximately 1.0x10^{-6} m^2/s at 20^{o}C)

D = pipe diameter (m)

v = mean flow velocity (m/s).

To ensure that the hydraulic diameter is equal to the diameter for a circular pipe (D) the following formula is used:

$$D = \frac{2 h_{rf} w_{rf}}{\left(h_{rf} + w_{rf}\right)} \quad (4.4)$$

where

h_{rf} = height of the rectangular flume (m); and

w_{rf} = width of the rectangular flume (m).

The average height of the surface roughness (ε) (m) is assumed to be one-half of the D_{50} (m), where D_{50} is the median grain size for the soil. One-half of the D_{50} is used because it is assumed that only one-half of the particle protrudes into the flow, while the bottom half is buried. The results of EFA testing from this study are presented in Appendix B. The conceptual depiction of the EFA results (Figure 4.2) shows two key components: (1) the critical shear stress (τ_c) where erosion of the soil starts to occur, and (2) the erosion rate versus shear stress relation once the critical shear has been reached. A summary of the critical shear stress values for each soil used in scour prediction is presented in Table 4.1. For erosion rate results

occurring after the critical shear stress was reached, a relation was developed on the logarithms of erosion rate (mm/hr) and shear stress minus critical shear stress for each soil as follows:

$$\dot{Z} = a(\tau - \tau_c)^b \quad (4.5)$$

An example of this for site 3-25 is shown in Figure 4.3, where a=0.177 and b=1.162 (i.e. $\dot{Z} = 0.177(\tau - \tau_c)^{1.162}$). Coefficient a and exponent b for each soil used in the scour prediction are presented in Table 4.1. Relations between the erosion rate results and soil properties are presented in Section 4.3.

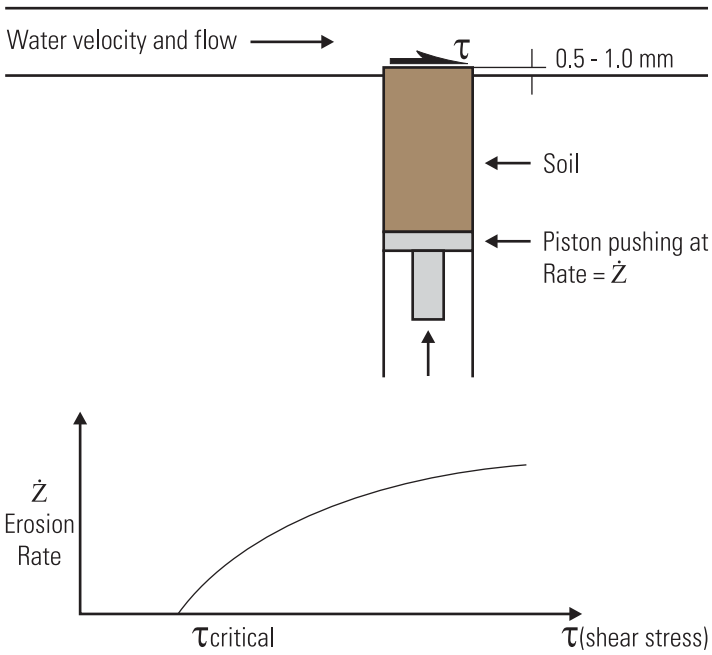

Figure 4.2. Erosion Function Apparatus conceptual diagram (modified from Briaud et al. 2003).

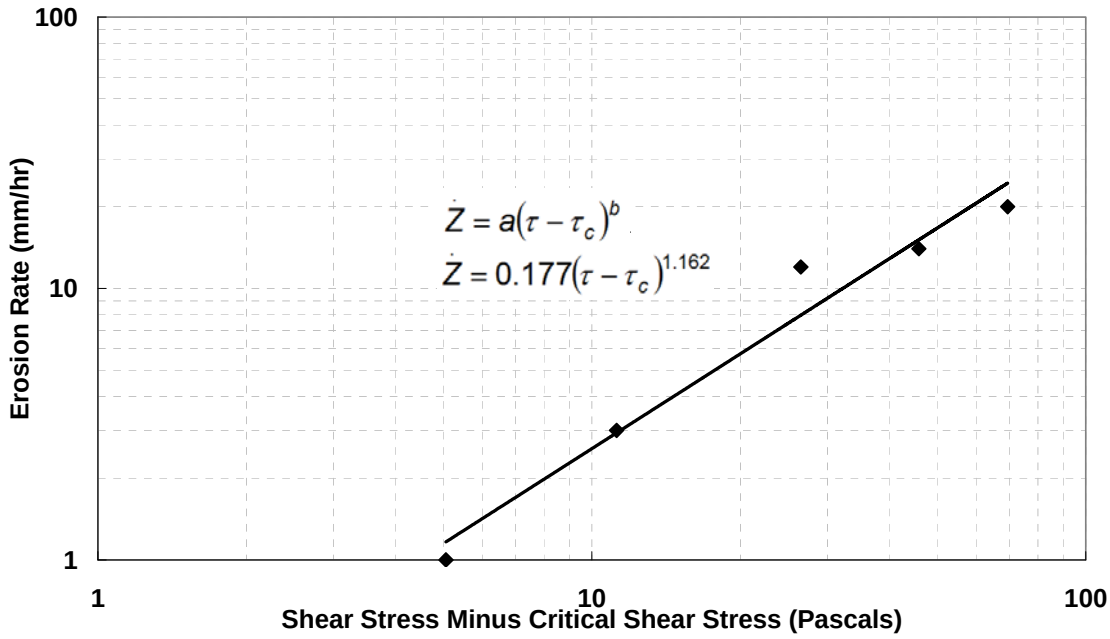

Figure 4.3. Erosion Function Apparatus relation between erosion rate and critical shear stress minus shear stress for site 3-25 Soil 1.

Table 4.1. Erosion Function Apparatus Results and Statistics of Critical Shear Stress, and Erosion Rate Parameters (coefficient *a*, and exponent *b*)

Sample	Critical Shear Stress (Pa)	Coefficient *a*	Exponent *b*	Coefficient of Determination R^2
1-1 Soil 1	4.25	0.286	1.123	0.57
1-4 Soil 1	13.20	0.233	0.738	0.58
1-4 Soil 2	1.23	0.860	1.465	0.90
1-4 Soil 3	16.05	0.441	0.665	0.93
1-4 Soil 4	13.28	0.163	0.990	0.93
1-6 Soil 1	1.23	0.337	1.222	0.94
1-7 Soil 1	10.80	0.080	1.673	0.93
1-7 Soil 2	5.74	0.052	2.086	1.00
3-25 Soil 1	9.70	0.177	1.162	0.96
4-5 Soil 1	0.99	0.305	1.948	0.93
4-5 Soil 2	8.90	0.038	1.796	0.89
5-17 Soil 1	18.79	0.269	0.467	0.63
5-20 Soil 1	19.13	0.283	0.520	0.86
6-22 Soil 1	8.80	0.048	1.698	0.88
7-1 Soil 1	2.56	0.072	2.279	0.85
7-1 Soil 2	1.77	0.550	2.342	0.99
7-18 Soil 1	19.58	0.330	0.630	0.63
8-3 Soil 1	8.50	1.026	0.605	0.31
8-50 Soil 1	5.15	0.700	2.036	0.93
9-1 Soil 1	2.50	0.030	2.577	0.81
9-2 Soil 1	5.20	0.146	1.200	0.94
9-2 Soil 2	8.80	0.686	0.948	0.54
Maximum	19.6	1.026	2.577	1.00
Minimum	1.0	0.030	0.467	0.31
Median	8.7	0.276	1.211	0.90
Average	8.5	0.323	1.371	0.82
Standard Deviation	6.1	0.281	0.653	0.19
10th-Percentile	1.3	0.05	0.61	0.57
90th-Percentile	18.5	0.70	2.26	0.96

4.2 SOIL PROPERTY TESTING

The following soil properties were determined from material in the Shelby-tube samples: liquid limit (*LL*), plastic limit (*PL*), plasticity index (*PI*), moisture content, unconfined compressive strength (Q_u), wet density (*WD*), particle-size distribution, mean diameter (D_{50}), percent sand (*Sa*), percent silt (*Si*), percent clay (*Cl*), and AASHTO and IDOT soil classification (Table 4.2).

The Q_u results were obtained from Shelby tubes using calibrated laboratory equipment performed according to AASHTO T 208 / ASTM D 2166. The compression machine is a Soiltest model U-600 with a 1,000-pound capacity. The device is capable of variable plate speeds from zero to 0.25 in. per minute. Load measurements were obtained by calibrated/verified proving rings. Stress calculations are determined by using uniform area correction.

The latitude, longitude, elevation, and full-particle size distribution are presented in Appendix B. The summary statistics (Table 4.2) show that the unconfined compressive strength and plasticity index ranged from 0.2 to 7.5 tons/ft^2 and 4 to 25, respectively. The results of the laboratory testing also were used to determine relations between soil properties and erosion potential (Section 4.3) as measured by the EFA.

Table 4.2. Soil Properties and Summary Statistics for Samples used in Scour Prediction

Sample	Soil Classification AASHTO	Soil Classification IDOT	Wet Density lbs/ft^3	Percent Moisture Content	Unconfined Compressive Strength (tons/ft^2)	Liquid Limit	Plastic Limit	Plasticity Index	Mean Particle Size (D_{50}) mm	Percent Gravel	Percent Sand	Percent Silt	Percent Clay
1-1 Soil 1	A-7-5(29)	Silty Clay	104.2	45.0	0.27	59	34	25	0.0041	0.5	18.2	54.5	20.9
1-4 Soil 1	A-6 (02)	Sand Loam	133.3	19.8	2.39	28	17	11	0.0148	30.4	16.3	46.8	32.1
1-4 Soil 2	A-4 (2)	Silt Loam	142.0	17.3	0.19	21	16	5	0.0100	0.8	32.4	29.7	16.4
1-4 Soil 3	A-4 (3)	Clay Loam	135.3	15.1	3.52	23	15	8	0.0217	13.9	32.9	36.2	15.9
1-4 Soil 4	A-4 (3)	Silty Clay-Loam	139.4	16.7	1.78	22	15	7	0.0149	6.4	37.7	41.2	16.5
1-6 Soil 1	A-7-6(20)	Clay	112.7	35.7	0.18	51	27	24	0.0084	4.8	15.0	61.5	23.5
1-7 Soil 1	A-6 (02)	Sand Loam	130.9	21.1	0.72	33	21	12	0.1296	21.5	14.7	65.0	20.3
1-7 Soil 2	A-4 (2)	Loam	119.8	23.4	0.60	27	18	9	0.0679	15.0	31.0	38.8	22.4
3-25 Soil 1	A-4 (0)	Loam	140.3	10.4	1.20	17	13	4	0.0591	4.6	30.7	42.1	20.9
4-5 Soil 1	A-6 (09)	Silty-Clay Loam	118.8	29.2	0.21	32	20	12	0.0148	0.0	12.0	65.6	21.5
4-5 Soil 2	A-4 (8)	Silty-Clay Loam	123.2	27.0	0.66	30	20	10	0.0204	0.0	31.3	46.1	18.1
5-17 Soil 1	A-4 (1)	Clay-Loam	143.0	11.7	5.47	21	14	7	0.0213	7.8	31.4	48.7	18.7
5-20 Soil 1	A-4 (3)	Clay-Loam	140.1	13.4	3.53	24	15	9	0.0274	6.3	32.0	42.7	18.7
6-22 Soil 1	A-4 (8)	Silty-Clay Loam	119.5	20.2	0.97	33	22	11	0.0167	0.9	4.0	66.9	29.0
7-1 Soil 1	A-4 (4)	Loam	118.6	23.6	0.21	27	17	10	0.0331	4.5	6.3	68.2	25.4
7-1 Soil 2	A-4 (3)	Loam	119.0	23.1	0.25	25	17	8	0.0304	1.2	29.1	49.8	21.1
7-18 Soil 1	A-4 (1)	Loam (Till)	143.1	9.8	7.53	19	13	6	0.0345	6.6	6.2	68.8	25.0
8-3 Soil 1	A-6 (17)	Silty-Clay Loam	119.7	23.5	0.81	38	21	17	0.0095	0.1	4.8	70.2	25.0
8-50 Soil 1	A-6 (10)	Silty Clay-Loam	121.1	24.1	0.51	30	18	12	0.0105	0.1	18.2	54.5	20.9
9-1 Soil 1	A-6 (06)	Clay Loam	125.5	24.9	0.18	28	16	12	0.0314	0.0	16.3	46.8	32.1
9-2 Soil 1	A-6 (12)	Silty Clay-Loam	118.0	23.7	0.47	33	19	14	0.0173	0.0	32.4	29.7	16.4
9-2 Soil 2	A-6 (14)	Silty Clay-Loam	118.5	21.3	0.49	34	19	15	0.0171	0.0	32.9	36.2	15.9
Maximum			143.1	45.0	7.5	59	34	25	0.1296	30.4	37.7	75.2	39.6
Minimum			104.2	9.8	0.2	17	13	4	0.0041	0.0	4.0	29.7	15.8
Median			122.2	22.2	0.6	28	17	11	0.0189	2.9	18.1	49.3	21.0
Average			126.6	21.8	1.5	29	18	11	0.0280	5.7	19.9	52.3	22.2
Standard Deviation			11.2	8.1	1.9	9.9	4.8	5.3	0.0275	8.0	11.5	13.5	5.7

4.3 EROSION RATE AND SOIL PROPERTY ANALYSIS

The soil property results from Section 4.2 were combined with the EFA results in Section 4.1 so that the relations between soil properties and erosion potential, as measured by the EFA, could be developed. The primary goal of the analysis is to develop relations that can predict the two components of the EFA results based on basic soil properties that generally are collected for bridge work. The two key components are (1) the critical shear stress (τ_c) where erosion of the soil starts to occur, and (2) the erosion rate versus shear stress relation once the critical shear has been reached (Figure 4.2 and Figure 4.3). The relations developed in this section can be used in SRICOS-EFA modeling if EFA data are not available.

The initial step in developing the relations was to do a linear regression analysis to relate the logarithms of τ_c, coefficient *a* and exponent *b* (key parameters in equation 4.5) to individual soil properties. The linear regression of the logarithms resulted in an estimation power function.

$$\tau_c = cS_i^{\,d} \tag{4.6}$$

$$a = eS_i^{\,f} \tag{4.7}$$

$$b = gS_i^{\,h} \tag{4.8}$$

where

S_i = soil property *i*

d, f, h = are exponents corresponding to soil properties *i*

c, e, g = coefficients

The resulting coefficient of determination (R^2) of each combination of soil property and key parameter is presented in Table 4.3. The equations using unconfined compressive strength as the soil property explain 82 and 61 percent of the variance in the logarithms for τ_c and *b*, respectively. No other soil properties result in a better R^2 than using Q_u for τ_c and *b*. The R^2 for the τ_c improves when using a natural logarithm function for Q_u and τ_c (Figure 4.4 and equation 4.9); the resulting R^2 is 0.95.

$$\tau_c = cLn(Q_u) + K \tag{4.9}$$

where

c = a coefficient

K = a constant

Therefore, this equation will be used for τ_c. The best-fit and envelope equations for predicting τ_c and *b* using a single soil property (Q_u) are presented and summarized in (Figure 4.4, Figure 4.5, and Table 4.4).

For coefficient *a*, no equation using any of the soil parameters gives an R^2 greater than 0.30. Depending on the application, a value of the coefficient *a* should be chosen from Table 4.4. The table provides the maximum and median values along with the values that were not exceeded by 90 and 10 percent of the values. More discussion of choosing coefficient *a* is in the last paragraph of this section.

Table 4.3. Coefficient of Determinations Resulting from Regression Analysis of Power Functions for Each Soil Property versus the τ_c , coefficient *a* and exponent *b*

	Coefficient of Determination (R^2)		
Soil Property	**Critical Shear Stress τ_c**	**Coefficient** *a*	**Exponent** *b*
Unconfined Compressive Strength (Q_u)	0.82	0.01	0.61
Moisture Content (*MC*)	0.39	0.01	0.28
Liquid Limit (*LL*)	0.12	0.00	0.03
Plasticity Limit (*PL*)	0.15	0.00	0.07
Plasticity Index (*PI*)	0.07	0.00	0.01
Percent finer than 0.075 mm	0.14	0.12	0.01
Percent coarser than 0.075 mm	0.08	0.20	0.00
Percent Sand (*Sa*)	0.05	0.25	0.00
Percent Silt (*Si*)	0.13	0.08	0.04
Percent Clay (*Cl*)	0.06	0.14	0.03
Mean particle size (D_{50})	0.08	0.24	0.04
Wet Density (*WD*)	0.27	0.01	0.23

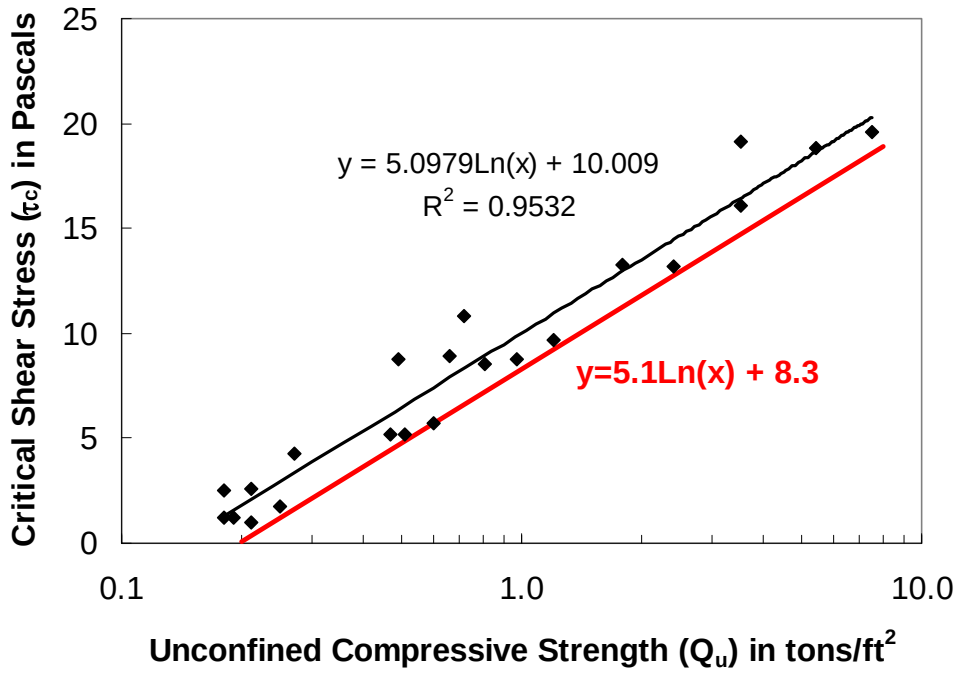

Figure 4.4. Best-fit (black line) and envelope (red line) natural logarithm functions of critical shear stress and unconfined compressive strength.

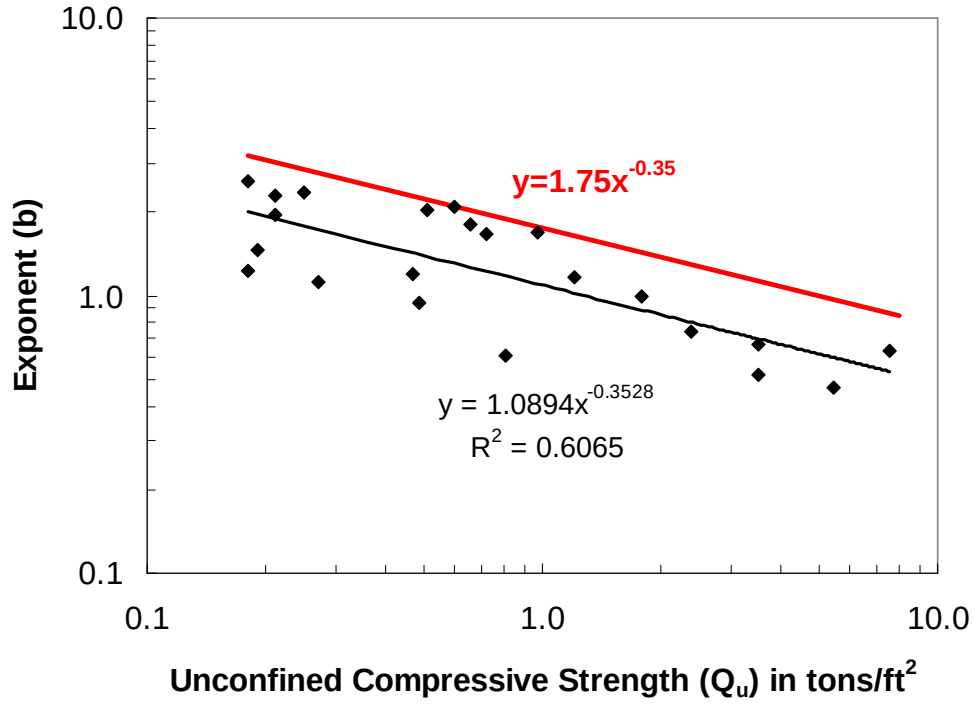

Figure 4.5. Best-fit (black line) and envelope (red line) power functions of exponent *b* and unconfined compressive strength.

Table 4.4. Erosion Parameter and Prediction Equations or Values

Erosion Parameter	Equation or Value	Eq. No.	Equation or Value Type
Critical Shear	$\tau_c = 5.098 \ln Q_u + 10.01$	4.10	best fit (single parameter)
	$\tau_c = 5.1 \ln Q_u + 8.3$	4.11	envelope fit
Coefficient *a*	$a = 1.0$		maximum
	$a = 0.7$		90th percentile
	$a = 0.3$		median
	$a = 0.1$		10th percentile
Exponent *b*	$b = 1.089 Q_u^{-0.353}$	4.12	best fit (single parameter)
	$b = 1.75 Q_u^{-0.35}$	4.13	envelope fit
	$b = 0.049 Q_u^{-0.236} MC^{0.668} Sa^{0.345} Si^{0.995} Cl^{-1.121}$	4.14	best fit (multiple parameter)

-Red text indicates envelope equation represented by red trendlines in Figure 4.4 and Figure 4.5

To attempt to improve on the equations, multiple-linear regression analysis was used to relate the logarithms of τ_c, coefficient *a*, and exponent *b* to multiple soil properties. The multiple-linear regression of the logarithms resulted in an estimation power function

$$\tau_c = cS_1^{d1}S_i^{di}\ldots$$

$$a = eS_1^{k1}S_i^{fi}\ldots$$

$$b = jS_1^{h1}S_i^{hi}\ldots$$

where

S_i = soil property i

d, k, h = are exponents corresponding to soil properties i

c, e, j = coefficients

The resulting coefficient of determination (R^2) of each combination is presented in Table 4.5. There was only one with substantial improvement in the R^2 and where two additional criteria were met:

(1) the exponents of the added soil properties were statistically significant (the corresponding 95-percent confidence interval for the parameter did not include zero), and

(2) the sign of the exponent was correct from a physical viewpoint. For example, critical shear stress should increase with increasing unconfined compressive strength.

These criteria were met for exponent *b* and the resulting equation is presented in Table 4.4. A comparison of measured and predicted exponent *b* values using equations 4.12, 4.13, and 4.14 is shown in Figure 4.6.

Further, applying the three equations (4.12, 4.13, and 4.14) for predicting exponent *b* to equation 4.5 (with coefficient $a = 0.3$ and using the best-fit equation (4.10) for τ_c), the predicted versus the measured EFA erosion rates are presented in Figure 4.7. Using the envelope fit (single parameter) (4.13) and best-fit (multiple parameter) (4.14) equations for predicting exponent *b* substantially overestimates the exponent and resulting erosion rates (Figure 4.6 and Figure 4.7).

Various combinations of values and equations for predicting coefficient *a*, exponent *b*, and critical shear were attempted to calculate the best-fit and upper-limit erosion rates. Best-fit and upper-limit approaches to estimating critical shear and erosion rates were developed based on Q_u of the soil only are presented in Figure 4.8 and Table 4.6. If EFA data are not available, these relations can be used in SRICOS-EFA modeling to determine a best fit and upper limit to predicted scour. Note that the sources of uncertainty in applying any of the equations developed in the section include the non-homogeneous nature of soils at any individual site and the statistically small data set used to develop the equations. Attention should be given to Table 4.2 to determine if the equations are applicable for a given site.

Table 4.5. Multiple-linear Regression Results on the Logarithms of Critical Shear, Coefficient *a*, Exponent *b*, and Various Soil Properties [Bold text indicates equation developed]

Critical Shear Regression Results	
Parameter	**R^2**
Qu, MC	0.83
Qu, MC, PI	0.84
Qu, MC, PL	0.83
Qu, MC, LL	0.84
Qu, MC, LL, Sa	0.84
Qu, MC, PI, Sa	0.84
Qu, MC, PI, Sa, Si	0.84
Qu, MC, PI, Sa, Si, Cl	0.86
Qu, MC, PI, D_{50}	0.86
Qu, MC, PI, D_{50}, Sa	0.90
Qu, MC, PI, Percent Finer	0.84
Qu, MC, PI, Percent Coarser	0.84
Sa, Si, Cl	0.16
Qu, MC, PI, D_{50}, WD	0.86
MC, D_{50}, WD	0.40
PI, Percent Coarser, D_{50}, WD	0.38
MC, PI	0.58
MC, PI, Sa	0.58

Coefficient *a* Regression Results	
Parameter	**R^2**
Qu, MC	0.01
Qu, MC, PI	0.08
Qu, MC, PL	0.04
Qu, MC, LL	0.09
Qu, MC, LL, Sa	0.37
Qu, MC, PI, Sa	0.38
Qu, MC, PI, Sa, Si	0.42
Qu, MC, PI, Sa, Si, Cl	0.55
Qu, MC, PI, D_{50}	0.44
Qu, MC, PI, D_{50}, Sa	0.47
Qu, MC, PI, Percent Finer	0.24
Qu, MC, PI, Percent Coarser	0.32
Sa, Silt, Cl	0.29
Qu, MC, PI, Sa, WD	0.38
MC, PI	0.06
MC, PI, Sa	0.37

Exponent *b* Regression Results	
Parameter	**R^2**
Qu, MC	0.62
Qu, MC, PI	0.73
Qu, MC, PL	0.66
Qu, MC, LL	0.74
Qu, MC, LL, Sa	0.79
Qu, MC, PI, Sa	0.79
Qu, MC, PI, Sa, Si	0.80
Qu, MC, PI, Sa, Si, Cl	0.87
Qu, MC, Sa, Si, Cl	**0.87**
Qu, MC, PI, D_{50}	0.85
Qu, MC, PI, D_{50}, Sa	0.85
Qu, MC, PI, Percent Finer	0.76
Qu, MC, PI, Percent Coarser	0.77
Sa, Si, Cl	0.19
Qu, MC, PI, D_{50}, WD	0.86
MC, D_{50}, WD	0.53
MC, PI	0.65
MC, PI, Sa	0.68

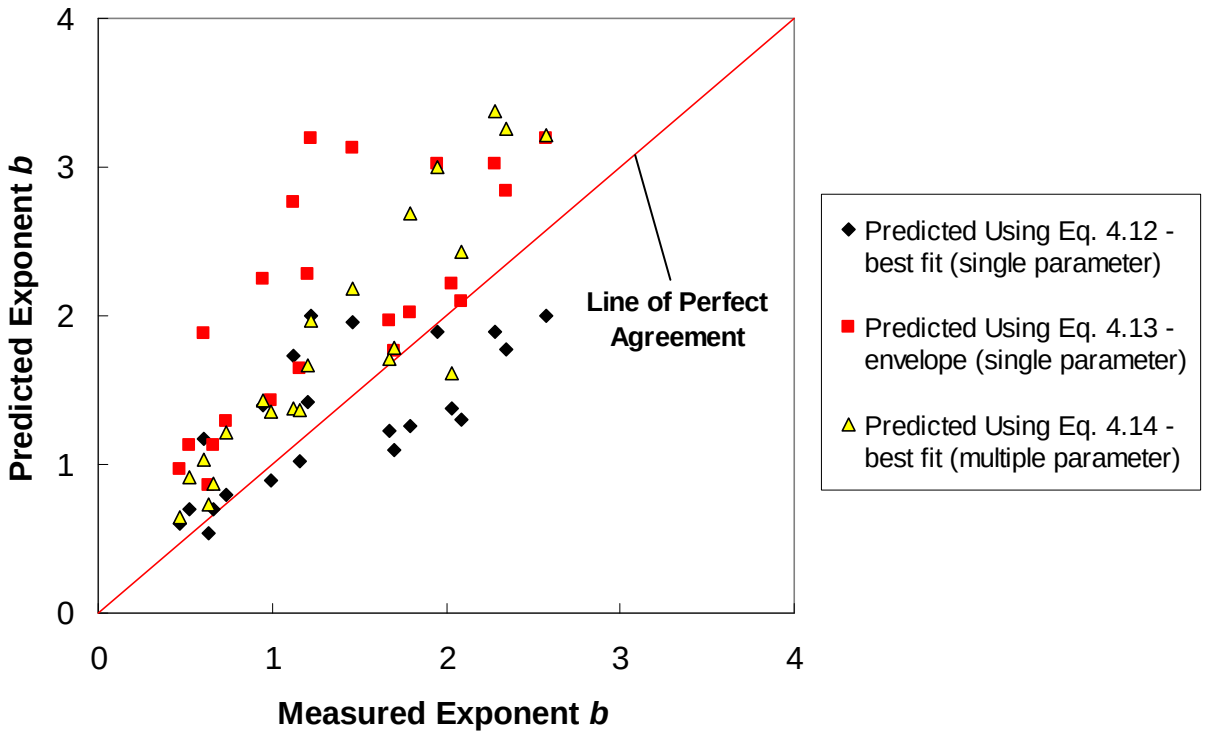

Figure 4.6. Measured and predicted exponent *b* using three equations.

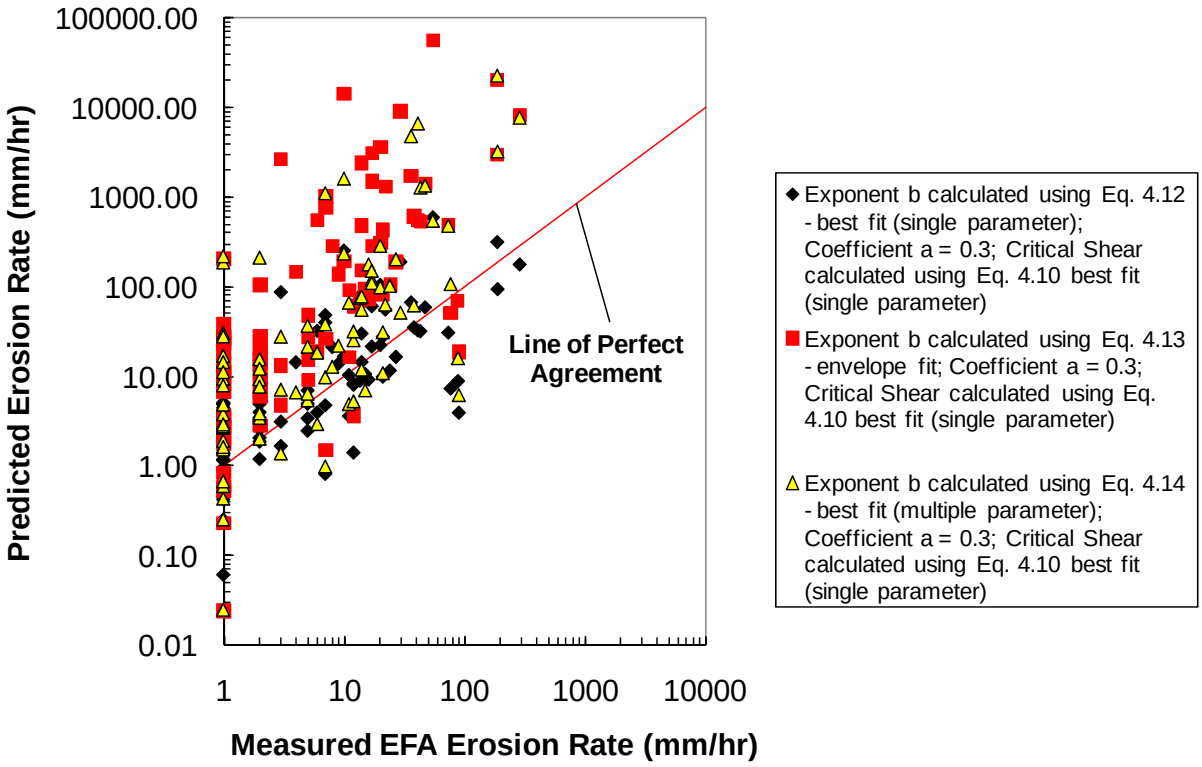

Figure 4.7. Predicted and measured EFA erosion rates with varying equations used for exponent *b*.

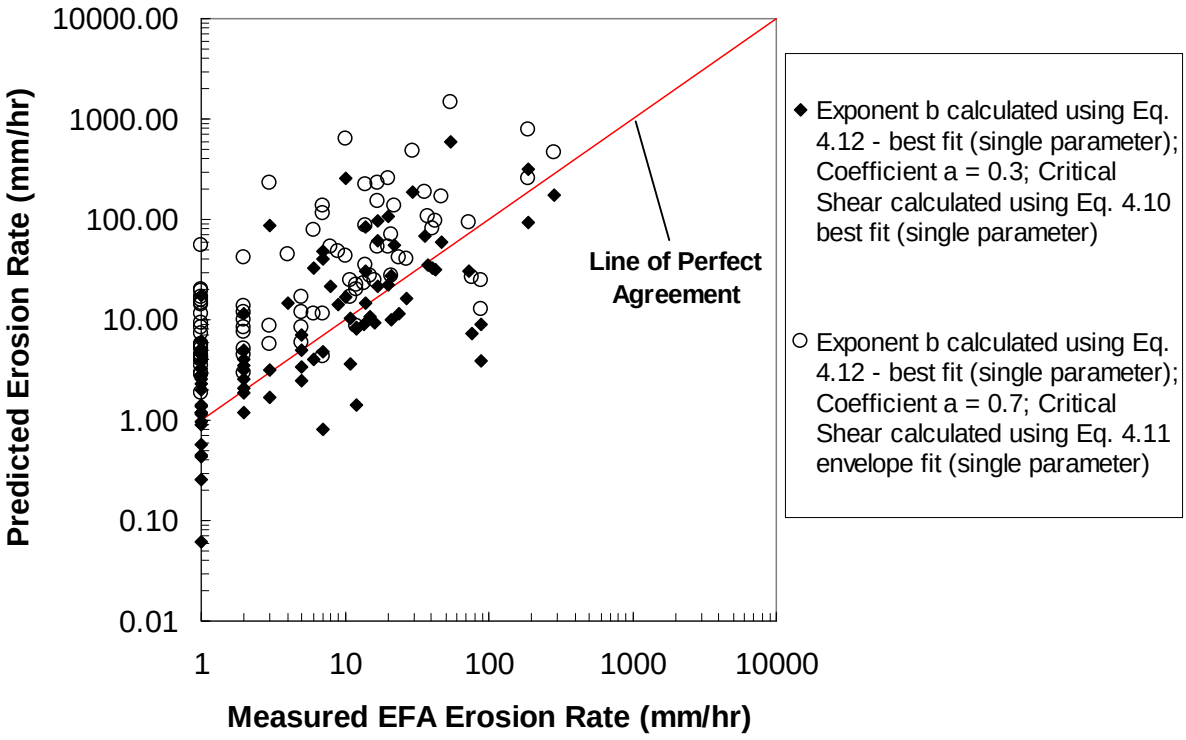

Figure 4.8. Predicted and measured EFA erosion rates using best-fit and upper-limit equation and parameter value combinations for predicting erosion rates based on only unconfined compressive strength of the soil.

Table 4.6. Best-fit and Upper-limit Equation and Parameter Value Combinations for Predicting Erosion Rates Based on Only Unconfined Compressive Strength of the Soil as Presented in Figure 4.8

Erosion Rate Estimation Goal	**Parameter**	**Equation No. or Parameter Value**	**Equation or Value Type**
Best Fit	Critical Shear	Eq. 4.10	best fit (single parameter)
	Coefficient *a*	$a = 0.3$	median
	Exponent *b*	Eq. 4.12	best fit (single parameter)
Upper Limit	Critical Shear	Eq. 4.11	envelope fit
	Coefficient *a*	$a = 0.7$	90th percentile
	Exponent *b*	Eq. 4.12	best fit (single parameter)

CHAPTER 5 SCOUR

This chapter presents measured historic scour, brief methods for each scour prediction type, comparison of results, and a reduction factor approach based on properties of the cohesive soils. This study used two scour prediction methods: (1) SRICOS-EFA methods for cohesive soils, and (2) HEC-18 method for non-cohesive soils.

5.1 MEASURED HISTORIC SCOUR

Scour holes may be filled on the recession limb of hydrographs or during low-flow conditions, causing the elevation of the stream channel bed to not reflect the actual historic scour elevation. To better measure the historic scour, ground penetrating radar (GPR), manual probing, digital level, and (or) echo sounder data were collected by USGS personnel at the 15 sites in Table 5.1. These scour elevations were then compared to historic cross-section elevations so that the measured depth of historic scour could be computed. Scour measurements were taken in the cross sections immediately upstream and downstream of the pier, and along the stream-wise direction of both sides of the pier.

The measured scour value at each bridge and the technique used to obtain that value are presented in Table 5.1. At 12 of the 15 sites, at least 1 pier was in the water at low flow in the main channel, and the pier in the main channel with the maximum pier and contraction scour was chosen for analysis. At the remaining three sites, the piers were perched in the overbank out of the low flow, and the pier in the overbank with the maximum pier and contraction scour was chosen for analysis. There was not a consistent pattern of where the maximum scour occurred. The maximum scour occurred in all the different possibilities, including the upstream or downstream side of the pier or cross section or along the pier in the stream-wise direction.

Data from the GPR were used at 9 of the 15 sites to determine the measured scour. At sites where the data from the GPR were not usable, manual probing data was used (3 of the 15 sites). When the pier was out of the water, data from digital level surveys were used (3 of the 15 sites). At one site, the GPR data were not usable and manual probing also was not possible. Echosounder data were used at this site, which only reflect stream channel bed at the time of the survey. At all 15 sites, uncertainty in the measured scour value can be attributed to historic bridges, construction disturbance, quality of historic cross sections, debris build-up near the bridge, and overall channel stability. Regardless, the measured scour data can be compared to predicted scour to evaluate the relative differences in various methods.

Although scour of cohesive soils occurs over time and not just in a single large storm event (like non-cohesive soils), there is still some value in determining the maximum historic flood that has occurred at each site. The maximum historic flood at the streamgage near each bridge (or an alternate nearby longer term streamgage (Table 2.1)) is presented in Table 5.1. Both the maximum for the current substructure life and streamgage period of record are listed in Table 5.1. The maximum for the period of record is listed because it was noted that previous historic bridges were present at all sites, and current contraction and possibly pier scour measurements may reflect scour that occurred before the current substructure was built. Using the maximum for the streamgage period of record may not fully represent all historic scour because bridges were most likely built before the streamgages were installed. Even with that consideration, all the current substructures at the bridge sites, except site 9-1, have experienced an approximately large flow, which is defined by Benedict (2003) as any flow that equals or exceeds 70 percent of the 100-year flow magnitude (Table 5.1). The 100-year flow magnitude was determined as described in Section 3.2. Again, the measured scour data can be compared to predicted scour to evaluate the relative differences in various modeling methods.

Table 5.1. Measured Scour and Technique Used for Each Bridge Site, and Maximum Historic Flood at a Nearby Streamgage

Bridge Site Identifier	Measured Pier and Contraction Scour (ft)	Technique Used	Year Bridge Substructure Built, Rebuilt, or Modified	Streamgage Used for Maximum Historic Flood	Peak Flow Period of Record	Maximum Peak Flow (ft^3/s)				100-yr Flood Estimate (ft^3/s)	Percent Different Between Peak Flow and 100-yr Flood	
						Period of Record		Substructure Life			Period of Record	Substructure (current) Life
						Date	Flow	Date	Flow			
1-1	2.56	Ground Penetrating Radar	1956	05532500	1914-2005	08/15/1987	9,770	---	---	7,767	26	26
1-4	2.20	Manual Probe	1965	05529000	1938; 1941-2005	07/04/1938	5,000	10/01/1986	4,900	7,339	-32	-33
1-6	1.59	Ground Penetrating Radar	1955	05529000	1938; 1941-2005	07/04/1938	5,000	10/01/1986	4,900	7,407	-32	-34
1-7	2.33	Manual Probe	1982	05531500	1946-2005	08/17/1987	3,540	---	---	2,820	26	26
3-25	1.90	Ground Penetrating Radar	1971	[A]05551700	1961-2005	07/18/1996	10,565	---	---	5,780	83	83
4-5	6.39	Ground Penetrating Radar	1976	05584500	1945-2005	03/05/1985	38,900	---	---	41,300	-6	-6
5-17	1.16	Ground Penetrating Radar	1981	[A]05590800	1973-2005	03/05/1979	3,402	---	---	4,080	-17	-17
5-20	0.22	Digital Level Survey (pier out of water)	1963	05590800	1973-2005	03/05/1979	4,030	---	---	4,650	-13	-13
6-22	1.42	Digital Level Survey (pier out of water)	1977	05577500	1948-2005	05/08/1996	10,700	---	---	14,300	-25	-25
7-1	10.8	Ground Penetrating Radar	1966	03379500	1915-2005	01/05/1950	47,000	05/19/1995	43,700	61,100	-23	-28
7-18	2.62	Ground Penetrating Radar	1962	05592500	1908-1912; 1915-1920; 1922-2005	06/29/1957	62,700	05/13/2002	41,000	60,500	4	-32
8-3	5.43	Manual Probe	1968	05587000	1921-1933; 1941-2005	04/12/1994	40,100	---	---	40,700	-1	-1
8-50	3.00	Digital Level Survey (pier out of water)	1979	05593575	1968-2005	05/17/1995	11,900	---	---	17,600	-32	-32
9-1	3.46	Ground Penetrating Radar	1987	05597000	1909-1912; 1915-2005	05/10/1961	42,900	05/01/1996	14,200	28,100	53	-49
9-2	5.11	Echosounder	1984	05599500	1916-1917; 1919; 1931-2005	05/02/1996	33,800	---	---	42,800	-21	-21

[A]A drainage area ratio-adjustment technique (Appendix A.4.4) was used to adjust the maximum peak flow for the site.

5.2 SRICOS-EFA METHOD FOR COMPLEX PIER SCOUR AND CONTRACTION SCOUR

The SRICOS-EFA method for complex pier scour and contraction scour in cohesive soils has two primary components. The first component includes the calculation of the maximum contraction and pier scour. The second component is an integrated approach that considers a time factor, soil properties, and continued interaction between the contraction and pier scour. (Briaud et al. 2003)

5.2.1 Maximum Complex Contraction and Pier Scour

A four-step procedure is used to calculate the maximum contraction and pier scour. The four steps include compiling input data and parameters, calculating maximum contraction scour, calculating maximum pier scour, and summing the two maximum scour predictions (Figure 5.1). Below are the steps partially excerpted from Briaud et al. (2003).

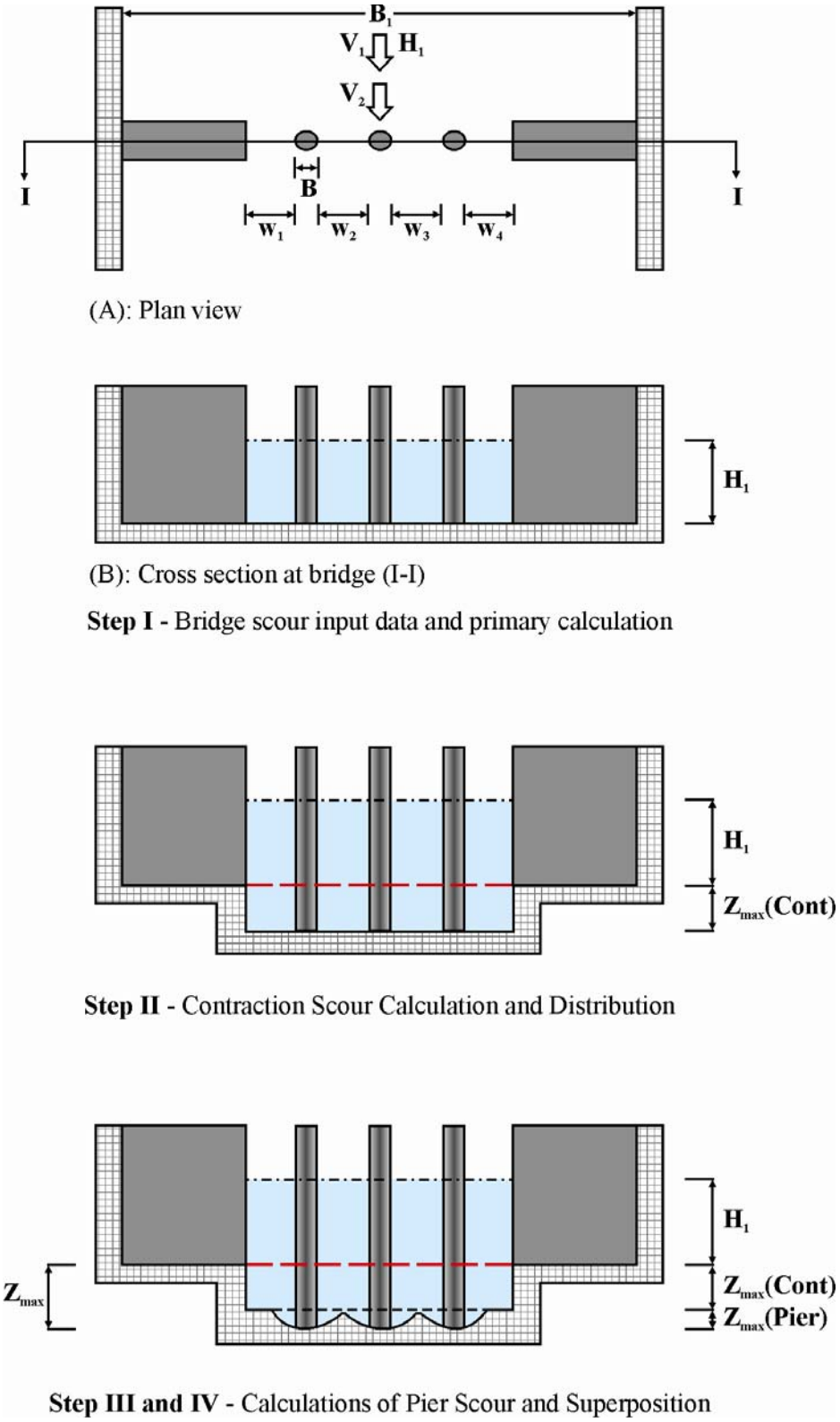

Figure 5.1. Maximum SRICOS complex contraction and pier scour schematic and data inputs (modified from Briaud et al. (2003) Figures 9.1, 9.2, and 9.3).

Step I: Input Data and Parameter Compilation

Flow, bridge and channel geometry, and soil data are needed for input into the equations for calculating maximum scour (Figure 5.1 and Table 5.2). Below is a summary of the data needed.

Table 5.2. Flow, Bridge and Channel Geometry, and Soil Data Input

V_1 = mean velocity in the approach section where the flow is not noticeably influenced by the existence of bridge contraction and piers (m/s)
H_1 = water depth in the approach section (m)
V_2 = mean velocity in the contraction section (at the location of the pier assuming that the bridge piers are not there). Also, sometimes referred to as V_{hec} in Briaud et al. (2003) since the velocity can be calculated using a program like HEC-RAS at the upstream bounding cross section to the bridge. Also, Briaud et al. (2003) showed that V_2 can be calculated by conservation of mass in rectangular channels using the following equation: $V_2 = 1.14 V_1 \left(\frac{B_1}{B_2} \right)$ (5.1) B_1 = approach channel width (m) B_2 = contracted channel width minus the total width of the piers (as shown in Figure 5.1 $B_2 = w_1 + w_2 + w_3 + w_4$)
B = individual pier width (m)
B' = is the pier projected width (m) if the pier is rectangular with a length to width ratio larger than 1 and the pier is at an angle to flow. B' equals B when the pier is not at an angle to flow. B' can be computed using the following equation: $B' = L \sin\alpha + B \cos\alpha$ (5.2) where, L = the pier length (m) α = the attack angle of the flow on the pier (degrees).
τ_c = critical shear stress of soil (Pa)

Step II: Maximum Contraction Scour Calculation

Using the data above on the flow, geometry, and soil properties, the maximum contraction scour can be calculated directly by equation 5.3:

$$Z_{\max}(Cont) = K_\theta K_L \times 1.90\left(\frac{1.49V_2}{\sqrt{gH_1}} - \frac{\left(\frac{\tau_c}{\rho}\right)^{0.5}}{gnH_1^{1/3}}\right)H_1 \quad \geq 0 \qquad (5.3)$$

where (parameters not defined in Step I above)

$Z_{\max}(Cont)$ = maximum contraction scour (m)

K_θ = factor for influence of the transition angle (equal to 1 for $Z_{\max}$ calculations)

K_L = factor for the influence of the length of the contracted channel (equal to 1 for $Z_{\max}$ calculations)

g = acceleration owing to gravity (9.81 m/s^2)

ρ = mass density of water (approximately 1,000 kg/m^3 at temperatures 4 to 20^{o}C)

n = Manning's coefficient (s/m$^{1/3}$)

If the value of the maximum contraction scour $Z_{\max}(Cont)$ is zero or negative, the flow and contraction is not severe enough to cause any contraction scour and the maximum contraction scour is zero.

Step III: Maximum Pier Scour Calculation

Depending on the results of Step II, the appropriate velocity and water depth for use in the maximum pier scour calculations can be determined

-If Step II results predict no contraction scour, the pier scour is calculated by using V_2 and H_1.

-If Step II results predict a maximum contraction scour depth $Z_{\max}(Cont)$ greater than zero, then the maximum pier scour depth is calculated by using the critical velocity V_c for the soil and the water depth H, which includes the contraction scour depth:

$$V_C = \sqrt{\frac{\tau_c H^{\frac{1}{3}}}{\rho g n^2}} \qquad (5.4)$$

$$H = H_1 + Z_{\max}(Cont) \qquad (5.5)$$

The maximum pier scour depth can be calculated by using equation 5.6:

$$Z_{\max}(Pier) = 0.18K_w K_{sp} K_{sh} R_e^{0.635} \qquad (5.6)$$

where

K_w is the correction factor for pier scour water depth, given by:

$$\text{For } \frac{H}{B} \leq 1.6 \qquad K_w = 0.85\left(\frac{H}{B}\right)^{0.34} \qquad (5.7)$$

$$\text{For } \frac{H}{B} > 1.6 \qquad K_w = 1$$

K_{sp} is the correction factor for pier spacing effect on the pier scour depth, when n piers of diameter B are installed in a row, given by:

$$K_{sp} = \frac{B_1}{(B_1 - nB)} \quad (5.8)$$

K_{sh} is the correction factor for pier shape effect on pier scour.

For rectangular piers with $\frac{L}{B} > 1$ $\quad K_{sh} = 1.1$

For all other shapes $\quad K_{sh} = 1.0$

Re is the Reynolds number:

$$\text{Re} = \frac{VB'}{\nu} \quad (5.9)$$

where

V is V_c (equation 5.4) if $Z_{\max}(Cont)$>0, or V_2 if $Z_{\max}(Cont)$=0

ν = kinematic viscosity of water (approximately 1.0x10^{-6} m^2/s at 20^{o}C)

Step IV: Maximum Pier Scour Calculation

The maximum bridge scour is (Figure 5.1):

$$Z_{\max} = Z_{\max}(Cont) + Z_{\max}(Pier) \quad (5.10)$$

5.2.2 Integrated SRICOS-EFA Method

The integrated approach uses the maximum scour predictions from the section above and adds consideration of time, additional soil properties, and continued interaction between the contraction and pier scour. The additional steps include calculation of initial development of scour and the time history of the bridge scour. In this study, the SRICOS-EFA Method program Version 1.02 (Texas A&M University 2001) was used to complete the integrated SRICOS-EFA method to predict complex scour for various streamflow and bridge conditions. The complete set of equations and methods are not repeated here, but a brief summary is given below.

-Calculate initial shear stress for a given streamflow

-Obtain corresponding erosion rate from the erosion function (measured in the EFA or from Table 4.6)

-With these two additional quantities, the following relation is used to find the scour depth for a given streamflow and duration:

$$Z(t) = \frac{t}{\frac{1}{\dot{Z}_i} + \frac{t}{Z_{\max}}} \quad (5.11)$$

where

$Z(t)$ = scour depth for a given streamflow and duration (hr)

$\dot{Z}_i$ = initial erosion rate (mm/hr)

$Z_{\max}$ = the maximum contraction and pier scour from equation 5.10 converted to mm

The scour depth will approach $Z_{\max}$ through time. The SRICOS-EFA Method program allows input for hydrographs and multiple soil layers. The program also has an option for a risk-based approach to scour (Briaud et al. 2003).

In this study, the following inputs and settings were used to obtain scour predictions from the SRICOS-EFA method:

1. Bridge and Hydraulic Characteristics as presented in Chapter 3
2. EFA results and soil properties as presented in Chapter 4
3. Hydrograph with 40 to 50 years of streamflow record (Chapter 2, Table 2.1)

4. The 500-year flood run for 5 days
5. Risk Based (inputting the 500- and 100-year floods with "No. of Runs" = 100 and "Hydrograph Time Length" = 100 years
6. The Z_{max} also was computed for both the 100- and 500-year floods.

5.3 HEC-18 MODELING

Hydraulic Engineering Circular No. 18 (HEC-18) (Richardson and Davis, 2001) scour-prediction methods for non-cohesive soils were used to predict scour at each site. These methods were computed in the implementation of HEC-18 in HEC-RAS (U.S. Army Corps of Engineers, 2008). The equations used in HEC-18 are not repeated in this text. The results of the HEC-18 modeling are presented in Appendixes D and E. Live-bed contraction scour (as indicated by results of equation 5.1 in the HEC-18 manual) occurred at all sites, which means that equations 5.2 and 5.3 in the HEC-18 manual were applied. To be consistent with IDOT general practices, the Colorado State University (CSU) equation 6.1 and the pertinent equations 6.2 – 6.10 in the HEC-18 manual were used to calculate pier scour. Similar to IDOT general practices, equations 6.5 – 6.8 were not used because K_4 was assumed to be 1 as a conservative measure. Also, IDOT uses equation 6.21 to calculate pressure-flow scour, but this equation was not applied in this study, as the pressure-flow scour would most likely be applied, in practice, to the results of SRICOS. In other words, only the components of HEC-18 that can be directly compared with SRICOS-EFA were computed. Abutment scour was not considered in HEC-18 nor SRICOS-EFA scour methods.

5.4 SRICOS-EFA AND HEC-18 SCOUR PREDICTION COMPARISONS

To compare with HEC-18 100- and 500-year storm analysis, three types of SRICOS runs were completed: (1) the risk-based analysis where the 100- and 500-year flood values are input, (2) running the 500-year flood for 5 days, and (3) running a 40- to 50-year hydrograph. Because historic bridges were present at all sites, it is best to compare the observed data with a 40- to 50-year hydrograph (50 years of hourly data is the maximum extent of a SRICOS run and 40 years was the minimum number of years for a site (Table 2.1)). On average, these three methods resulted in consistent values for pier and pier plus contraction scour. Lastly, the 100- and 500-year SRICOS Z_{max} were used in the comparison (Appendix E).

On average, the HEC-18 results predict the highest amount of scour, followed by the SRICOS Z_{max} results, and the three types of SRICOS runs (with a 1.5 safety factor applied as recommended by the SRIOCS program or 1-ft minimum scour depth as decided in this study) predict the lowest amount of scour (Figure 5.2, 5.3, 5.4). The Z_{max} does not have a safety factor because it is treated like the HEC-18 results where a safety factor is not used. Despite uncertainties in the field determination of scour as discussed in Section 5.1, the predicted scour in Figure 5.4 shows that the maximums of the SRICOS runs (with safety factor applied) give a reasonable best-fit approach, but the SRICOS Z_{max} and HEC-18 estimates are always higher than observed in this study. Only the closest sample to the scour hole (and any samples above the scour hole that would have needed to be eroded) was used to compare with observed data. This is shown by the 15 observed scour rows in the tables in Appendix E and the corresponding 15 points per method in Figure 5.4.

Additionally, every soil type collected was modeled for each bridge as a hypothetical situation to compare with HEC-18. In other words, if the bridge was assumed to have only one soil type, it was determined how the SRICOS results compare with the HEC-18 results. The SRICOS Z_{max} gives a reasonable upper limit to scour prediction as all the estimates are near or

below the HEC-18 estimates (Figure 5.3). Eighty-three percent of the Z_{max} predictions show a 45- to 77-percent reduction in the HEC-18 predictions that are over 10 ft (Figure 5.3).

To further explore a reduction-factor approach, a factor was applied to each HEC-18 result to make it match the maximum of the three types of SRICOS runs (with a safety factor) for each bridge site and soil. The Q_u value for the soil was then matched with the reduction factor, and the results were ranked in order of increasing Q_u (Table 5.3). The results showed potential groupings based on Q_u using an envelope approach as discussed in Table 5.3.

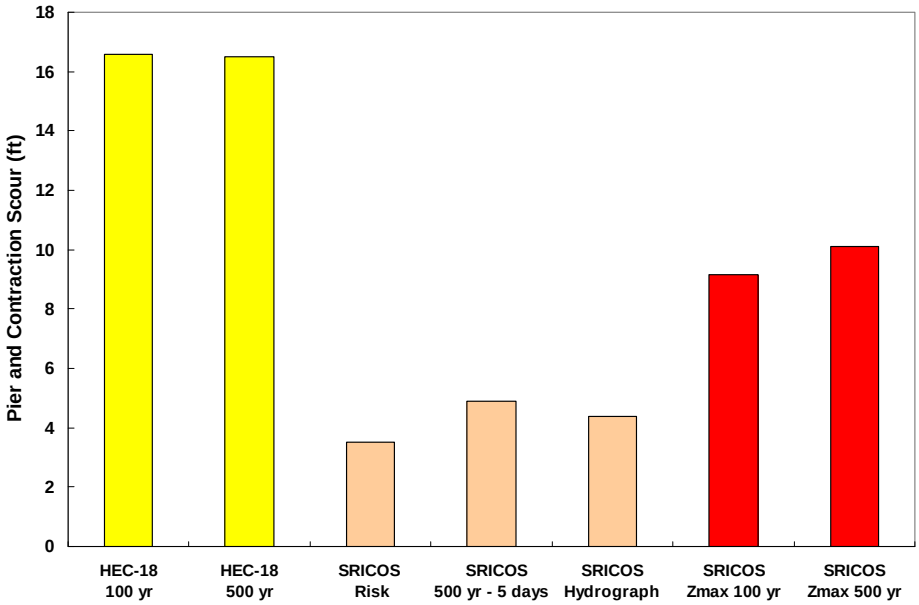

Figure 5.2. Average HEC-18 and SRICOS results for all bridge sites and soils. SRICOS runs have a 1.5 safety factor or 1-ft minimum scour depth except Z_{max}.

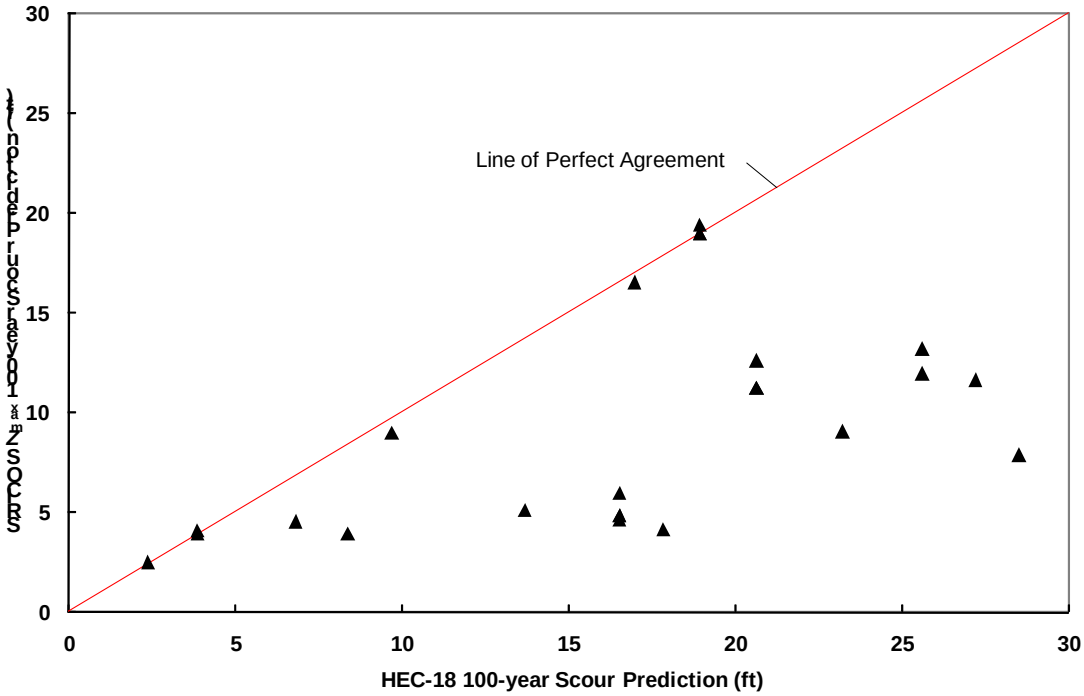

Figure 5.3. HEC-18 and SRICOS Z_{max} 100-year scour prediction for each bridge site and soil.

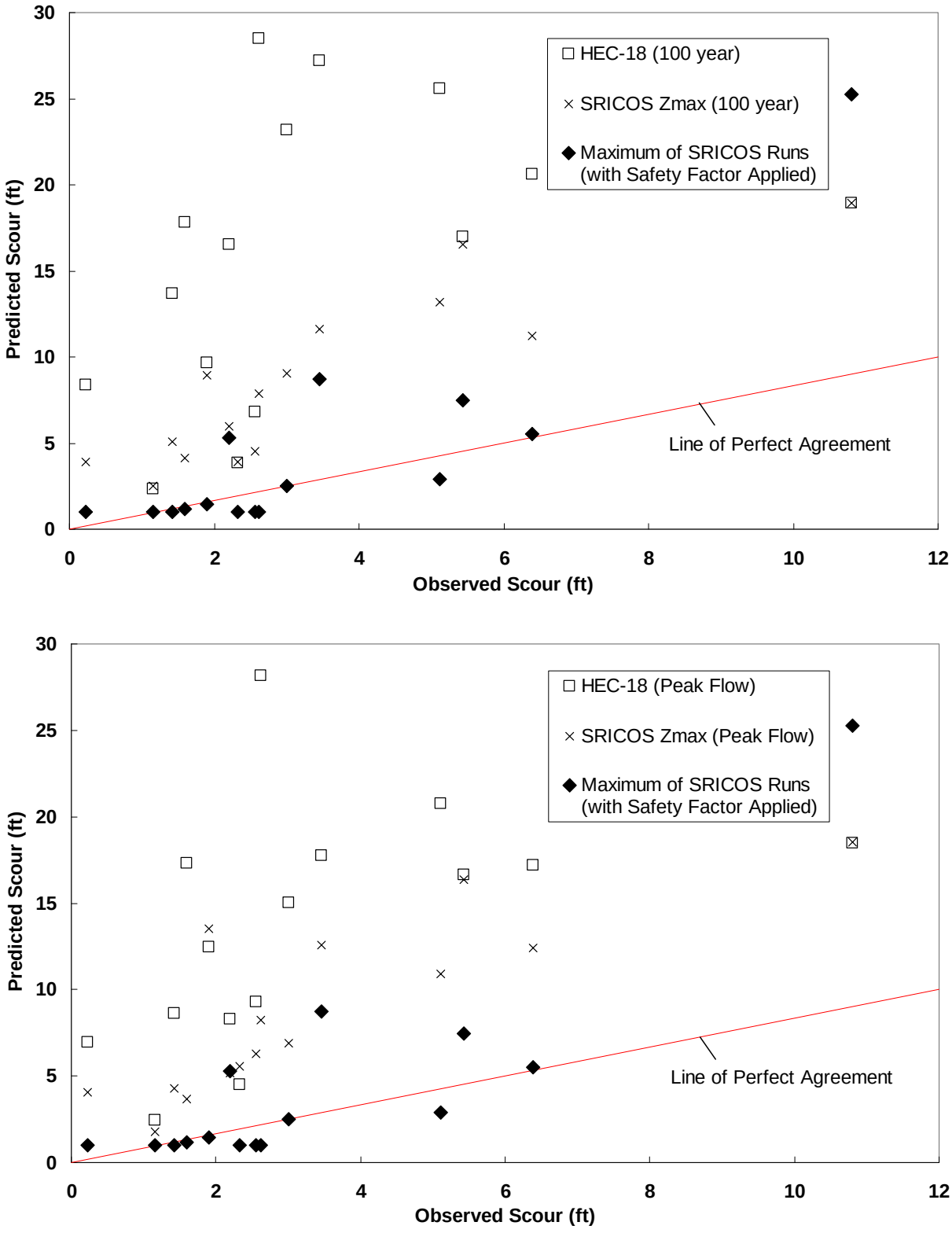

Figure 5.4. Observed and predicted scour for each bridge site (top HEC-18 and Z_{max} computed using the 100-yr flow; bottom HEC-18 and Z_{max} computed using the peak flow).

Table 5.3. Reduction factor for each HEC-18 result to make it match the maximum of the three types of SRICOS runs (with a safety factor) for each bridge site and soil, and potential reduction groupings based on Q_u using an envelope approach.

Q_u (TSF)	Percent Reduction in Scour Depth	Reduction Grouping and Potential Percent Reduction	Discussion of Groupings and Sites
0.18	93	Q_u (0-0.4 TSF) 0 percent reduction	This group of soils has percent reductions that fall near or below zero, so a potential zero percent reduction may be appropriate.
0.18	68		
0.19	68		
0.21	34		
0.21	9		
0.25	-45		
0.27	85		
0.47	89	Q_u (>0.4-1.0 TSF) 25 percent reduction	This group of soils has a percent reduction near 50 percent. As a safety, a percent reduction of half that (25 percent) may be appropriate.
0.49	89		
0.51	89		
0.60	74		
0.66	85		
0.72	74		
0.81	56		
0.97	93		
1.20	85	Q_u (>1.0-8.0 TSF) 50 percent reduction	This group of soils has a percent reduction near 50 percent, but the HEC-18 scour estimate for this site is only 2.37 ft. The remainder of the values are between 85 and 96 percent. As a safety, a percent reduction of around 50 percent may be appropriate, and is still below the minimum reduction factor.
1.78	94		
2.39	94		
3.52	94		
3.53	88		
5.47	58		
7.53	96		

The reduction factors presented in Table 5.3 were applied to each bridge site and soil. These results and comparison with the SRICOS Z_{max} calculation are presented in Table 5.4. The bold values in Table 5.4 represent the lowest of the three prediction methods for each bridge site and soil. Less than half of the reduction-factor method values were the lowest estimate of scour; whereas, the Z_{max} method was the lowest estimate for over half. These results show that the reduction factor method (using a single soil property) may not always be the lowest and that computing Z_{max} (using a soil property and hydraulic properties) may give an even lower estimate of scour. The Z_{max} is the equilibrium maximum contraction and pier scour of cohesive soils for a bridge site over time. This "upper limit" of scour prediction can then be used for sites where the reduction-factor method result is higher than Z_{max}.

The results of Z_{max} calculated using an envelope critical shear value (calculated using equation 4.11 in Table 4.4) is presented in Table 5.5. Using these envelope values, Z_{max} would still be the lowest prediction method at all the same bridge sites and soils except for one.

Note that the sources of uncertainty in applying the methods of this study include uncertainty of scour measurements, a statistically small data set, non-homogeneous nature of soils that may introduce error into estimated soil properties, uncertainty of hydraulic models, and uncertainty associated with flow data. Also, attention should be given to the site characteristics used in this study to determine if the methods are applicable for a given site.

Table 5.4. Scour Prediction Values Using HEC-18, and HEC-18 with a Reduction Factor (Table 5.3) Applied Based on Q_u, and SRICOS Z_{max}. Bold Values Represent the Lowest of the Three Prediction Methods for Each Bridge Site and Soil

		Scour Prediction (ft)		
Sample	Q_u (tons/ft^2)	HEC-18 100 year	Reduction Factor	Z_{max} 100 year
1-1 Soil 1	0.27	6.81	6.81	**4.53**
1-4 Soil 1	2.39	16.52	8.26	**4.83**
1-4 Soil 2	0.19	16.52	16.52	**5.95**
1-4 Soil 3	3.52	16.52	8.26	**4.61**
1-4 Soil 4	1.78	16.52	8.26	**4.83**
1-6 Soil 1	0.18	17.83	17.83	**4.13**
1-7 Soil 1	0.72	3.86	**2.90**	3.91
1-7 Soil 2	0.60	3.86	**2.90**	4.06
3-25 Soil 1	1.20	9.69	**4.85**	8.96
4-5 Soil 1	0.21	20.63	20.63	**12.60**
4-5 Soil 2	0.66	20.63	15.47	**11.22**
5-17 Soil 1	5.47	2.37	**1.19**	2.49
5-20 Soil 1	3.53	8.37	4.19	**3.90**
6-22 Soil 1	0.97	13.68	10.26	**5.08**
7-1 Soil 1	0.21	**18.93**	**18.93**	18.96
7-1 Soil 2	0.25	**18.93**	**18.93**	19.41
7-18 Soil 1	7.53	28.50	14.25	**7.86**
8-3 Soil 1	0.81	16.97	**12.73**	16.52
8-50 Soil 1	0.51	23.21	17.41	**9.04**
9-1 Soil 1	0.18	27.20	27.20	**11.63**
9-2 Soil 1	0.47	25.60	19.20	**13.19**
9-2 Soil 2	0.49	25.60	19.20	**11.94**

Table 5.5. EFA Measured Envelope Equation Critical Shear and the Resulting SRICOS Z_{max} Scour Prediction

		Critical Shear Stress (τ_c) (Pa)		SRICOS Z_{max} (ft)	
Sample	Q_u (tons/ft^2)	EFA Measured	Envelope Eq. 4.11	EFA	Envelope
1-1 Soil 1	0.27	4.25	1.62	4.53	4.65
1-4 Soil 1	2.39	13.20	12.74	4.83	4.87
1-4 Soil 2	0.19	1.23	0.00	5.95	5.51
1-4 Soil 3	3.52	16.05	14.72	4.61	4.71
1-4 Soil 4	1.78	13.28	11.24	4.83	5.00
1-6 Soil 1	0.18	1.23	0.00	4.13	3.23
1-7 Soil 1	0.72	10.80	6.62	3.91	4.01
1-7 Soil 2	0.60	5.74	5.69	4.06	4.06
3-25 Soil 1	1.20	9.70	9.23	8.96	9.00
4-5 Soil 1	0.21	0.99	0.34	12.60	12.74
4-5 Soil 2	0.66	8.90	6.18	11.22	11.63
5-17 Soil 1	5.47	18.79	16.97	2.49	2.67
5-20 Soil 1	3.53	19.13	14.73	3.90	4.30
6-22 Soil 1	0.97	8.80	8.14	5.08	5.16
7-1 Soil 1	0.21	2.56	0.34	18.96	20.50
7-1 Soil 2	0.25	1.77	1.23	19.41	19.75
7-18 Soil 1	7.53	19.58	18.60	7.86	8.31
8-3 Soil 1	0.81	8.50	7.23	16.52	16.69
8-50 Soil 1	0.51	5.15	4.87	9.04	9.06
9-1 Soil 1	0.18	2.50	0.00	11.63	12.32
9-2 Soil 1	0.47	5.20	4.45	13.19	13.48
9-2 Soil 2	0.49	8.80	4.66	11.94	13.40

5.5 TIERED SCOUR PREDICTION APPLICATION

Development of a tiered approach to predicting pier and contraction scour using the results in this study is outlined in this section. The four levels of this approach are listed below in order of complexity.

Levels of Pier and Contraction Scour Prediction Methods:

1. Reduction factors for HEC-18 based on Q_u groupings
2. SRICOS Z_{max} calculation
3. SRICOS simulation based on soil property regressions
4. SRICOS simulation based on EFA results for a given site

In Level 1, a reduction factor is used to adjust the scour estimates from HEC-18. The reduction factor is based on Q_u groupings and results of the SRICOS runs as shown in Table 5.3 and summarized in the list below.

Q_u (0-0.4 TSF): 0 percent reduction in the HEC-18 result
Q_u (>0.4-1.0 TSF): 25 percent reduction in the HEC-18 result
Q_u (>1.0-8.0 TSF): 50 percent reduction in the HEC-18 result

The results from a HEC-18 prediction of pier and contraction scour for a 100-year flood event are reduced by a certain percentage based on the Q_u of the soil near the elevation of the scour zone for the pier.

In Level 2, the SRICOS Z_{max} is calculated for the 100-year flood. The Z_{max} is the equilibrium maximum contraction and pier scour of cohesive soils for a bridge site over time. This "upper limit" of scour prediction can then be used for sites where the reduction factor method result is higher than Z_{max}. A four-step procedure is used to calculate the maximum contraction and pier scour as outlined in Section 5.2.1.

In Level 3, SRICOS simulation is performed based on soil property regressions to obtain critical shear values and erosion rates instead of running an EFA test on soils from the bridge site. Two relations are used: (1) to estimate critical shear and (2) to estimate the erosion rate after critical shear is reached. A best-fit and upper-limit approach to estimating critical shear and erosion rates are presented in Table 4.6 based on Q_u of the soil only. The bridge and hydraulic information needed to run SRICOS can be obtained from HEC-18 and HEC-RAS input and output. Also, the risk, constant flow, and continuous streamflow options can be used in SRICOS as outlined in Section 5.2.2. To retrieve or estimate streamflow, methods in Chapter 2 can be followed.

In Level 4, Shelby-tube samples are taken at the site, similar to the sites in this study. The samples are then run in the EFA to get critical shear and erosion rates for input into SRICOS. The bridge, hydraulic, and streamflow information can be obtained and used as outlined in ***Level 3***.

CHAPTER 6 CONCLUSIONS

The Scour Rate In Cohesive Soils-Erosion Function Apparatus (SRICOS-EFA) methodology outlined in the National Cooperative Highway Research Program Report 24-15 (Briaud et al. 2003) provides a potentially useful methodology for assessing scour in cohesive soils. Field-validation data are limited in testing the SRICOS-EFA method in addressing the issue of scour in cohesive soils. To further test the SRICOS-EFA method in Illinois, the U.S. Geological Survey (USGS), in cooperation with the Illinois Center for Transportation and the Illinois Department of Transportation (IDOT), began a study in 2006 at 15 selected bridge sites throughout the State. Additionally, soil properties were determined for each soil so that the development of relations between soil properties and erosion potential, as determined by the EFA, could be studied. Hydraulic Engineering Circular No. 18 (HEC-18) scour-prediction methods for non-cohesive soils also were used to predict scour at each site.

On average, the HEC-18 results predict the highest scour, followed by the SRICOS Z_{max} results, and the three types of SRICOS runs (with a safety factor) predicted the lowest amount of scour. When compared to observed data, the SRICOS runs (with a safety factor) give a reasonable best-fit approach, and the SRICOS Z_{max} and HEC-18 estimates are always higher than observed.

A reduction factor was determined for each HEC-18 result to make it match the maximum of the three types of SRICOS runs (with a safety factor) for each bridge site and soil. The unconfined compressive strength (Q_u) for the soil was then matched with the reduction factor, and the results were ranked in order of increasing Q_u. The results were grouped by Q_u and a percent reduction was assigned to each group using an envelope approach based primarily on the minimum reduction factor in each group. The reduction factors were applied to each bridge site and soil. These results, and comparison with the SRICOS Z_{max} calculation, show that less than half of the reduction-factor method values were the lowest estimate of scour; whereas, the Z_{max} method was the lowest estimate for over half. These results show that the reduction-factor method (using a single soil property) may not always give the lowest estimate and that computing Z_{max} (using a single soil property and hydraulic properties) may give an even lower estimate of scour. Eighty-three percent of the Z_{max} predictions show a 45- to 77-percent reduction in the HEC-18 predictions that are over 10 ft. The Z_{max} is the equilibrium maximum contraction and pier scour of cohesive soils for a bridge site over time as determined by the SRICOS method. This “upper limit” of scour prediction can then be used for sites where the reduction-factor method result is higher than Z_{max}.

Using the results in this study, a tiered approach to predicting pier and contraction scour was developed. The four levels of this approach are listed below in order of complexity.

Levels of Pier and Contraction Scour Prediction Methods:

1. Reduction factors for HEC-18 based on Q_u groupings
2. SRICOS Z_{max} calculation
3. SRICOS simulation based on soil property regressions
4. SRICOS simulation based on EFA results for a given site

Levels 1 and 2 can be completed without EFA data, but level 3 needs some surrogate EFA data. In this study, equations based on soil properties were developed to obtain critical shear values and erosion rates that can be used instead of running EFA tests on soils. A best-fit and upper-limit approach to estimating critical shear and erosion rates were developed based on Q_u of the soil only.

Levels 3 and 4 require streamflow for input into SRICOS. In this study, streamflow data needed in the SRICOS modeling either were retrieved from historic data records or estimated.

Historic daily data were disaggregated from daily to hourly intervals using methods outlined in this report. Hourly streamflow data were needed at most sites to provide an accurate description of flood events for the purpose of scour estimation. The estimation techniques are useful for ungaged sites and sites where historic hourly data are needed, but not available.

The sources of uncertainty in applying the methods of this study include uncertainty of scour measurements, a statistically small data set, non-homogeneous nature of soils that may introduce error into estimated soil properties, uncertainty of hydraulic models, and uncertainty associated with flow data. Attention should be given to the specific site characteristics used in this study to determine whether the methods presented are applicable to a given site for prediction of pier and contraction scour.

An automated tool or program would be a useful addition to the streamflow estimation process in the future. Also, real-time or continuous monitoring of scour at bridges throughout Illinois, coupled with SRICOS-EFA modeling, would be useful to expand the data set and further verify the results of this study.

REFERENCES

Benedict, S. T., *Clear-water abutment and contraction scour in the Coastal Plain and Piedmont Provinces of South Carolina, 1996–99*, Water-Resources Investigations Report 03–4064, U.S. Geological Survey, Reston, VA, 2003, 137 p.

Brandimarte, L., A. Montanari, J.-L. Briaud, and P. D'Odorico, "Stochastic flow analysis for predicting scour of cohesive soils," *Journal of Hydraulic Engineering*, Vol. 132, No. 5, May 2006, pp.

Briaud, J., Ting, F., Chen, H.C., Gudavilli, R., Kwak, K., Philogene, B., Han, S., Perugu, S., Wei, G., Nurtjahyo, P., Cao, Y., and Li, Y., SRICOS: Prediction of scour rate at bridge piers, The Texas A&M University System TX-00/2937-1, 1999, pp. 1-126.

Briaud, J.-L., Ting, F.C.K., Chen, H.C., Gudavalli, S.R., and Kwak, K., 2002, Maximum scour depth around a bridge pier in sand and in clay: Are they equal? In: *Proceedings of the International Deep Foundations Congress*, Orlando, FL, pp. 385-395.

Briaud, J.-L., H.-C. Chen, L. P. Nurtjahyo, and J. Wang, *Complex pier scour and contraction scour in cohesive soils*, NCHRP Report 24-15, National Cooperative Highway Research Program, National Research Board National Research Council, Washington, D.C., 2003, 266 p.

Briaud, J.-L., H.-C. Chen, L. P. Nurtjahyo, and J. Wang, "The SRICOS-EFA method for complex fine grained soils," *Journal of Geotechnical and Geoenvironmental Engineering*, Vol. 130, No. 11, 2004, pp. 1180-1191.

Briaud, J.-L. and H.-C., Chen, "The EFA, erosion function apparatus: an overview," *Proceedings of the International Conference on Soil Mechanics and Geotechnical Engineering*, Osaka, Japan, September 2005, pp.

Ghelardi, V. M., Estimation of long term bridge scour in cohesive soils at Maryland bridges using EFA/SRICOS, Master Thesis, University of Maryland, College Park, MD, 2004, 76 p.

Kwak, K., J.-L. Briaud, and H.-C. Chen, "SRICOS: Computer Program for Bridge Pier Scour," *Proceedings of the 15th International Conference on Soil Mechanics and Geotechnical Engineering*, A.A. Balkema Publishers, Rotterdam, The Netherlands, 2001, Vol. 3, pp. 2235-2238.

Moody, L.F., Friction factors for pipe flow: *Transaction of the American Society of Mechanical Engineers*, v. 66, 1944, pp. 671-684.

Richardson, E.V. and S. R. Davis, *Evaluating Scour at Bridges*, Hydraulic Engineering Circular No. 18, Fourth Edition, FHWA NHI 01-001, Federal Highway Administration, U.S. Department of Transportation, Washington, DC, 2001, 380 p.

Texas A&M University, *SRICOS-EFA (Scour Rate In Cohesive Soils-Erosion Function Apparatus) Method program*, *Version 1.02*, College Station, TX, July 17, 2001, Patent No. US6260409B1.

U.S. Army Corps of Engineers, *HEC-RAS River Analysis System, Hydraulic Reference Manual – Version 4.0*, Hydrologic Engineering Center, Davis, CA, 2008, various chapters plus appendices.

U.S. Geological Survey, *User's Manual for the National Water Information System of the U.S. Geological Survey: Automated Data Processing System (ADAPS)*, Open-File Report 03–123, U.S. Geological Survey, Reston, VA, 2003, 413 p.

APPENDIX A – ESTIMATION OF STREAMFLOW

ABBREVIATIONS, ACRONYMS, AND SYMBOLS

A	tri-diagonal matrix relating daily streamflow y_i and adjusted daily streamflow y'_i
A	drainage area
a	parameter in the plotting position formula lying in the range $0 \le a \le 1$.
a(*x*)	an arbitrary smooth function of *x*, pre-factor drainage area *A* in $q(x) = a(x)A^{b(x)}$
b	vector containing sequence of observed daily streamflow values y_i
b(*x*)	arbitrary smooth function of *x*, exponent of drainage area *A* in $q(x) = a(x)A^{b(x)}$
CPI	Current Precipitation Index
FDC	Flow Duration Curve
ft^3/s	cubic feet per second
IDL	Interactive Data Language
K	parameter of the CPI equation
m	subscript representing the month
mm	millimeters
n	number of days in a streamflow record
NWS	National Weather Service
p	exceedance probability or percentile
P	daily precipitation
POR	period of record
Q	daily discharge
q(*p*)	discharge quantile having exceedance probability *p*
q(*p*(*t*))	flow value quantile *q* for a given exceedance probability *p* on day *t*
$q'_{i+j/24}$	disaggregated hourly discharge on hour *j* on day *i*
q(*x*)	streamflow or streamflow statistic
QPPQ	quantile-probability-probability-quantile
RMSE	root mean square error
t_i	time, day *i*
V_i	volume of flow on day *i*
x	an arbitrary real-valued variable
x	vector containing sequence of adjusted daily streamflow values y'_i
Y(*t*)	function of time generated by linearly interpolating between y'_i values
y_i	daily streamflow value on day *i*
y'_i	adjusted daily streamflow value on day *i*

A.1 DAILY-TO-HOURLY DISAGGREGATION OF STREAMFLOW DATA

A.1.1 Existing techniques for disaggregation of streamflow data

Many techniques to address disaggregation of streamflow have been developed (see, for example, Salas 1993 and references therein). These techniques were mostly developed in the context of stochastic streamflow simulation, where it was found that streamflow simulated at an annual time step was not consistent with streamflow simulated at a monthly time step (i.e., the probability distribution of the sum of simulated monthly streamflows in a year would differ from the distribution of the simulated annual time streamflows). This class of techniques usually requires assumptions about the probability distribution of streamflow values (most such methods were originally developed for normally distributed flows) followed by adjustments to obtain a different distribution, and in the end they provide stochastic flow values at the finer time scale rather than a unique set of non-random values. These properties make such methods inappropriate for the present problem.

A simple method to compute a unique, non-random set of disaggregated rainfall values was presented by Ormsbee (1989) using a linear interpolation process (see also Hingray and Ben Haha, 2005). This method has several desirable properties: (a) it is deterministic and thus requires no assumptions about the probability distribution of the streamflow and provides a unique set of disaggregated values; (b) it is conservative (the total discharge at the disaggregated time scale is equal to the discharge at the original time scale); (c) it is simple and computationally efficient; (d) it has no free parameters to be estimated; (e) the minima and maxima of the disaggregated values are more extreme than those of the original series, as is observed in both precipitation and streamflow processes; and (f) the disaggregated values are non-negative. One particular potential drawback of this method, in the context of rainfall disaggregation, is that no intermittency (periods of zero rain rate) is introduced at the disaggregated time scale. Normally, this is not a major concern in streamflow disaggregation context (days with zero flow would be preserved, but no periods of zero flow would be introduced on days with positive daily streamflow). The Ormsbee (1989) method was investigated for use in this project because of its apparent appropriateness to the problem of disaggregation of daily streamflow data, but it was discovered that the disaggregated process has discontinuities at the beginning and end of each day (Figure A.1a).

A.1.2 A New Streamflow Disaggregation Technique

To overcome the discontinuity problem with the Ormsbee (1989) method, an alternative conservative linear interpolation disaggregation method was developed (Figure A.1, panels B and C). It provides path-wise continuous disaggregated values and retains all the desirable properties of the Ormsbee method except (a) it requires somewhat more computational capacity than the original method, since a set of linear equations must be solved, but very long daily time series can be quickly disaggregated using sparse matrix techniques; and (b) under certain circumstances (usually when a large day-to-day change in streamflow is encountered), negative hourly streamflow values may result. This second drawback is addressed by setting the negative values to zero and slightly adjusting the rest of the values in the series to retain conservation of discharge, though a more elegant correction method may be possible.

A generalized form of the method in which the daily values of streamflow are raised to some positive power different than one before disaggregation and the disaggregated values are back-transformed and adjusted to obtain conservation also was developed (Figure A.1d) and is used herein for certain records. This generalized form, which results in convex hydrographs for exponents between zero and one or concave hydrographs for exponents greater than one, was found to be useful in the case of “flashy” records where the peaks are under-estimated for the linear case. In this case, it is desirable to set the exponent to a value less than one so that the

peaks will be increased. The optimal value of the exponent can be obtained by calibration against the observed hourly record, if any, and the set of historical peaks.

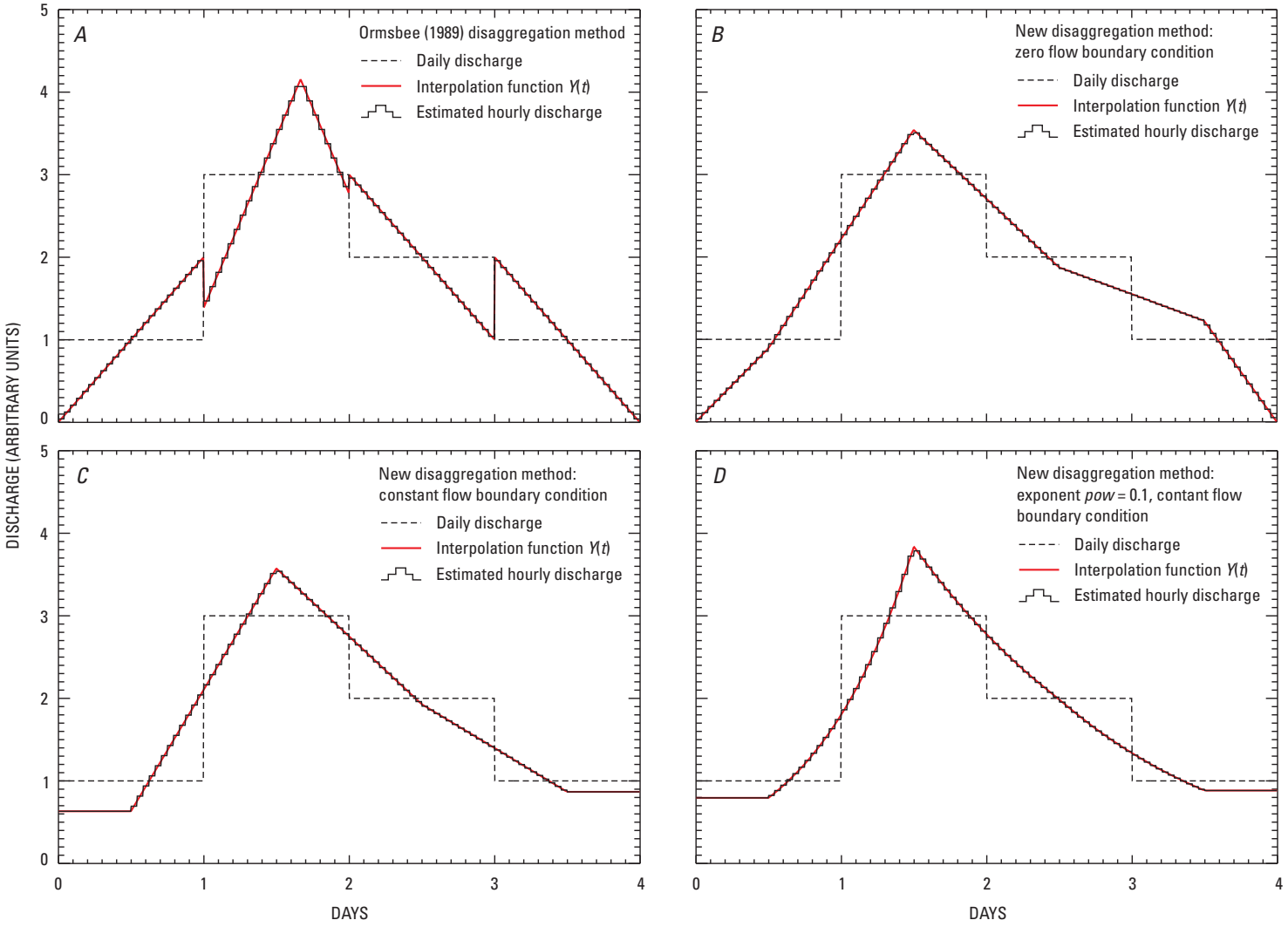

Figure A.1. Daily-to-hourly streamflow disaggregation examples: (a) Ormsbee (1989) method, (b) new method with zero flow boundary condition, (c) new method with constant flow boundary condition, and (d) new method using power-law transform with exponent *pow* = 0.1.

A.1.2.1 Details of the method

Let $y_i, i = 1,2,\ldots,n$ denote the daily mean streamflow value on day *i*, which is assumed to occur over the time interval between t_{i-1} and t_i, and choose time units (here, days) so that without loss of generality, $t_i - t_{i-1} = 1$. The method proceeds by solving for a new set of *y* values, denoted by $y'_i, i = 1,2,\ldots,n$, that apply at noon each day, i.e., at time $t_{i-1/2}$, such that the integral under the continuous function *Y*(*t*) defined by a set of straight line segments connecting the y'_i values preserves the original daily volume V_i (notice $V_i = y_i$ because $t_i - t_{i-1} = 1$ by assumption).

Mathematically, on day *i*, $1 < i < n$, that is, except at the beginning and end of the series, *Y*(*t*) as defined above is given by

$$Y(t) = (y'_i - y'_{i-1})(t - t_{i-1-1/2}) + y'_{i-1} \text{ for } t_{i-1} < t < t_{i-1/2} \quad \text{(A.1)}$$

(i.e., for the first half of the day) and by

$$Y(t) = (y'_{i+1} - y'_i)(t - t_{i-1/2}) + y'_i \text{ for } t_{i-1/2} < t < t_i \quad \text{(A.2)}$$

(i.e., for second half of the day). Using equations (A.1) and (A.2) then the values of *Y*(*t*) at the beginning, middle, and end of the day are

$$Y(t_{i-1}) = (1/2)(y'_i + y'_{i-1}), \quad \text{(A.3a)}$$

$$Y(t_{i-1/2}) = y'_i, \quad \text{(A.3b)}$$

and

$$Y(t_i) = (1/2)(y'_i + y'_{i+1}). \quad \text{(A.3c)}$$

For *Y*(*t*) defined by straight lines from $t = t_{i-1}$ to $t = t_{i-1/2}$ and from $t = t_{i-1/2}$ to $t = t_i$, V_i, the volume of flow on day *i*, i.e., the integral under *Y*(*t*) from t_{i-1} to t_i, is given by

$$V_i = y_i = \frac{1}{2}\left\{\frac{1}{2}\left[Y(t_{i-1}) + Y(t_{i-1/2})\right] + \frac{1}{2}\left[Y(t_{i-1/2}) + Y(t_i)\right]\right\} = \frac{1}{4}Y(t_{i-1}) + \frac{1}{2}Y(t_{i-1/2}) + \frac{1}{4}Y(t_i). \quad \text{(A.4)}$$

Plugging the values of *Y*(*t*) from equations (A.3) above into equation (A.4) then gives

$$y_i = \frac{1}{4}\left[\frac{1}{2}(y'_i + y'_{i-1})\right] + \frac{1}{2}y'_i + \frac{1}{4}\left[\frac{1}{2}(y'_i + y'_{i+1})\right] = \frac{1}{8}y'_{i-1} + \frac{3}{4}y'_i + \frac{1}{8}y'_{i+1}. \quad \text{(A.5)}$$

Equation (A.5) gives the basic equation expressing the adjusted daily flow values y'_i in terms of the original daily flow values y_i in the interior of a sequence of positive flow values. The definition of the boundary conditions is presented below.

For positive values at the beginning and end of the daily time series and unknown values before and after the series, a constant discharge boundary condition is assumed. At the beginning of the series, this boundary condition is expressed by assuming that *Y*(*t*) takes the value $Y(t) = y'_1$ on the first half of the first day, i.e., for $0 < t < 1/2$, then

$$V_1 = y_1 = \frac{7}{8}y'_1 + \frac{1}{8}y'_2, \quad \text{(A.6)}$$

and similarly, if $Y(t) = y'_n$ during the second half of the last day of the sequence, for $t_{n-1/2} < t < t_n$, then

$$V_n = y_n = \frac{1}{8}y'_{n-1} + \frac{7}{8}y'_n. \quad \text{(A.7)}$$

Using equations (A.5) to (A.7), for this boundary condition, the system of linear equations that needs to be solved in order to find the values of $y_i, i = 1,2,\ldots,n$, for example for $n = 4$, can then be written as

$$\begin{bmatrix} y_1 \\ y_2 \\ y_3 \\ y_4 \end{bmatrix} = \begin{bmatrix} 7/8 & 1/8 & & \\ 1/8 & 3/4 & 1/8 & \\ & 1/8 & 3/4 & 1/8 \\ & & 1/8 & 7/8 \end{bmatrix} \begin{bmatrix} y'_1 \\ y'_2 \\ y'_3 \\ y'_4 \end{bmatrix} \text{ or } \mathbf{b} = \mathbf{Ax}, \qquad \text{(A.8)}$$

where $\mathbf{b} = \begin{bmatrix} y_1 \\ y_2 \\ y_3 \\ y_4 \end{bmatrix}$, $\mathbf{A} = \begin{bmatrix} 7/8 & 1/8 & & \\ 1/8 & 3/4 & 1/8 & \\ & 1/8 & 3/4 & 1/8 \\ & & 1/8 & 7/8 \end{bmatrix}$, and $\mathbf{x} = \begin{bmatrix} y'_1 \\ y'_2 \\ y'_3 \\ y'_4 \end{bmatrix}$.

Equation (A.8) is then generalized to larger values of *n*. The same system of equations applies for $n = 2$ and $n = 3$, keeping the y_1 and y_n equations as in equation (A.8).

Another boundary condition is needed if a sequence of positive daily flow values is preceded or followed by a zero daily value. In this case, it is necessary to modify the basic relation given by equation (A.5) in order that all the disaggregated flow values on the day with zero flow may be assigned zero flow without violating conservation of mass. This situation must be treated as a boundary condition in which flow is assumed to vanish at the boundaries of the positive sequence, i.e., at time $t = t_0$ for a positive sequence beginning on day 1 or at time $t = t_n$ for a positive sequence ending on day *n*. For the beginning of the positive sequence, it can be shown that the applicable equation relating y_1 and the y' values is $y_1 = \frac{5}{8}y'_1 + \frac{1}{8}y'_2$, and at the end, $y_n = \frac{1}{8}y'_{n-1} + \frac{5}{8}y'_n$. Thus, if the 4-day system given in equation (A.8) were bounded on both sides by zeroes, the system of equations would become:

$$\begin{bmatrix} y_1 \\ y_2 \\ y_3 \\ y_4 \end{bmatrix} = \begin{bmatrix} 5/8 & 1/8 & & \\ 1/8 & 3/4 & 1/8 & \\ & 1/8 & 3/4 & 1/8 \\ & & 1/8 & 5/8 \end{bmatrix} \begin{bmatrix} y'_1 \\ y'_2 \\ y'_3 \\ y'_4 \end{bmatrix}. \qquad \text{(A.9)}$$

To observe the effect of these two boundary conditions on disaggregation results, compare Figure A.1B and A.1C.

The case of *n* = 1 remains. Selecting the constant flow boundary condition (applicable when the flows on the days before and after are unknown) results in the solution $y' = y = Y(t)$, and no sub-daily flow variation occurs. Having no sub-daily flow variation seems unsatisfactory, but it is hard to imagine a practical situation when a single day would need to be disaggregated, except when the zero flow boundary condition applies (i.e., a single positive day preceded and followed by zero days). In that case, the solution is $y' = 2y$, and the resulting *Y*(*t*) function is a triangle beginning and ending at zero and having a discharge of $y' = 2y$ at noon.

A.1.2.2 Solution of the linear system ***b*** = ***Ax***

For a sequence of daily values a few decades long, the system of equations (A.8) or (A.9), in particular the matrix **A,** becomes quite large. However, **A** is sparse, having at most three non-zero entries per row centered on the diagonal (a tri-diagonal matrix). Thus, sparse matrix methods can be expected to be quite effective and were implemented to solve these systems. In particular, the LINBCG routine provided in the Interactive Data Language (IDL) version 6.3 distribution (RSI 2006), which is based on the LINBCG routine given in section 2.7 of Press et al. (1992) and solves a sparse system of linear equations using the iterative bi-conjugate gradient method, was used.

A.1.2.3 Obtaining the Disaggregated Flow Values

Once the y' values that define the continuous piece-wise linear function $Y(t)$ are computed, the disaggregated streamflow estimates are computed by averaging over the desired intervals under $Y(t)$. For hourly discharges obtained from daily, these are computed as

$$q'_{i+j/24} = \frac{1}{2}\left[Y\left(t_{i-1+(j-1)/24}\right) + Y\left(t_{i-1+j/24}\right)\right],\ j = 1,2,\ldots,24 \qquad \text{(A.10)}$$

where $q'_{i+j/24}$ is the disaggregated average hourly discharge for hour j on day i. Recall that the computation of the y' values that define the function $Y(t)$ did not depend on the time step of the disaggregated data. The disaggregation time step enters only in this final step of computing the disaggregated values q' from the $Y(t)$ function. Thus, this method could be used to obtain streamflow estimates at any sub-daily time scale.

A.2 FLOW-DURATION CURVES

Most of the methods for extending or transferring daily streamflow used here and described in the next two sub-sections make use of the characteristics of a streamflow record as indicated by its flow-duration curve (FDC). This is shown as a plot of stream discharge as a function of its cumulative probability of occurrence. By tradition, in the construction of FDCs the cumulative probability is expressed in terms of the exceedance probability rather than the cumulative non-exceedance probability, which is standard in probability and statistics. Mathematically, if Q is a random variable representing the daily mean streamflow at a certain site, its FDC is the function $q(p)$, where q is some value (called the "quantile") of the daily discharge Q and p is the exceedance probability, i.e., $p = \Pr(Q > q)$, so the quantile $q(p)$ is the streamflow having exceedance probability p.

FDCs were computed from an observed streamflow record by ranking the daily mean streamflow values from smallest to largest and assigning each an exceedance probability. The exceedance probability was computed from the observed record using the plotting position formula

$$p(q_i) = 1 - \frac{i - a}{n + 1 - 2a}, \qquad \text{(A.11)}$$

where $i = 1,2,\ldots,n$ (n is the number of days in the record) is the rank (smallest to largest) of observed daily mean streamflow q_i. As suggested by Helsel and Hirsch (2002), the Cunnane plotting position formula, equation (A.11) with $a = 0.4$, was used. Thus, the FDC was computed by sorting the observed record and applying the plotting position formula, equation (A.11). When there were "ties" on positive values of q, that is, multiple instances of the same positive discharge q, a small random value selected from a uniform distribution on the interval [-0.005, 0.005 ft^3/s] was added. Values of this magnitude will not change the daily streamflow value (which are published with a precision of at most 0.01 ft^3/s) but will enable a unique value of q to be associated with each p value. Multiple values of $q = 0$ were allowed to remain and were treated separately in the methods that follow. Examples of FDCs used in this project are given in Figures A.2c, A.3d, A.4b, and A.5b.

In the context of extending an observed record or estimating the record at an ungaged site, once it is computed or estimated, the utility of the FDC is to provide a flow value quantile q for a given exceedance probability p on day t, i.e., $q(p(t))$. The methods using FDCs described below differ in how the FDC is computed or estimated and how the exceedance probability for a given day is estimated, but they all follow the basic scheme of estimating the FDC then the $p(t)$.

A.3 METHODS OF EXTENDING DAILY STREAMFLOW RECORDS

A.3.1 Method IIA: The QPPQ Method

When a nearby gage record was available that satisfied certain criteria listed below, it was designated as a "base gage" and used to extend the record at a site where additional years of record were needed. The required criteria for a base gage were: (a) the percentile of streamflow on any given day is highly correlated with the percentile of streamflow at the site where the record will be extended at the time scale of interest (here, daily); and (b) its period of record (POR) overlaps with the POR of the record to be extended for several years, including wet and dry years; and its POR also covers the period for which the extended record is needed.

When such a gage was available, the QPPQ method (developed for estimation of flow at ungaged sites by Fennessey, 1994; see also Waldron and Archfield, 2006; Mohamoud, 2008; Archfield et al., 2010) was used to estimate the discharges at the site of interest during the extension period. The QPPQ method makes use of the FDCs of the two gage records during their period of overlapping record. For the QPPQ method, once the FDCs of the observed records at the base gage and at the site needing extension during their overlapping period are computed, they are related by the assumption that the time history of their exceedance probabilities are identical. This assumption can of course be tested during the overlapping period and is the reason why high correlation between the records is a criterion for selecting a base gage. During the record extension period, this assumption is used to estimate the discharge for the record being extended as follows: (a) the observed discharge $q_b(t)$ at the base gage on some day t is related to its exceedance probability $p_b(t)$ by means of its FDC $q_b(p_b)$, which is the meaning of the first two letters ("QP") of the name of the method; (b) the exceedance probability at the gage whose record is being extended is assumed to be identical to $p_b(t)$, i.e., $p(t) = p_b(t)$; and (c) the discharge $q(t)$ at the gage whose record is being extended is computed using its FDC $q(p)$, which is the meaning of the last two letters of the name of the method ("PQ"). Symbolically, the QPPQ method can be expressed as

$$q_b(t) \xrightarrow{q_b(p)} p_b(t) = p(t) \xrightarrow{q(p)} q(t).$$

In step (1), when the $p_b(t)$ value is being computed for a given observed value $q_b(t)$ at the base gage during the extension period, if $q_b(t)$ lies between two observed values in the FDC $q_b(p_b)$, the $p_b(t)$ is computed by linear interpolation between observed values. However, if $q_b(t)$ exceeds the largest or is smaller than the smallest value observed during the overlapping period, the computation is more complicated. In the latter case, because low flows are less important in the present study, interpolation between $(q,p) = (q_{\min}, p_{\max})$ and $(q,p) = (0,1)$ was used. In the former case, because high flows are especially important in the present study, more care was taken. In this case, extrapolation of the trend at the high end of the FDC ratios, i.e., $q(p)/q_b(p)$, was used to obtain a relation between q_b and q at large values of q_b.

This method was applied to extend the records from three gaging stations. The first, station 05531300, is the primary gage for site 1-7, required extension of its record over the period beginning in 1957 and ending in 1989, when the gaging station was established. This extension made use of station 05531500 as the base gage, because it is the nearest gage in terms of drainage area ratio on the same stream that covers the period of record needed. The second, station 05590400, which was operated during 1965-1979 at site 5-17, was extended by this method to cover the period 1980-2007. This extension made use of station 05590800 as the base gage, because it is the only nearby station that covers the period of record needed. The third, station 03378900, the primary gage for site 7-1 and operated from 1965 to 1982, required extension to cover the period from 1983 to 2007. The extension made use of the record from station 03379500 because it is the nearest gage in terms of drainage area ratio on the same stream that covers the period of record needed.

Figure A.2 illustrates the application of this method to the extension of the record at station 05590400. The dotted line in the figure indicates an example computation. On day *t*, the observed discharge at the base gage is about 500 ft^3/s (panel B), which corresponds to a percentile p_t of about 0.10 (solid line, panel C), and a discharge of about 300 ft^3/s on the FDC of the extension gage (dashed line, panel C). So on day *t*, the extension gage is assigned an estimated discharge of 300 ft^3/s (panel D). The scatterplot in panel A illustrates the degree to which the FDC percentiles at the base gage are correlated with the FDC percentiles at the extension gage during the calibration period.

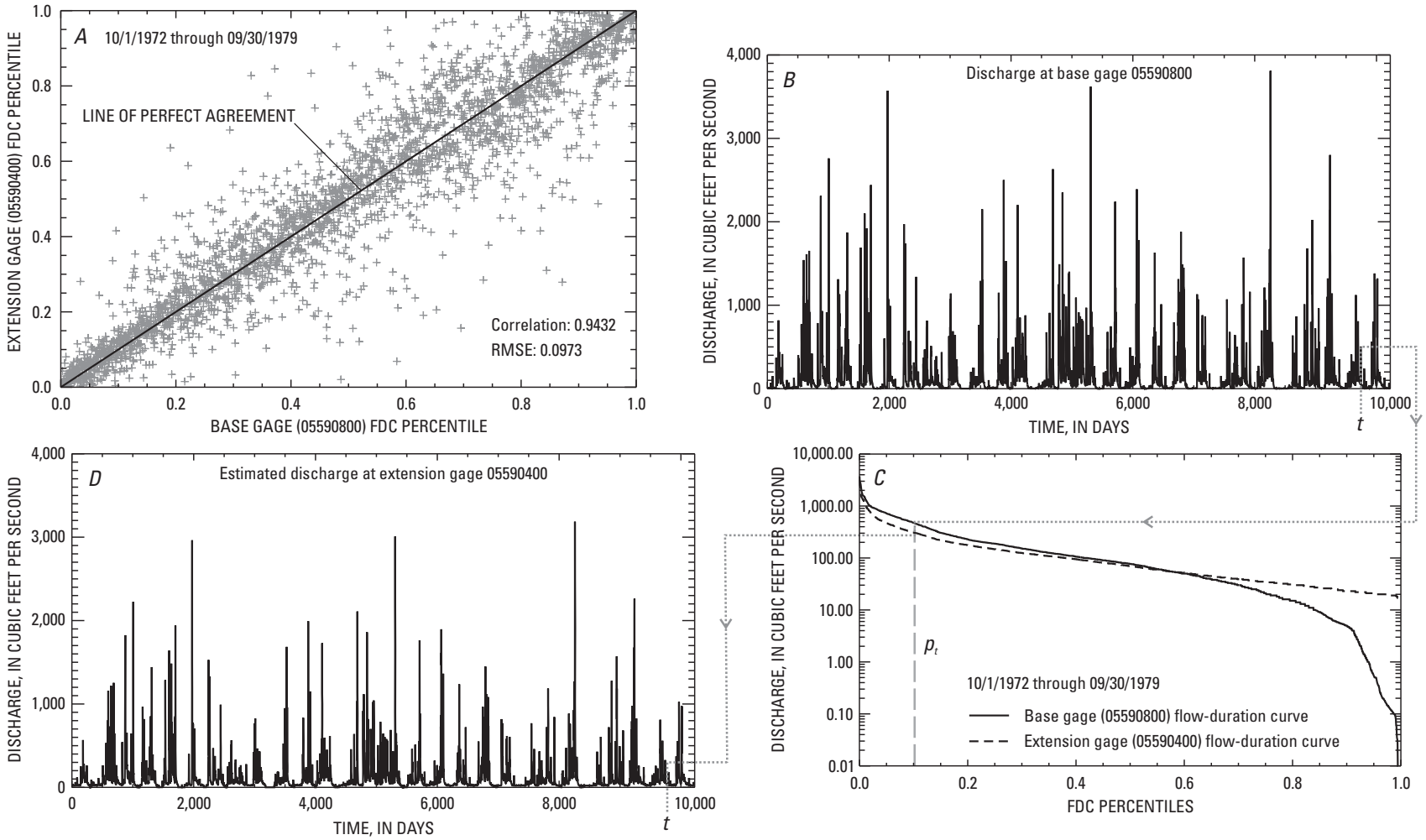

Figure A.2. Illustration of the QPPQ method of streamflow record extension as applied to station 05590400 (Kaskaskia River near Pesotum, Illinois), at scour investigation site 5-17: (a) scatterplot of FDC percentiles for the base gage, station 05590800, and the extension gage, station 05590400, during the calibration period, 10/1/1972 through 9/30/1979; (b) time series of observed discharges at the base gage during the extension period, 10/1/1979 through 9/30/2007; (c) flow-duration curves (FDCs) at the base and extension gages during the calibration period; and (d) time series of estimated discharges at station 05590400 during the extension period.

A.3.2. Method IIB: The QPPQ Method Using a Precipitation Index (QPPQ-CPI)

When no nearby streamgage was available to serve as the base gage in the QPPQ method, the approach of Smakhtin and Masse (2000) was used to essentially synthesize a base gage record, after which the QPPQ method was applied to this synthetic base gage record and the observed record at the gage needing extension. The synthesis is done using daily precipitation totals, which are smoothed or filtered by means of equation (A.12) to create what Smakhtin and Masse called the "current precipitation index" *CPI*. The *CPI* is computed as

$$CPI(t) = \begin{cases} K * CPI(t-1) + P(t) = \sum_{s=0}^{t} K^s P(t-s) \text{ for } t \geq 1 \\ 0 \text{ for } t = 0 \end{cases}, \quad \text{(A.12)}$$

where $P(t)$ is the total precipitation on day t, and K, which lies in the range $0 < K < 1$, is a parameter to be estimated. To avoid effects from the transient caused by the initialization of the CPI computation at $t = 0$, the computation was started 1 year before the beginning of the period for which it was needed.

To implement the QPPQ transform method using the CPI values, the following steps were carried out: (a) The annual CPI duration curve, denoted $CPI(p)$, and monthly CPI duration curve, denoted $CPI_m(p)$, $m = 1,2,\ldots,12$, and the annual and monthly streamflow FDCs of the record being extended, $q(p)$ and $q_m(p)$, during their common POR were computed. Here a "monthly" duration curve (whether based on CPI or streamflow values) includes daily values for days only during a given month m (for all years in the record), while the "annual" duration curve includes all (daily) values regardless of their month of occurrence. (b) Assuming the time histories of exceedance probabilities of the record being extended $p_Q(t)$ and of the CPI duration curve $p_{CPI}(t)$ are identical, the CPI series during the extension period is used to estimate the discharge series during the extension period by the QPPQ method described above. In this case, symbolically, $CPI(t) \xrightarrow{CPI(p)} p_{CPI}(t) = p(t) \xrightarrow{q(p)} q(t)$ when the annual duration curves are used and similarly when the monthly duration curves are used.

Similar to the base gage QPPQ record extension method discussed in section A.3.1, extrapolation of the CPI duration curve was needed when a CPI value at time t, $CPI(t)$, during the extension period, was smaller or larger than any observed during the observation period. For extrapolation of low values, the same approach as described above for the base gage QPPQ method was used, that is, linear interpolation between $(CPI(t), p) = (CPI_{\min}, p_{\max})$ and $(CPI(t), p) = (0,1)$. However, regarding extrapolation on the high end, it was found that the Weibull distribution provided a good fit to the upper tail of the CPI distributions, so a user-guided fit of the Weibull distribution to the tail of the distribution using a least-squares method (see, for example, van Donk et al. 2005) was used to provide estimates of $p_{CPI}(t)$ for very high values of $CPI(t)$ during the extension period.

Carrying out the QPPQ transform estimation of discharge at the site of interest during its POR allows the accuracy of the method to be tested, a determination of whether monthly or annual FDCs were preferable to be made, the best precipitation gage to be selected, and the optimal value of K to be computed (assumed to be the same for each month even in the case of monthly FDCs). In the present application, split-sample testing (calibrating on one part of the observed record and validating on the remaining part) was used to more thoroughly test the method, but when estimating the actual unobserved portion of the record, usually the whole observed period was used for calibration.

This method was tested on all four gage records requiring extension (see Table 2.1: 05531300 near site 1-7, 05590400 at site 5-17, 05590800 at site 5-20, and 03378900 near site 7-1) using one or two nearby daily rain gage records, a range of K values, and both annual and monthly FDCs, but the streamflow-based QPPQ method (Section A.3.1) was found to be more accurate whenever a nearby streamflow record covering the period needed was available. This

result left only gaging station 05590800 to be estimated by this method. It was also found that monthly flow and CPI duration curves were generally preferable. For the application to the record from station 05590800, precipitation data from the Monticello, Illinois, NWS Coop station to extend the record to cover the period from 1957 until 1972 when the gaging station was established. A value of $K = 0.85$ was determined from calibration to the period of observed record, 1972-2007.

Figure A.3 illustrates the application of this method at station 05590800. The dotted line in the figure indicates an example computation for a day *t*. On this day, assumed to be in January, the CPI value computed from the observed precipitation is about 23 mm (panel B), which corresponds to a percentile p_t of about 0.14 (panel C). This percentile corresponds to a discharge of about 300 ft^3/s during January (panel D), so the discharge on day *t* is assigned this value (panel E).

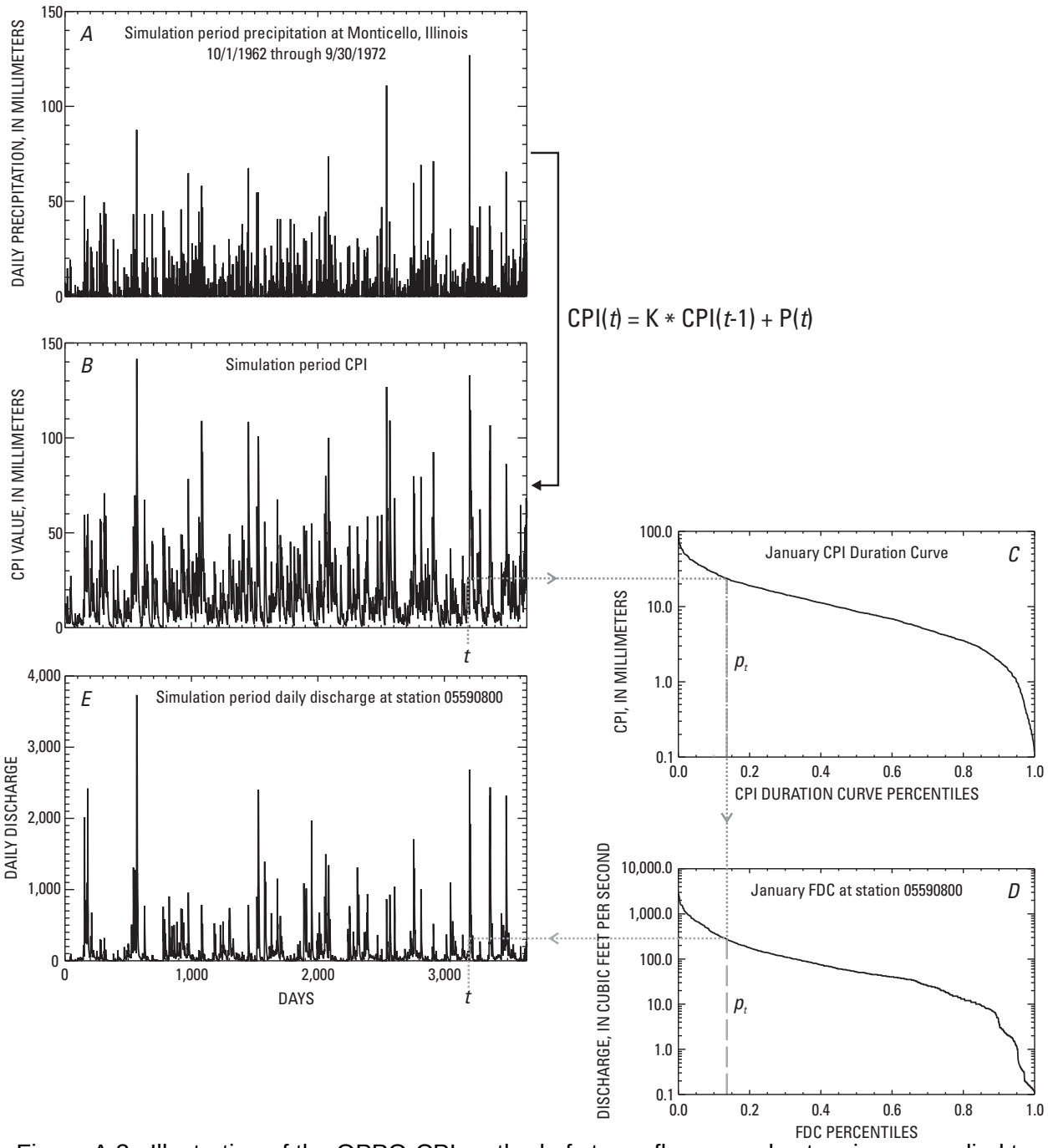

Figure A.3. Illustration of the QPPQ-CPI method of streamflow record extension as applied to station 05590800 (Lake Fork at Atwood, Illinois): (a) daily precipitation at Monticello NWS Coop gage during the simulation period, 10/1/1962 through 9/30/1972; (b) current precipitation index (CPI) computed from daily precipitation at Monticello during the simulation period using K = 0.85; (c) the January CPI duration curve during the calibration period, 10/1/1972 through 9/30/2007; (d) the January discharge FDC at station 05590800 during the calibration period; and (e) simulated daily discharge at station 05590800.

A.3.3 Comments on record extension techniques

The accuracy of either of these methods for extending an observed streamflow record obviously depends strongly on the existence of a representative streamflow or precipitation data sequence. The precipitation-based (CPI) version of this method often appears to be attractive, because of the sparseness of streamflow-gage records relative to daily precipitation-gage records. While it is clear that the process of estimating runoff from precipitation may not be well-modeled using the simple one-parameter equation used to compute the CPI value, it is worth emphasizing that the CPI value does not need to actually model the amount of runoff, only its time-ordering, as the fundamental assumption is that the sequence of the associated exceedance probabilities matches. However, at the sites in this study where record extension was needed, the streamflow-based QPPQ method was found to be more accurate than the CPI-based QPPQ method (as implemented here using a single daily rainfall gage) when a nearby gage (whether on the same stream or not) was available. Therefore only at station 05590800, where the only nearby station, 05590400, did not have a sufficient period-of-record, was the QPPQ-CPI method used. Whether combinations of daily precipitation records or some spatially averaged source of precipitation such as estimates from weather radar might improve the QPPQ-CPI results should be investigated. In the implementation of the CPI method used in this study, daily precipitation records at different gages in or near the watersheds draining to the gage of interest were tested, but no combinations of precipitation gage records or spatially averaged precipitation data were tested.

Methods of record extension that are regression based, such as the suite of maintenance-of-variance-extension (MOVE) methods (see, for example, Hirsch, 1982 and Vogel and Stedinger, 1985) were not considered for use in this study. MOVE methods are designed to preserve the mean and variance of the extended record. In the present case, the upper (high flow) tail of the discharge distribution is of particular concern, so methods that focus on the discharge distribution (the FDC) were considered more appropriate.

A.4 METHODS OF TRANSFERRING GAGE RECORDS

A.4.1 Hydrologic Similarity and its Consequences

All the methods used in this study to estimate the discharge at ungaged sites make use of one or two observed records transformed in some way, i.e., “transferred” to the site of interest. In making the transformation from the gaged site or sites to the ungaged site, all make use of the observation that discharges in a hydrologically similar region often can be estimated using drainage area in a power-law form to parameterize the estimation equation, i.e.,

$$q(x) = a(x)A^{b(x)}, \qquad \text{(A.13)}$$

where A is the drainage area; $q(x)$ is some streamflow statistic such as FDC quantile or discharge on a certain day; x is the parameter specifying which quantile is being considered; and $a(x)$ and $b(x)$ are parameters that are smooth, often monotonic, functions of x. Since drainage area A measures the size or “scale” of a basin, the hydrologic similarity equation is often said to describe the “scaling” properties of streamflow and has been applied most often to peak flows (Gupta and Dawdy, 1995; Gupta and Waymire, 1990; Gupta et al., 2007) and also to annual streamflow (Vogel and Sankarasubramanian, 2000).

The present applications of hydrologic similarity are to daily streamflow estimation by transference of daily streamflow from a neighboring site or sites. The first two methods of transference require three sites, preferably (and as implemented here) all on the same stream, two gaged (one upstream and one downstream) and one ungaged. Let $q_u(t)$, $q_d(t)$, and $q(t)$ denote the discharge records at the these three sites, $q_u(p)$, $q_d(p)$, and $q(p)$ their FDCs, and A_u, A_d, and A their drainage areas. If the hydrologic similarity equation (3) with the same a and b

functions applies at all three locations, then for a given value of $x(t)$ or $x(p)$, $q/q_d = (A/A_d)^b$ and $q_u/q_d = (A_u/A_d)^b$ or, taking logs, $\ln(q/q_d) = b\ln(A/A_d)$ and $\ln(q_u/q_d) = b\ln(A_u/A_d)$. Dividing these last two equations gives

$$\frac{\ln(q/q_d)}{\ln(q_u/q_d)} = \frac{\ln(A/A_d)}{\ln(A_u/A_d)}. \qquad \text{(A.14a)}$$

Since the only unknown in equation (A.14a) is *q*, the discharge at the ungaged site, equation (A.14a) provides an estimation method for *q* as long as hydrologic similarity (equation (A.13)) holds, without having to know the functions *a*(*x*) and *b*(*x*), which have dropped out, because the observed values at the upstream and downstream sites were used. Solving equation (A.14a) explicitly for *q* gives

$$q = q_d(A/A_d)^s \text{ where } s = \frac{\ln(q_u/q_d)}{\ln(A_u/A_d)} = \frac{\ln q_u - \ln q_d}{\ln A_u - \ln A_d}. \qquad \text{(A.14b)}$$

While the interpretation of *q* differs between the methods, equation (A.14a) or (A.14b) provides the equation of estimation for *q* for the first two record transference methods used herein.

Another view of equations (A.14a) and (A.14b) can be seen by taking logs,

$$\ln q = s\ln(A/A_d) + \ln(q_d) = \frac{\ln q_u - \ln q_d}{\ln A_u - \ln A_d}(\ln A - \ln A_d) + \ln(q_d), \qquad \text{(A.14c)}$$

which shows that $\ln q$ describes a line in $\ln q - \ln A$ space joining (q_d,A_d) and (q_u,A_u), having slope *s* and intercept $\ln q_d - s\ln A_d$. It also shows that $\ln q$ is a weighted average of $\ln q_u$ and $\ln q_d$, which has implications for estimating the extremes of $\ln q$.

A.4.2 Method IIIA: Drainage Area-based Interpolation

When gage records covering the period of interest exist at nearby sites both upstream and downstream from the site of interest, as occurs for sites 1-1 and 1-6, interpolation between those records appears promising, because the two gage records should constrain the range of possible hydrologic behavior at the site of interest. Two types of approaches to drainage area-based interpolation were tested.

A.4.2.1 Interpolation of daily discharge

The most conceptually straightforward approach is to interpolate the daily discharges on day *t* at upstream and downstream stations to estimate the flows at the site of interest. If $q(t)$ is the discharge on day *t* at the site of interest having drainage area *A*, $q_u(t)$ is the discharge on day *t* at the upstream station having drainage area A_u, and $q_d(t)$ is the discharge on day *t* at the downstream station having drainage area A_d, using equation (A.14), $q(t)$ can be estimated by this method as:

$$q(t) = q_d(t)(A/A_d)^{s(t)}, \text{ where } s(t) = \frac{\ln(q_d(t)/q_u(t))}{\ln(A_d/A_u)}. \qquad \text{(A.15)}$$

In this case, the hydrologic similarity assumption leads to a line in $\ln q - \ln A$ space connecting ($q_d(t)$,A_d) and ($q_u(t)$,A_u), having a different slope and intercept each day, and using that to estimate $q(t)$ at its drainage area *A*. This method is not ideal, as the averaging of $q_u(t)$ and $q_d(t)$ involved in the computation of $q(t)$ by this method reduces its extremes because the extremes of $q_u(t)$ and $q_d(t)$ are not perfectly synchronized.

A.4.2.2. Interpolation of FDCs

A second approach to interpolation is to assume that it is not the daily discharges but instead the FDCs $q(p)$, $q_u(p)$, and $q_d(p)$ that are linearly related in $\ln q - \ln A$ space. In this case, equation (A.14) becomes

$$q(p) = q_d(p)(A/A_d)^{s(p)}, \text{ where } s(p) = \frac{\ln(q_d(p)/q_u(p))}{\log(A_d/A_u)}. \qquad \text{(A.16)}$$

An additional assumption is needed with this approach, since $q(p)$ in equation (A.16) only gives the FDC at the site of interest, not the discharge on day t. Two methods were tested to provide this additional piece of information. One is to use the FDC exceedance probabilities at the upstream and downstream sites on day t, $p_u(t)$ and $p_d(t)$. Since $p_u(t)$ and $p_d(t)$ are not generally the same, it is necessary to combine their values in some way to estimate an exceedance probability at the site of interest, $p(t)$. The method used herein was again a drainage area interpolation method, assuming a linear relation between p and log$A$. In this case, the estimating equation is given by

$$p(t) = s_p(t)\ln(A/A_d) + p_d(t), \text{ where } s_p(t) = \frac{p_d(t) - p_u(t)}{\ln(A_d/A_u)}. \qquad \text{(A.17)}$$

Equation (A.14) shows that this value of $p(t)$ is a weighted average of the upstream and downstream values $p_u(t)$ and $p_d(t)$. The result of this averaging is that $p(t)$ is less likely to take on extreme values near 0 and 1. To overcome this effect, the value of $p(t)$ computed using equation (A.17) was treated only as an ordering, not the actual exceedance probability value, and the largest value of $p(t)$ was mapped to the largest exceedance probability associated with the estimated FDC, the second largest to the second largest and so on, giving a new exceedance probability series, say $p'(t)$. Given this exceedance probability value $p'(t)$ obtained from $p_u(t)$ and $p_d(t)$ by the previously described method, the daily discharge q(t) at the ungaged site is computed in this method using equation (A.16) as $q(p'(t))$.

The other assumption tested for finding the appropriate $p(t)$ for use in estimating $q(t)$ by using interpolated FDCs was to go back to the daily interpolation method given by equation (A.15); use it to estimate a set of "provisional" discharges at the site of interest, now denoted by $q'(t)$; and compute a FDC for those discharges, denoted by $q'(p)$. Then the interpolated daily discharges were used to obtain a $p(t)$ value, i.e., the $q'(t)$ on a given day was used, through its FDC $q'(p)$, to obtain a $p(t)$ value, which then was used with the interpolated FDC $q(p)$, obtained using equation (A.16), to obtain a discharge value on that day as $q(p(q'(t)))$.

This last method, where the distribution of discharge values comes from the interpolated FDC, but the $p(t)$ value and hence the order in which they are used comes from the interpolated discharges, was found to be the most accurate when tested on trios of observed gage records; thus it was the method of interpolation used also at the ungaged sites where interpolation was appropriate (sites 1-1 and 1-6).

Figure A.4 illustrates the application of this method for estimation of streamflow at site 1-1. Panels A1 and A2 are the hydrographs at the gaging stations upstream and downstream from the site 1-1 for an example period (10/1/1985 through 9/10/1988). Panel B shows the FDCs that are used in the computation. The lowest and upper-most FDCs are those from the upstream and downstream gaging stations, respectively. Interpolation between these using drainage area ratios (equation A.16) gives the interpolated FDC (solid red line). The FDC computed from the daily discharges interpolated by drainage area ratios (equation A.15) is given by the dash-dot line. Panel C shows the resulting estimated hydrograph at site 1-1. The dotted gray line in the figure indicates an example computation for one day. The discharges at the upstream and downstream gages on day t are combined using interpolation (equation A.15) to obtain an estimated value of about 5,200 ft^3/s, which is found on the interpolated daily

discharge FDC (dot-dash line in panel B) to find the corresponding percentile p_t of about 0.001. Moving vertically at this percentile from the dot-dash FDC to the solid red FDC in panel B gives an interpolated FDC discharge of about 6,800 ft^3/s, and the estimated discharge at site 1-1 is given this value on day *t* (panel C).

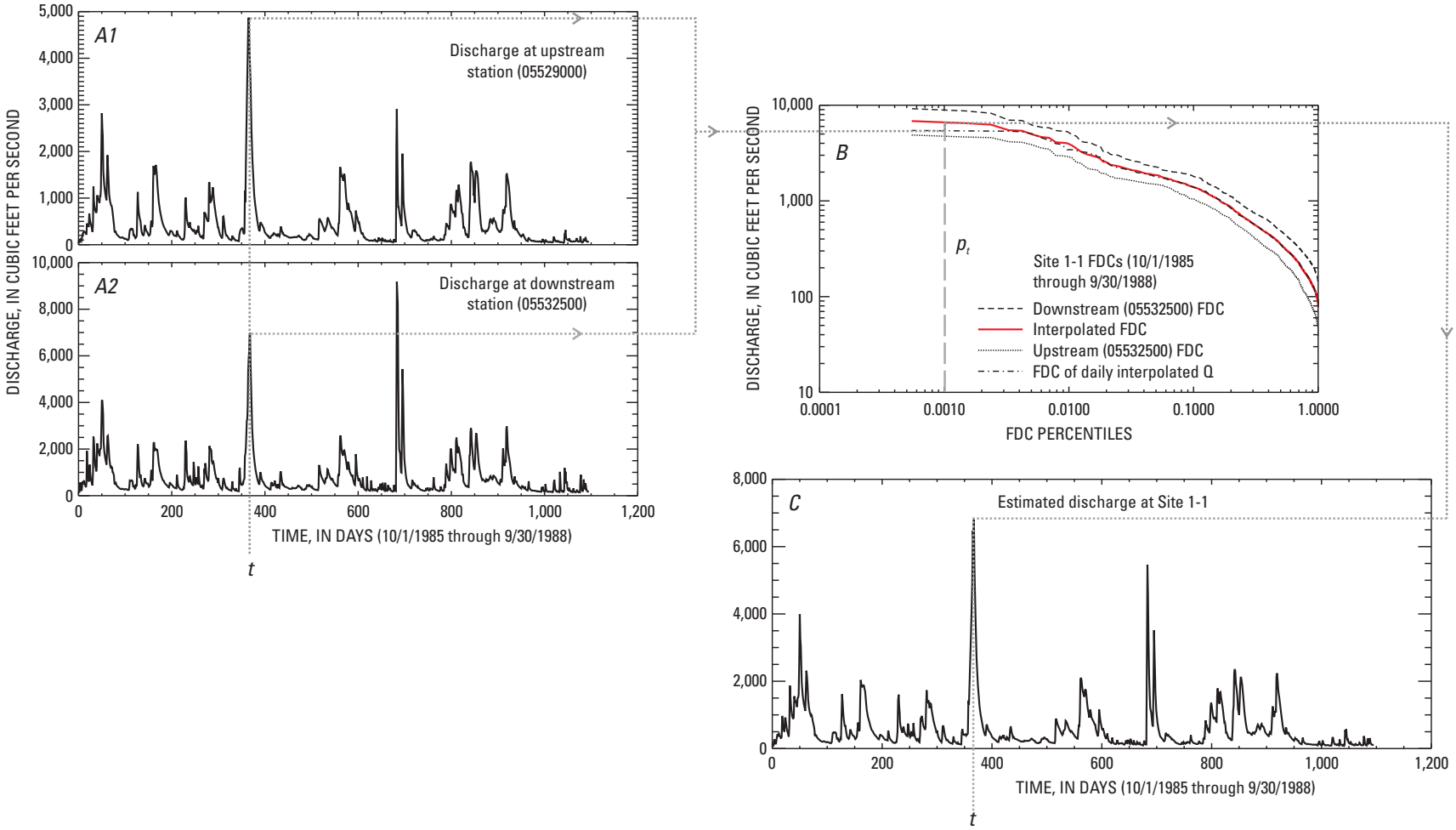

Figure A.4. Illustration of the drainage area-based interpolation method of streamflow transfer as applied at scour investigation site 1-1 from 10/1/1985 through 9/30/1988: (a) daily streamflow time series at the upstream (station 05529000, A1) and downstream (station 05532500, A2) gaging stations; (b) flow duration curves (FDCs) at upstream and downstream stations using observed data, estimated using drainage area-based interpolation of upstream and downstream FDCs at site 1-1, and estimated using drainage area-based interpolation of daily upstream and downstream discharges at site 1-1; and (c) estimated discharge time series at site 1-1.

A.4.3 Method IIIB: Constrained Drainage Area-based Extrapolation

When a pair of gages with streamflow records exists near an ungaged site of interest, all three on the same stream, but both gages are upstream or downstream from the site of interest, interpolation is not an option. If the distance between the gages and the ungaged site is small (measured by drainage-area ratio; as applied here the drainage area at the ungaged site is within 95% of the drainage area at the upstream streamflow gage), and no major hydrologic controls occur in between, then estimation based on extrapolation of the relation between the observed gage records should be relatively accurate. The general form of the estimating equation is the same as in Method IIIA above, i.e., equation (A.14), but the details, as implemented here, are slightly different. At the two sites where this method was implemented, sites 1-7 and 7-1 (see Table 2.1 and Figure A.5), the record at the “primary” gage nearer the scour investigation site, in this case a short distance downstream, also had to be extended. This extension was carried by the QPPQ method (Method IIA), based on the gage which was somewhat further downstream. In the QPPQ method, the time sequence of *p* (percentile) values is provided by the base gage, so this choice was continued for the extrapolation for the sake of consistency with the extended record at the primary gage. Only one gage record is involved in this choice of *p* sequence, so it does not suffer from the averaging issues that arose in some of the choices tested in the discussion of interpolation methods above.

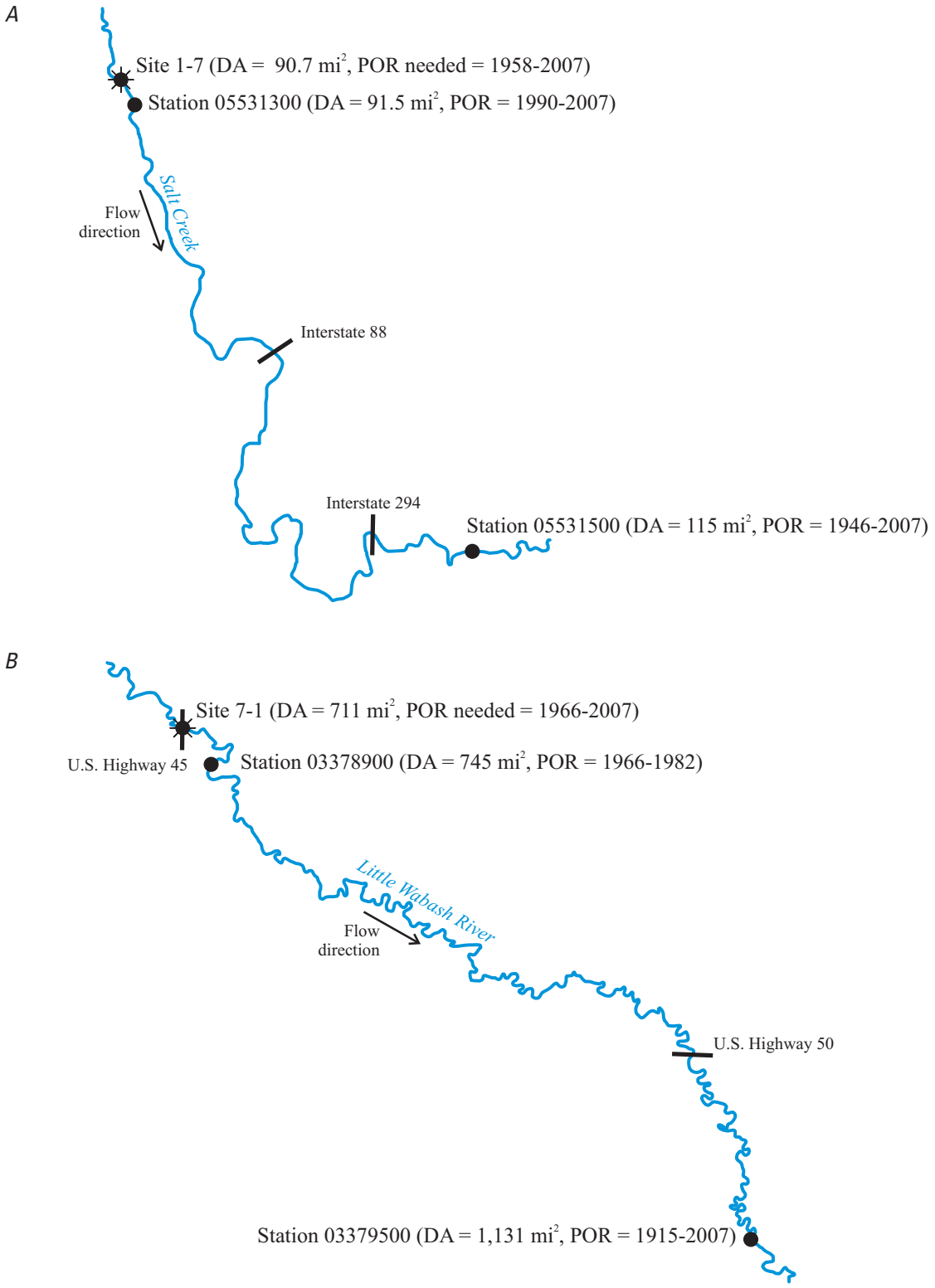

Figure A.5. Configuration of scour investigation sites and streamflow gaging stations used to estimate daily stream at the site when using estimation method IIB (Constrained Drainage Area-based Extrapolation): (a) site 1-7; (b) site 7-1. [DA: drainage area; POR: period-of-record.]

The steps to implement constrained drainage area-based extrapolation in this case are as follows:

(a) Define the downstream observed discharge record as the base gage $q_b(t)$, the upstream partly observed, partly extended discharge record as the extension gage $q_e(t)$, and the unobserved record at the site interest as $q(t)$.

(b) Form the FDCs at the base and partly extended gages $q_b(p)$ and $q_e(p)$ using the POR for which the record at the ungaged site is needed.

(c) Apply equation (A.14b) to estimate the FDC $q(p)$ at the site of interest, i.e., $q(p) = q_b(p)(A/A_b)^s$ where $s = \frac{\ln(q_e(p)/q_b(p))}{\ln(A_e/A_b)}$.

(d) Use the QPPQ method to estimate the daily flows $q(t)$ at the site of interest, starting with the flows at the base gage, $q_b(t)$, from which the sequence of exceedance probabilities $p_b(t)$ were obtained, with extrapolation, as needed, carried in the manner described in the QPPQ method discussion above. The sequence of probabilities at the site of interest $p(t)$ are taken as equal to $p_b(t)$, and from $p(t)$ are obtained the daily flows $q(t)$ via the FDC $q(p)$. Symbolically, as in the original QPPQ method above, this process can be expressed as $q_b(t) \xrightarrow{q_b(p)} p_b(t) = p(t) \xrightarrow{q(p)} q(t)$.

Figure A.6. illustrates the application of this method to estimation of streamflow at site 7-1. The dotted line in the figure indicates an example computation. The base gage discharge on day *t* is about 1,800 ft^3/s (panel A). This corresponds to a percentile p_t of about 0.17 (dashed line in panel B) and an estimated discharge of about 800 ft^3/s for an extrapolated site with a drainage area of 711 mi^2 (solid line in panel B), which is the drainage area at site 7-1. Therefore, the estimated discharge at site 7-1 on day *t* is assigned the value 800 ft^3/s (panel C).

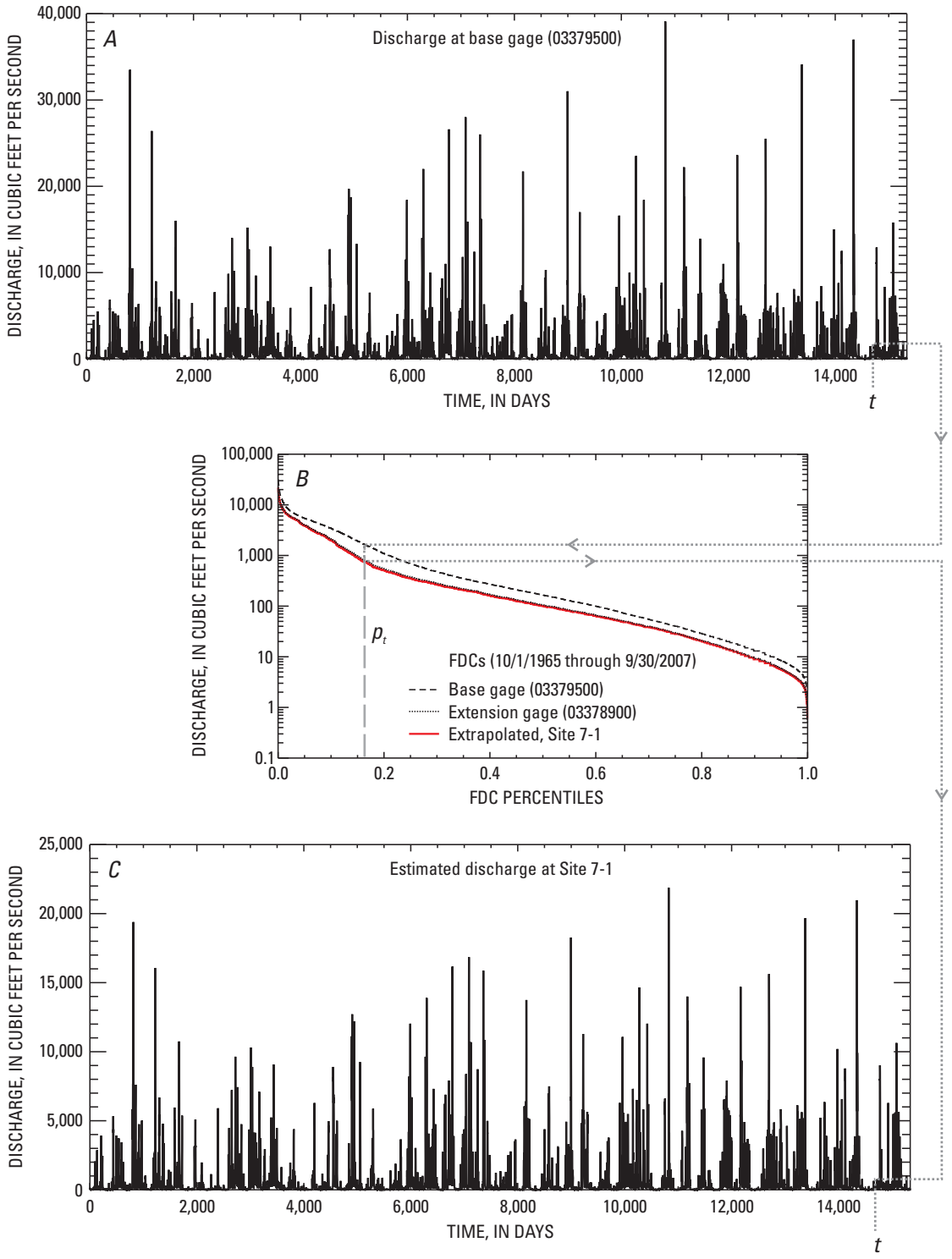

Figure A.6. Illustration of constrained drainage area-based extrapolation method of streamflow transfer as applied at scour investigation site 7-1 from 10/1/1965 through 9/30/2007: (a) observed discharge time series at the base gage, station 03379500; (b) flow-duration curves at the base gage (using observed data), at the extension gage, 03378900 (using partly observed and partly estimated data), and estimated at site 7-1; and (c) estimated discharge time series at site 7-1.

A.4.4 Method IIIC: Estimation by Drainage-area Ratio Method

In the absence of any gage record at the site of interest, any nearby records on the same stream, or a regional FDC study to provide FDC estimates at ungaged sites, the usual option short of development of a full rainfall-runoff model (which also will have significant uncertainty because of the lack of calibration data) is to find a nearby record on another stream draining a watershed deemed to be hydrologically similar (which could be considered as a type of "base gage") and re-scale this observed record using the ratio of the drainage areas (see for example, Hirsch, 1979; Koltun and Roberts, 1990; Ries and Friesz, 2000; Perry et al., 2004; Emerson et al., 2005; Hortness, 2006; Mohamoud, 2008). Mathematically, this method can be expressed as $Q(t) = (A/A_b)Q_b(t)$, where $Q(t)$ is the estimated discharge on day t at the site of interest, A is the drainage area at the site of interest, $Q_b(t)$ is the observed discharge at the base gage, and A_b is the drainage area at the base gage. Clearly, this method involves the greatest assumptions of any of the methods used here, so it also has the largest uncertainty associated with it. This method was used to estimate the daily record at site 3-25 for the complete period of interest.

REFERENCES TO APPENDIX A

Archfield, S., R. Vogel, P. Steeves, S. Brandt, P. Weiskel, and S. Garabedian, *The Massachusetts Sustainable-Yield Estimator: A Decision-Support Tool to Assess Water Availability at Ungaged Sites in Massachusetts*, Scientific Investigations Report 2009-5227, U.S. Geological Survey, Reston, VA, 2010, 41 p.

Emerson, D.G., A.V. Vecchia, and A.L. Dahl, *Evaluation of Drainage-Area Ratio Method Used to Estimate Streamflow for the Red River of the North Basin, North Dakota and Minnesota*, Scientific Investigations Report 2005-5017, U.S. Geological Survey, Reston, VA, 2002, 13 p.

Fennessey, N. M., A Hydro-Climatological Model of Daily Streamflow for the Northeast United States, PhD Dissertation, Tufts University, Medford, MA, November 1994, 269 p.

Gupta, V.K. and D.R. Dawdy, "Physical interpretations of regional variations in the scaling exponents of flood quantiles," *Hydrological Processes*, Vol. 9, 1995, pp. 347-361.

Gupta, V.K., and E. Waymire, "Multiscaling properties of spatial rainfall and river flow distributions," *Journal of Geophysical Research*, Vol. 95(D3), 1990, pp. 1999-2009.

Gupta, V.K., B.M. Troutman, and D.R. Dawdy, "Towards a nonlinear geophysical theory of floods in river networks: An overview of 20 years of progress," *Nonlinear Dynamics in Geosciences*, A.A. Tsonis and J.B. Elsner, Eds., Springer Science+Business Media, LLC, New York, NY, 1997, pp. 120-151.

Hirsch, R.M., "A comparison of four streamflow record extension techniques", *Water Resources Research*, Vol. 18, 1982, pp. 1081-1088.Helsel, D. R. and R. M. Hirsch, *Statistical Methods in Water Resources*, Techniques of Water-Resources Investigations of the United States Geological Survey, Book 4: Hydrologic Analysis and Interpretation, Chapter A3, U.S. Geological Survey, Reston, VA, 2002, 510 p.

Hingray, B. and M. Ben Haha, "Statistical performances of various deterministic and stochastic models for rainfall series disaggregation," *Atmospheric Research*, Vol. 77, 2005, pp. 152-175.

Hirsch, R.M., "An evaluation of some record reconstruction techniques," *Water Resources Research*, Vol. 15, 1979, pp. 1781-1790.

Hortness, J.E., *Estimating Low-flow Frequency Statistics for Unregulated Streams in Idaho*, Scientific Investigations Report 2006-5035, U.S. Geological Survey, Reston, VA, 2006, 31 p.

Koltun, G.F. and J.W. Roberts, *Techniques for Estimating Flood-Peak Discharges of Rural, Unregulated Streams in Ohio*, Water-Resources Investigation Report 89-4126, U.S. Geological Survey, Reston, VA, 1990, 68 p.

Mohamoud, Y.M., "Prediction of daily flow duration curves and streamflow for ungauged catchments using regional flow duration curves," *Hydrological Sciences Journal*, Vol. 53, 2008, pp. 706-724.

RSI, *IDL Reference Guide*, RSI, Boulder, CO, 2006, 5386 p.

Ormsbee, L. E., “Rainfall disaggregation model for continuous hydrologic modeling,” *Journal of Hydraulic Engineering*, Vol. 115, 1989, pp. 507-525.

Perry, C.A., Wolock, D.M., and Artman, J.C., 2004, *Estimates of Flow Duration, Mean Flow, and Peak-Discharge Frequency Values for Kansas Stream Locations*, Scientific Investigations Report 2004–5033, U.S. Geological Survey, Reston, VA, 2004, 651 p.

Press, W. H., B. P. Flannery, S. A. Teukolsky, and W. T. Vetterling, *Numerical Recipes in C: The Art of Scientific Computing*, Cambridge University Press, Cambridge, MA, 1992, 994 p.

Ries, K.G., III, and P.J. Friesz, *Methods for Estimating Low-Flow Statistics for Massachusetts Streams*, Water-Resources Investigations Report 2000-4135, U.S. Geological Survey, Reston, VA, 2000, 81 p.

Salas, J. D., “Analysis and modeling of hydrologic time series,” *Handbook of Hydrology*, D. R. Maidment, Ed., McGraw-Hill, Inc., New York, NY, 1993, pp. 19.32-19.36.

Smakhtin, V. Y. and B. Masse, “Continuous daily hydrograph simulation using duration curves of a precipitation index,” *Hydrological Process*es, Vol. 14, 2000, pp. 1083-1100.

van Donk, S. J., L. E. Wagner, E. L. Skidmore, and J. Tatarko, “Comparison of the Weibull model with measured wind speed distributions for stochastic wind generation,” *Transactions of the ASAE*, Vol. 48, 2005, pp. 503-510.

Vogel, R.M. and J.R. Stedinger, “Minimum variance streamflow record augmentation procedures,” *Water Resources Research*, Vol. 21, 1985, pp. 715-723.

Vogel, R.M. and A. Sankarasubramanian, “Spatial scaling properties of annual streamflow in the United States,” *Hydrological Sciences Journal*, Vol. 15, 2000, pp. 465-476.

Waldron, M. C. and S. A. Archfield, *Factors Affecting Firm Yield and the Estimation of Firm Yield for Selected Streamflow-Dominated Drinking-Water-Supply Reservoirs in Massachusetts*, Scientific Investigations Report 2006–5044, U.S. Geological Survey, Reston, VA, 2006, 39 p.

APPENDIX B – EROSION FUNCTION APPARATUS AND GRAIN-SIZE ANALYSIS RESULTS

Site 1-1 Des Plaines River at Cermak Erosion Function Apparatus and Grain-Size Analysis Results Soil 1
(Elevation 600.80 to 598.80 feet) (Latitude: 41°51.0214, Longitude: 87°49.6460)

Water Mass Density (ρ) =	1,000	kg/m^3
Kinematic Viscosity (υ) =	0.000001	m^2/s
Flume Height (h_{rf}) =	0.0508	m
Flume Width (w_{rf}) =	0.1016	m
Flume Area (A) =	0.0052	m
Flume Perimeter (P) =	0.3048	m
Hydraulic Diameter (D) =	0.0677	m

Mean Particle Size (D_{50}) =	0.0041	mm
Surface Roughness (ε) =	0.0000021	m
Relative Roughness (ε/D) =	0.0000304	

Velocity v (m/s)	Reynold's Number Re	Friction Factor f	Shear Stress τ (N/m^2)	Erosion Rate (mm/hr)
2.0	135,467	0.0170	8.5	1.0
2.5	169,333	0.0163	12.7	4.0
3.0	203,200	0.0158	17.7	14.0
4.0	270,933	0.0150	30.0	3.0
5.0	338,667	0.0144	45.1	29.4

% Smaller than Size Shown		Diameter (mm)	Sieve
	100.00	75	3
	100.00	63	2.5
	100.00	50	2
	100.00	37.5	1.5
	100.00	25	1
	100.00	19	3/4
	100.00	12.5	1/2
	100.00	9.5	3/8
	99.91	4.75	# 4
	99.43	2	# 10
	98.61	0.850	#20
	97.68	0.425	#40
T-88	94.94	0.150	#100
minutes	92.86	0.075	#200
1	85.46	0.043	
5	79.71	0.020	
15	71.08	0.012	
30	64.38	0.009	
60	57.71	0.006	
90	52.95	0.005	
120	51.07	0.004	
250	46.35	0.003	
1,440	30.55	0.001	

Site 1-4 Des Plaines River at Palatine Road Erosion Function Apparatus and Grain-Size Analysis Results Soil 1
(Elevation 625.10 to 627.10 feet) (Latitude: 42°06.54, Longitude: 87°53.33)

Water Mass Density (ρ) =	1,000	kg/m^3
Kinematic Viscosity (υ) =	0.000001	m^2/s
Flume Height (h_{rf}) =	0.0508	m
Flume Width (w_{rf}) =	0.1016	m
Flume Area (A) =	0.0052	m
Flume Perimeter (P) =	0.3048	m
Hydraulic Diameter (D) =	0.0677	m

Mean Particle Size (D_{50}) =	0.0148	mm
Surface Roughness (ε) =	0.0000074	m
Relative Roughness (ε/D) =	0.0001093	

Velocity v (m/s)	Reynold's Number Re	Friction Factor f	Shear Stress τ (N/m^2)	Erosion Rate (mm/hr)
2.5	169,333.3	0.0169	13.2	0.0
3.0	203,200.0	0.0164	18.5	1.0
4.0	270,933.3	0.0157	31.4	1.0
5.0	338,666.7	0.0153	47.8	5.0

% Smaller than Size Shown		Diameter (mm)	Sieve
	100.00	75	3
	100.00	63	2.5
	100.00	50	2
	100.00	37.5	1.5
	92.73	25	1
	87.81	19	3/4
	80.44	12.5	1/2
	78.54	9.5	3/8
	73.74	4.75	# 4
	69.66	2	# 10
	65.59	0.850	#20
	61.64	0.425	#40
T-88	53.58	0.150	#100
minutes	48.05	0.075	#200
1	39.00	0.044	
5	33.57	0.020	
15	29.48	0.012	
30	26.77	0.009	
60	23.38	0.006	
90	21.36	0.005	
120	20.02	0.004	
250	18.02	0.003	
1,440	13.58	0.001	

Site 1-4 Des Plaines River at Palatine Road Erosion Function Apparatus and Grain-Size Analysis Results Soil 2
(Elevation 623.60 to 625.10 feet) (Latitude: 42°06.54, Longitude: 87°53.33)

Water Mass Density (ρ) =	1,000	kg/m^3
Kinematic Viscosity (υ) =	0.000001	m^2/s
Flume Height (h_{rf}) =	0.0508	m
Flume Width (w_{rf}) =	0.1016	m
Flume Area (A) =	0.0052	m
Flume Perimeter (P) =	0.3048	m
Hydraulic Diameter (D) =	0.0677	m

Mean Particle Size (D_{50}) =	0.0100	mm
Surface Roughness (ε) =	0.0000050	m
Relative Roughness (ε/D) =	0.0000738	

Velocity v (m/s)	Reynold's Number Re	Friction Factor f	Shear Stress τ (N/m^2)	Erosion Rate (mm/hr)
1.0	67,733.3	0.0197	2.5	1.0
1.5	101,600.0	0.0182	5.1	11.0
2.0	135,466.7	0.0173	8.7	9.0
2.5	169,333.3	0.0166	13.0	38.0

% Smaller than		Diameter	
Size Shown		(mm)	Sieve
	100.00	75	3
	100.00	63	2.5
	100.00	50	2
	100.00	37.5	1.5
	100.00	25	1
	100.00	19	3/4
	100.00	12.5	1/2
	99.75	9.5	3/8
	99.55	4.75	# 4
	99.21	2	# 10
	98.68	0.850	#20
	98.21	0.425	#40
T-88	96.08	0.150	#100
minutes	94.56	0.075	#200
1	82.97	0.038	
5	69.80	0.018	
15	53.81	0.011	
30	42.54	0.008	
60	34.10	0.006	
90	29.42	0.005	
120	25.67	0.004	
250	22.90	0.003	
1,440	15.88	0.001	

Site 1-4 Des Plaines River at Palatine Road Erosion Function Apparatus and Grain-Size Analysis Results Soil 3
(Elevation 622.40 to 623.60 feet) (Latitude: 42°06.54, Longitude: 87°53.33)

Water Mass Density (ρ) =	1,000	kg/m^3
Kinematic Viscosity (υ) =	0.000001	m^2/s
Flume Height (h_{rf}) =	0.0508	m
Flume Width (w_{rf}) =	0.1016	m
Flume Area (A) =	0.0052	m
Flume Perimeter (P) =	0.3048	m
Hydraulic Diameter (D) =	0.0677	m

Mean Particle Size (D_{50}) =	0.0217	mm
Surface Roughness (ε) =	0.0000109	m
Relative Roughness (ε/D) =	0.0001602	

Velocity v (m/s)	Reynold's Number Re	Friction Factor f	Shear Stress τ (N/m^2)	Erosion Rate (mm/hr)
3.0	203,200.0	0.0168	18.9	1.0
4.0	270,933.3	0.0162	32.4	2.0
5.0	338,666.7	0.0157	49.1	5.0
6.0	406,400.0	0.0154	69.3	7.0

% Smaller than Size Shown		Diameter (mm)	Sieve
	100.00	75	3
	100.00	63	2.5
	100.00	50	2
	100.00	37.5	1.5
	95.31	25	1
	95.31	19	3/4
	94.38	12.5	1/2
	93.80	9.5	3/8
	90.25	4.75	# 4
	86.12	2	# 10
	82.35	0.850	#20
	79.81	0.425	#40
T-88	72.80	0.150	#100
minutes	68.26	0.075	#200
1	58.76	0.043	
5	49.29	0.020	
15	42.94	0.012	
30	37.41	0.009	
60	32.69	0.006	
90	29.55	0.005	
120	28.78	0.004	
250	24.91	0.003	
1,440	18.22	0.001	

Site 1-4 Des Plaines River at Palatine Road Erosion Function Apparatus and Grain-Size Analysis Results Soil 4
(Elevation 619.60 to 622.40 feet) (Latitude: 42°06.54, Longitude: 87°53.33)

Water Mass Density (ρ) =	1,000	kg/m^3
Kinematic Viscosity (υ) =	0.000001	m^2/s
Flume Height (h_{rf}) =	0.0508	m
Flume Width (w_{rf}) =	0.1016	m
Flume Area (A) =	0.0052	m
Flume Perimeter (P) =	0.3048	m
Hydraulic Diameter (D) =	0.0677	m

Mean Particle Size (D_{50}) =	0.0149	mm
Surface Roughness (ε) =	0.0000075	m
Relative Roughness (ε/D) =	0.0001100	

Velocity v (m/s)	**Reynold's Number Re**	**Friction Factor f**	**Shear Stress τ (N/m^2)**	**Erosion Rate (mm/hr)**
2.5	169,333.3	0.0170	13.3	0.0
3.0	203,200.0	0.0164	18.5	1.0
4.0	270,933.3	0.0157	31.4	2.0
5.0	338,666.7	0.0153	47.8	5.0
6.0	406,400.0	0.0149	67.1	11.0

% Smaller than Size Shown		Diameter (mm)	Sieve
	100.00	75	3
	100.00	63	2.5
	100.00	50	2
	100.00	37.5	1.5
	100.00	25	1
	100.00	19	3/4
	99.28	12.5	1/2
	99.02	9.5	3/8
	96.86	4.75	# 4
	93.55	2	# 10
	90.07	0.850	#20
	87.14	0.425	#40
T-88	80.08	0.150	#100
minutes	75.41	0.075	#200
1	64.85	0.043	
5	55.16	0.020	
15	47.09	0.012	
30	40.62	0.009	
60	34.19	0.006	
90	32.59	0.005	
120	29.39	0.004	
250	24.63	0.003	
1,440	16.99	0.001	

Site 1-6 Des Plaines River at Touhy Erosion Function Apparatus and Grain-Size Analysis Results Soil 1
(Elevation 611.58 to 613.58 feet) (Latitude: 42°00.6295, Longitude: 87°51.6644)

Water Mass Density (ρ) =	1,000	kg/m^3
Kinematic Viscosity (υ) =	0.000001	m^2/s
Flume Height (h_{rf}) =	0.0508	m
Flume Width (w_{rf}) =	0.1016	m
Flume Area (A) =	0.0052	m
Flume Perimeter (P) =	0.3048	m
Hydraulic Diameter (D) =	0.0677	m

Mean Particle Size (0-3) (D_{50}) =	0.0084	mm
Surface Roughness (ε) =	0.0000042	m
Relative Roughness (ε/D) =	0.0000620	

Velocity v (m/s)	**Reynold's Number Re**	**Friction Factor f**	**Shear Stress τ (N/m^2)**	**Erosion Rate (mm/hr)**
1.0	67,733	0.0197	2.5	1.0
2.5	169,333	0.017	12.9	7.0
3.0	203,200	0.016	18.0	14.0
4.0	270,933	0.0153	30.6	10.0
5.0	338,667	0.0148	46.3	54.6
6.0	406,400	0.0144	64.8	173.3

% Smaller than Size Shown		Diameter (mm)	Sieve
	100.00	75	3
	100.00	63	2.5
	100.00	50	2
	100.00	37.5	1.5
	100.00	25	1
	100.00	19	3/4
	99.57	12.5	1/2
	99.05	9.5	3/8
	97.78	4.75	# 4
	95.24	2	# 10
	92.37	0.850	#20
	89.07	0.425	#40
T-88	81.84	0.150	#100
minutes	78.90	0.075	#200
1	73.67	0.043	
5	63.34	0.020	
15	56.38	0.012	
30	51.22	0.009	
60	45.19	0.006	
90	42.61	0.005	
120	40.06	0.004	
250	35.79	0.003	
1,440	27.50	0.001	

Site 1-7 Salt Creek at Route 83 Erosion Function Apparatus and Grain-Size Analysis Results
Soil 1
(Elevation 656.39 to 658.39 feet) (Latitude: 41°53.3585, Longitude: 87°57.7394)

Water Mass Density (ρ) =	1,000	kg/m^3
Kinematic Viscosity (υ) =	0.000001	m^2/s
Flume Height (h_{rf}) =	0.0508	m
Flume Width (w_{rf}) =	0.1016	m
Flume Area (A) =	0.0052	m
Flume Perimeter (P) =	0.3048	m
Hydraulic Diameter (D) =	0.0677	m

Mean Particle Size (0-3) (D_{50}) =	0.1296	mm
Surface Roughness (ε) =	0.0000648	m
Relative Roughness (ε/D) =	0.0009567	

Velocity v (m/s)	Reynold's Number Re	Friction Factor f	Shear Stress τ (N/m^2)	Erosion Rate (mm/hr)
1.5	101,600	0.022	6.2	0.0
2.0	135,467	0.022	10.8	0.0
2.5	169,333	0.0212	16.6	1.0
3.0	203,200	0.0209	23.5	12.0
4.0	270,933	0.0207	41.4	17.0

% Smaller than		Diameter	
Size Shown		(mm)	Sieve
	100.00	75	3
	100.00	63	2.5
	100.00	50	2
	100.00	37.5	1.5
	100.00	25	1
	95.47	19	3/4
	92.08	12.5	1/2
	90.95	9.5	3/8
	86.79	4.75	# 4
	78.46	2	# 10
	70.66	0.850	#20
	63.86	0.425	#40
T-88	51.48	0.150	#100
minutes	46.05	0.075	#200
1	38.60	0.043	
5	34.16	0.020	
15	29.73	0.012	
30	26.03	0.009	
60	23.83	0.006	
90	21.63	0.005	
120	20.92	0.004	
250	18.75	0.003	
1,440	13.90	0.001	

Site 1-7 Salt Creek at Route 83 Erosion Function Apparatus and Grain-Size Analysis Results
Soil 2
(Elevation 654.39 to 656.39 feet) (Latitude: 41°53.3585, Longitude: 87°57.7394)

Water Mass Density (ρ) =	1,000	kg/m^3
Kinematic Viscosity (υ) =	0.000001	m^2/s
Flume Height (h_{rf}) =	0.0508	m
Flume Width (w_{rf}) =	0.1016	m
Flume Area (A) =	0.0052	m
Flume Perimeter (P) =	0.3048	m
Hydraulic Diameter (D) =	0.0677	m

Mean Particle Size (0-3) (D_{50}) =	0.0679	mm
Surface Roughness (ε) =	0.0000340	m
Relative Roughness (ε/D) =	0.0005012	

Velocity v (m/s)	Reynold's Number Re	Friction Factor *f*	Shear Stress τ (N/m^2)	Erosion Rate (mm/hr)
0.6	40,640	0.023	1.0	0.0
1.0	67,733	0.022	2.7	0.0
1.5	101,600	0.0204	5.7	0.0
2.0	135,467	0.0197	9.9	1.0
3.0	203,200	0.0189	21.3	16.0

% Smaller than		Diameter	
Size Shown		(mm)	Sieve
	100.00	75	3
	100.00	63	2.5
	100.00	50	2
	100.00	37.5	1.5
	100.00	25	1
	98.90	19	3/4
	97.39	12.5	1/2
	96.94	9.5	3/8
	93.25	4.75	# 4
	84.99	2	# 10
	76.91	0.850	#20
	70.51	0.425	#40
T-88	58.19	0.150	#100
minutes	52.12	0.075	#200
1	42.58	0.043	
5	35.94	0.020	
15	30.97	0.012	
30	27.65	0.009	
60	24.35	0.006	
90	22.69	0.005	
120	21.08	0.004	
250	17.81	0.003	
1,440	13.99	0.001	

Site 3-25 Indian Creek at Route 24 Erosion Function Apparatus and Grain-Size Analysis Results Soil 1
(Elevation 654.39 to 656.39 feet) (Latitude: 41°31.3879, Longitude: 88°48.9834)

Water Mass Density (ρ) =	1,000	kg/m^3
Kinematic Viscosity (υ) =	0.000001	m^2/s
Flume Height (h_{rf}) =	0.0508	m
Flume Width (w_{rf}) =	0.1016	m
Flume Area (A) =	0.0052	m
Flume Perimeter (P) =	0.3048	m
Hydraulic Diameter (D) =	0.0677	m

Mean Particle Size (0-3) (D_{50}) =	0.0591	mm
Surface Roughness (ε) =	0.0000296	m
Relative Roughness (ε/D) =	0.0004363	

Velocity v (m/s)	**Reynold's Number Re**	**Friction Factor f**	**Shear Stress τ (N/m^2)**	**Erosion Rate (mm/hr)**
2.0	135,467	0.0194	9.7	1.0
2.5	169,333	0.0190	14.8	1.0
3.0	203,200	0.0186	20.9	3.0
4.0	270,933	0.0181	36.2	12.0
5.0	338,667	0.0178	55.6	14.0
6.0	406,400	0.0176	79.2	20.0

% Smaller than		Diameter	
Size Shown		(mm)	Sieve
	100.00	75	3
	100.00	63	2.5
	100.00	50	2
	100.00	37.5	1.5
	100.00	25	1
	100.00	19	3/4
	100.00	12.5	1/2
	99.56	9.5	3/8
	97.90	4.75	# 4
	95.35	2	# 10
	92.17	0.850	#20
	88.19	0.425	#40
T-88	69.76	0.150	#100
minutes	57.67	0.075	#200
1	42.23	0.043	
5	36.62	0.020	
15	31.03	0.012	
30	26.37	0.009	
60	23.58	0.006	
90	21.74	0.005	
120	19.91	0.004	
250	18.12	0.003	
1,440	14.87	0.001	

Site 4-5 LaMoine River at Route 61 Erosion Function Apparatus and Grain-Size Analysis Results Soil 1
(Elevation 495.25 to 497.25 feet) (Latitude: 40°19'51.9, Longitude: 90°53'46.6)

Water Mass Density (ρ) =	1,000	kg/m^3
Kinematic Viscosity (υ) =	0.000001	m^2/s
Flume Height (h_{rf}) =	0.0508	m
Flume Width (w_{rf}) =	0.1016	m
Flume Area (A) =	0.0052	m
Flume Perimeter (P) =	0.3048	m
Hydraulic Diameter (D) =	0.0677	m

Mean Particle Size (D_{50}) =	0.0148	mm
Surface Roughness (ε) =	0.0000074	m
Relative Roughness (ε/D) =	0.0001093	

Velocity v (m/s)	Reynold's Number Re	Friction Factor f	Shear Stress τ (N/m^2)	Erosion Rate (mm/hr)
0.6	40,640	0.022	1.0	0.0
1.0	67,733	0.020	2.5	1.0
1.5	101,600	0.0184	5.2	2.0
2.0	135,467	0.018	9.0	24.0
2.5	169,333	0.0175	13.7	73.2
3.0	203,200	0.0164	18.5	47.0
4.0	270,933	0.0157	31.4	285.7

% Smaller than Size Shown		Diameter (mm)	Sieve
	100.00	75	3
	100.00	63	2.5
	100.00	50	2
	100.00	37.5	1.5
	100.00	25	1
	100.00	19	3/4
	100.00	12.5	1/2
	100.00	9.5	3/8
	100.00	4.75	# 4
	100.00	2	# 10
	99.99	0.850	#20
	99.71	0.425	#40
T-88	90.27	0.150	#100
minutes	85.01	0.075	#200
1	75.53	0.040	
5	58.77	0.019	
15	43.91	0.012	
30	36.01	0.009	
60	32.08	0.006	
90	30.11	0.005	
120	28.14	0.004	
250	25.23	0.003	
1,440	21.65	0.001	

Site 4-5 LaMoine River at Route 61 Erosion Function Apparatus and Grain-Size Analysis Results Soil 2
(Elevation 493.25 to 495.25 feet) (Latitude: 40°19'51.9, Longitude: 90°53'46.6)

Water Mass Density (ρ) =	1,000	kg/m^3
Kinematic Viscosity (υ) =	0.000001	m^2/s
Flume Height (h_{rf}) =	0.0508	m
Flume Width (w_{rf}) =	0.1016	m
Flume Area (A) =	0.0052	m
Flume Perimeter (P) =	0.3048	m
Hydraulic Diameter (D) =	0.0677	m

Mean Particle Size (0-3) (D_{50}) =	0.0204	mm
Surface Roughness (ε) =	0.0000102	m
Relative Roughness (ε/D) =	0.0001507	

Velocity v (m/s)	**Reynold's Number Re**	**Friction Factor f**	**Shear Stress τ (N/m^2)**	**Erosion Rate (mm/hr)**
1.5	101,600	0.0187	5.3	0.0
2.0	135,467	0.018	8.9	0.0
2.5	169,333	0.0172	13.4	1.0
3.0	203,200	0.0167	18.8	1.0
4.0	270,933	0.0161	32.2	10.0
5.0	338,667	0.0157	49.1	41.0

% Smaller than Size Shown		Diameter (mm)	Sieve
	100.00	75	3
	100.00	63	2.5
	100.00	50	2
	100.00	37.5	1.5
	100.00	25	1
	100.00	19	3/4
	100.00	12.5	1/2
	100.00	9.5	3/8
	100.00	4.75	# 4
	100.00	2	# 10
	99.99	0.850	#20
	99.91	0.425	#40
T-88	96.69	0.150	#100
minutes	85.34	0.075	#200
1	70.19	0.041	
5	49.57	0.020	
15	36.79	0.012	
30	28.93	0.009	
60	24.99	0.006	
90	24.03	0.005	
120	23.05	0.004	
250	21.11	0.003	
1,440	19.60	0.001	

Site 5-17 Kaskaskia River at County Road 1550N Erosion Function Apparatus and Grain-Size Analysis Results Soil 1
(Elevation 81.41- 83.71 feet) (Latitude: 39°52'44.9, Longitude: 88°22'36.8)

Water Mass Density (ρ) =	1,000	kg/m^3
Kinematic Viscosity (υ) =	0.000001	m^2/s
Flume Height (h_{rf}) =	0.0508	m
Flume Width (w_{rf}) =	0.1016	m
Flume Area (A) =	0.0052	m
Flume Perimeter (P) =	0.3048	m
Hydraulic Diameter (D) =	0.0677	m

Mean Particle Size (D_{50}) =	0.0213	mm
Surface Roughness (ε) =	0.0000106	m
Relative Roughness (ε/D) =	0.0001570	

Velocity v (m/s)	**Reynold's Number Re**	**Friction Factor f**	**Shear Stress τ (N/m^2)**	**Erosion Rate (mm/hr)**
3.0	203,200	0.0167	18.8	0.0
4.0	270,933	0.016	32.0	1.0
5.0	338,667	0.0157	49.1	1.0
6.0	406,400	0.0154	69.3	2.0

% Smaller than		Diameter	
Size Shown		(mm)	Sieve
	100.00	75	3
	100.00	63	2.5
	100.00	50	2
	100.00	37.5	1.5
	100.00	25	1
	100.00	19	3/4
	99.16	12.5	1/2
	98.35	9.5	3/8
	96.13	4.75	# 4
	92.21	2	# 10
	87.86	0.850	#20
	82.42	0.425	#40
T-88	67.61	0.150	#100
minutes	61.20	0.075	#200
1	56.86	0.043	
5	49.55	0.020	
15	41.33	0.012	
30	34.94	0.009	
60	30.38	0.006	
90	29.47	0.005	
120	28.56	0.004	
250	25.86	0.003	
1,440	18.91	0.001	

Site 5-20 Lake Fork at County Road 100N Erosion Function Apparatus and Grain-Size Analysis Results Soil 1
(Elevation 639.89 – 642.39 feet) (Latitude: 39°48'23.205, Longitude: 88°28'36.488)

Water Mass Density (ρ) =	1,000	kg/m^3
Kinematic Viscosity (υ) =	0.000001	m^2/s
Flume Height (h_{rf}) =	0.0508	m
Flume Width (w_{rf}) =	0.1016	m
Flume Area (A) =	0.0052	m
Flume Perimeter (P) =	0.3048	m
Hydraulic Diameter (D) =	0.0677	m

Mean Particle Size (D_{50}) =	0.0274	mm
Surface Roughness (ε) =	0.0000137	m
Relative Roughness (ε/D) =	0.0002021	

Velocity v (m/s)	**Reynold's Number Re**	**Friction Factor f**	**Shear Stress τ (N/m^2)**	**Erosion Rate (mm/hr)**
2.0	135,467	0.018	9.0	0.0
3.0	203,200	0.017	19.1	0.0
4.0	270,933	0.016	32.0	1.0
5.0	338,667	0.016	50.0	2.0
6.0	406,400	0.016	72.0	2.0

% Smaller than Size Shown		Diameter (mm)	Sieve
	100.00	75	3
	100.00	63	2.5
	100.00	50	2
	100.00	37.5	1.5
	100.00	25	1
	100.00	19	3/4
	98.92	12.5	1/2
	98.01	9.5	3/8
	96.34	4.75	# 4
	93.68	2	# 10
	90.28	0.850	#20
	85.95	0.425	#40
T-88	70.53	0.150	#100
minutes	62.97	0.075	#200
1	57.00	0.043	
5	46.74	0.020	
15	38.35	0.012	
30	34.62	0.009	
60	29.98	0.006	
90	28.13	0.005	
120	26.27	0.004	
250	23.53	0.003	
1,440	18.31	0.001	

Site 6-22 Spring Creek at Route 97 Erosion Function Apparatus and Grain-Size Analysis Results Soil 1
(Elevation 639.89 – 642.39 feet) (Latitude: 39°48'54.455, Longitude: 89°41'58.227)

Water Mass Density (ρ) =	1,000	kg/m^3
Kinematic Viscosity (υ) =	0.000001	m^2/s
Flume Height (h_{rf}) =	0.0508	m
Flume Width (w_{rf}) =	0.1016	m
Flume Area (A) =	0.0052	m
Flume Perimeter (P) =	0.3048	m
Hydraulic Diameter (D) =	0.0677	m

Mean Particle Size (D_{50}) =	0.0167	mm
Surface Roughness (ε) =	0.0000084	m
Relative Roughness (ε/D) =	0.0001233	

Velocity v (m/s)	**Reynold's Number Re**	**Friction Factor f**	**Shear Stress τ (N/m^2)**	**Erosion Rate (mm/hr)**
2.0	135,467	0.0176	8.8	0.0
2.5	169,333	0.0170	13.3	1.0
3.0	203,200	0.0165	18.6	1.0
4.0	270,933	0.0159	31.8	13.6
5.0	338,667	0.0154	48.1	26.9

% Smaller than		Diameter	
Size Shown		(mm)	Sieve
	100.00	75	3
	100.00	63	2.5
	100.00	50	2
	100.00	37.5	1.5
	100.00	25	1
	100.00	19	3/4
	100.00	12.5	1/2
	100.00	9.5	3/8
	100.00	4.75	# 4
	99.12	2	# 10
	98.32	0.850	#20
	97.39	0.425	#40
T-88	93.20	0.150	#100
minutes	87.13	0.075	#200
1	75.06	0.040	
5	55.19	0.020	
15	41.24	0.012	
30	33.29	0.009	
60	29.30	0.006	
90	26.33	0.005	
120	25.34	0.004	
250	23.35	0.003	
1,440	19.67	0.001	

Site 7-1 Little Wabash at Route 45 Erosion Function Apparatus and Grain-Size Analysis Results
Soil 1
(Elevation 431.18 – 432.18 feet) (Latitude: 38°47'02, Longitude: 88°30'28.7)

Water Mass Density (ρ) =	1,000	kg/m^3
Kinematic Viscosity (υ) =	0.000001	m^2/s
Flume Height (h_{rf}) =	0.0508	m
Flume Width (w_{rf}) =	0.1016	m
Flume Area (A) =	0.0052	m
Flume Perimeter (P) =	0.3048	m
Hydraulic Diameter (D) =	0.0677	m

Mean Particle Size (0-3) (D_{50}) =	0.0331	mm
Surface Roughness (ε) =	0.0000166	m
Relative Roughness (ε/D) =	0.0002446	

Velocity v (m/s)	**Reynold's Number Re**	**Friction Factor f**	**Shear Stress τ (N/m^2)**	**Erosion Rate (mm/hr)**
0.6	40,640	0.023	1.0	0.0
1.0	67,733	0.021	2.6	0.0
1.5	101,600	0.019	5.3	1.0
2.0	135,467	0.018	9.0	2.0
2.5	169,333	0.0178	13.9	43.0
3.0	203,200	0.0174	19.6	36.0

% Smaller than		Diameter	
Size Shown		(mm)	Sieve
	100.00	75	3
	100.00	63	2.5
	100.00	50	2
	100.00	37.5	1.5
	100.00	25	1
	100.00	19	3/4
	100.00	12.5	1/2
	100.00	9.5	3/8
	100.00	4.75	# 4
	95.52	2	# 10
	93.32	0.850	#20
	91.43	0.425	#40
T-88	78.65	0.150	#100
minutes	64.19	0.075	#200
1	54.96	0.043	
5	43.68	0.020	
15	34.25	0.012	
30	28.61	0.009	
60	24.84	0.006	
90	22.98	0.005	
120	22.05	0.004	
250	19.25	0.003	
1,440	16.87	0.001	

Site 7-1 Little Wabash at Route 45 Erosion Function Apparatus and Grain-Size Analysis Results
Soil 2
(Elevation 430.18 – 431.18 feet) (Latitude: 38°47'02, Longitude: 88°30'28.7)

Water Mass Density (ρ) =	1,000	kg/m^3
Kinematic Viscosity (υ) =	0.000001	m^2/s
Flume Height (h_{rf}) =	0.0508	m
Flume Width (w_{rf}) =	0.1016	m
Flume Area (A) =	0.0052	m
Flume Perimeter (P) =	0.3048	m
Hydraulic Diameter (D) =	0.0677	m

Mean Particle Size (0-3) (D_{50}) =	0.0304	mm
Surface Roughness (ε) =	0.0000152	m
Relative Roughness (ε/D) =	0.0002244	

Velocity v (m/s)	Reynold's Number Re	Friction Factor f	Shear Stress τ (N/m^2)	Erosion Rate (mm/hr)
1.0	67,733	0.02	2.5	1.0
1.5	101,600	0.019	5.3	12.0
2.0	135,467	0.018	9.0	76.6

% Smaller than Size Shown		Diameter (mm)	Sieve
	100.00	75	3
	100.00	63	2.5
	100.00	50	2
	100.00	37.5	1.5
	100.00	25	1
	100.00	19	3/4
	100.00	12.5	1/2
	100.00	9.5	3/8
	100.00	4.75	# 4
	98.79	2	# 10
	97.72	0.850	#20
	96.76	0.425	#40
T-88	85.05	0.150	#100
minutes	67.43	0.075	#200
1	57.56	0.043	
5	43.92	0.020	
15	33.91	0.012	
30	30.31	0.009	
60	26.71	0.006	
90	24.89	0.005	
120	24.00	0.004	
250	21.29	0.003	
1,440	16.16	0.001	

Site 7-18 Kaskaskia at Route 51 Erosion Function Apparatus and Grain-Size Analysis Results
Soil 1
(Elevation 455.90 – 457.00 feet) (Latitude: 38°57'36.5, Longitude: 89°05'18.6)

Water Mass Density (ρ) =	1,000	kg/m^3
Kinematic Viscosity (υ) =	0.000001	m^2/s
Flume Height (h_{rf}) =	0.0508	m
Flume Width (w_{rf}) =	0.1016	m
Flume Area (A) =	0.0052	m
Flume Perimeter (P) =	0.3048	m
Hydraulic Diameter (D) =	0.0677	m

Mean Particle Size (0-3) (D_{50}) =	0.0345	mm
Surface Roughness (ε) =	0.0000172	m
Relative Roughness (ε/D) =	0.0002545	

Velocity v (m/s)	Reynold's Number Re	Friction Factor f	Shear Stress τ (N/m^2)	Erosion Rate (mm/hr)
2.5	169,333	0.0174	13.6	0.0
3.0	203,200	0.0174	19.6	1.0
4.0	270,933	0.017	33.8	2.0
5.0	338,667	0.0165	51.6	2.0
6.0	406,400	0.0162	72.9	5.0

% Smaller than		Diameter	
Size Shown		(mm)	Sieve
	100.00	75	3
	100.00	63	2.5
	100.00	50	2
	100.00	37.5	1.5
	100.00	25	1
	100.00	19	3/4
	99.11	12.5	1/2
	98.56	9.5	3/8
	96.67	4.75	# 4
	93.42	2	# 10
	89.52	0.850	#20
	84.63	0.425	#40
T-88	70.66	0.150	#100
minutes	61.43	0.075	#200
1	53.74	0.043	
5	43.54	0.020	
15	35.08	0.012	
30	31.68	0.009	
60	28.31	0.006	
90	26.61	0.005	
120	24.93	0.004	
250	21.55	0.003	
1,440	15.92	0.001	

Site 8-3 Macoupin Creek at Route 67 Erosion Function Apparatus and Grain-Size Analysis Results Soil 1
(Elevation 428.08 – 430.08 feet) (Latitude: 39°14'03.5, Longitude: 90°23'40.1)

Water Mass Density (ρ) =	1,000	kg/m^3
Kinematic Viscosity (υ) =	0.000001	m^2/s
Flume Height (h_{rf}) =	0.0508	m
Flume Width (w_{rf}) =	0.1016	m
Flume Area (A) =	0.0052	m
Flume Perimeter (P) =	0.3048	m
Hydraulic Diameter (D) =	0.0677	m

Mean Particle Size (D_{50}) =	0.0095	mm
Surface Roughness (ε) =	0.0000048	m
Relative Roughness (ε/D) =	0.0000704	

Velocity v (m/s)	**Reynold's Number Re**	**Friction Factor *f***	**Shear Stress τ (N/m^2)**	**Erosion Rate (mm/hr)**
1.0	67,733	0.02	2.5	0.0
1.5	101,600	0.018	5.1	0.0
2.0	135,467	0.017	8.5	0.0
Interpolated			10.9	1.0
2.5	169,333	0.017	13.3	3.0
3.0	203,200	0.016	18.0	6.0
4.0	270,933	0.015	30.0	15.0
5.0	338,667	0.015	46.9	8.0
6.0	406,400	0.014	63.0	6.0

% Smaller than		Diameter	
Size Shown		(mm)	Sieve
	100.00	75	3
	100.00	63	2.5
	100.00	50	2
	100.00	37.5	1.5
	100.00	25	1
	100.00	19	3/4
	100.00	12.5	1/2
	100.00	9.5	3/8
	100.00	4.75	# 4
	99.97	2	# 10
	99.49	0.850	#20
	98.79	0.425	#40
T-88	97.02	0.150	#100
minutes	95.91	0.075	#200
1	90.24	0.038	
5	72.09	0.018	
15	55.95	0.011	
30	45.84	0.008	
60	39.81	0.006	
90	37.79	0.005	
120	35.78	0.004	
250	31.76	0.003	
1,440	26.00	0.001	

Site 8-50 Little Crooked Creek at Route 177 Erosion Function Apparatus and Grain-Size Analysis Results Soil 1
(Elevation 420.27 – 422.27 feet) (Latitude: 38°26'29, Longitude: 89°25'01)

Water Mass Density (ρ) =	1,000	kg/m^3
Kinematic Viscosity (υ) =	0.000001	m^2/s
Flume Height (h_{rf}) =	0.0508	m
Flume Width (w_{rf}) =	0.1016	m
Flume Area (A) =	0.0052	m
Flume Perimeter (P) =	0.3048	m
Hydraulic Diameter (D) =	0.0677	m

Mean Particle Size (0-3) (D_{50}) =	0.0105	mm
Surface Roughness (ε) =	0.0000053	m
Relative Roughness (ε/D) =	0.0000777	

Velocity v (m/s)	Reynold's Number Re	Friction Factor f	Shear Stress τ (N/m^2)	Erosion Rate (mm/hr)
1.0	67,733	0.020	2.5	0.0
1.5	101,600	0.018	5.1	0.0
2.0	135,467	0.017	8.7	7.0
2.5	169,333	0.017	13.0	89.6
3.0	203,200	0.016	18.2	88.0

% Smaller than Size Shown		Diameter (mm)	Sieve
	100.00	75	3
	100.00	63	2.5
	100.00	50	2
	100.00	37.5	1.5
	100.00	25	1
	100.00	19	¾
	100.00	12.5	½
	100.00	9.5	3/8
	99.88	4.75	# 4
	99.87	2	# 10
	99.69	0.850	#20
	99.40	0.425	#40
T-88	96.86	0.150	#100
minutes	93.52	0.075	#200
1	77.44	0.043	
5	64.41	0.020	
15	53.24	0.012	
30	45.79	0.009	
60	38.36	0.006	
90	34.64	0.005	
120	32.82	0.004	
250	28.23	0.003	
1,440	22.30	0.001	

Site 9-1 Big Muddy River at Route 149 near Plumfield Erosion Function Apparatus and Grain-Size Analysis Results Soil 1
(Elevation 352.7 – 354.7 feet) (Latitude: 37°53'29.8, Longitude: 89°01'12.5)

Water Mass Density (ρ) =	1,000	kg/m^3
Kinematic Viscosity (υ) =	0.000001	m^2/s
Flume Height (h_{rf}) =	0.0508	m
Flume Width (w_{rf}) =	0.1016	m
Flume Area (A) =	0.0052	m
Flume Perimeter (P) =	0.3048	m
Hydraulic Diameter (D) =	0.0677	m

Mean Particle Size (D_{50}) =	0.1642	mm
Surface Roughness (ε) =	0.0000821	m
Relative Roughness (ε/D) =	0.0012118	

Velocity v (m/s)	**Reynold's Number Re**	**Friction Factor f**	**Shear Stress τ (N/m^2)**	**Erosion Rate (mm/hr)**
1.0	67,733	0.024	3.0	0.0
1.5	101,600	0.023	6.5	1.0
2.0	135,467	0.022	11.0	1.0
2.5	169,333	0.022	17.2	1.0
3.0	203,200	0.022	24.8	3.0
4.0	270,933	0.022	44.0	22.8

% Smaller than		Diameter	
Size Shown		(mm)	Sieve
	100.00	75	3
	100.00	63	2.5
	100.00	50	2
	100.00	37.5	1.5
	100.00	25	1
	100.00	19	¾
	100.00	12.5	½
	100.00	9.5	3/8
	100.00	4.75	# 4
	100.00	2	# 10
	99.96	0.850	#20
	99.78	0.425	#40
T-88	87.19	0.150	#100
minutes	70.89	0.075	#200
1	55.57	0.043	
5	44.53	0.020	
15	36.24	0.012	
30	32.56	0.009	
60	28.89	0.006	
90	27.07	0.005	
120	26.19	0.004	
250	23.50	0.003	
1,440	18.51	0.001	

Site 9-2 Big Muddy River at Route 127 near Murphysboro Erosion Function Apparatus and Grain-Size Analysis Results Soil 1
(Elevation 332.6 – 334.6 feet) (Latitude: 37°45'29.5, Longitude: 89°19'39.5)

Water Mass Density (ρ) =	1,000	kg/m^3
Kinematic Viscosity (υ) =	0.000001	m^2/s
Flume Height (h_{rf}) =	0.0508	m
Flume Width (w_{rf}) =	0.1016	m
Flume Area (A) =	0.0052	m
Flume Perimeter (P) =	0.3048	m
Hydraulic Diameter (D) =	0.0677	m

Mean Particle Size (D_{50}) =	0.0173	mm
Surface Roughness (ε) =	0.0000087	m
Relative Roughness (ε/D) =	0.0001277	

Velocity v (m/s)	**Reynold's Number Re**	**Friction Factor f**	**Shear Stress τ (N/m^2)**	**Erosion Rate (mm/hr)**
1.5	101,600	0.0185	5.2	0.0
2.0	135,467	0.0176	8.8	1.0
2.5	169,333	0.0170	13.3	1.0
5.0	338,667	0.0154	48.1	17.0
6.0	406,400	0.0151	68.0	20.0

% Smaller than Size Shown		Diameter (mm)	Sieve
	100.00	75	3
	100.00	63	2.5
	100.00	50	2
	100.00	37.5	1.5
	100.00	25	1
	100.00	19	¾
	100.00	12.5	½
	100.00	9.5	3/8
	100.00	4.75	# 4
	100.00	2	# 10
	99.98	0.850	#20
	99.86	0.425	#40
T-88	98.40	0.150	#100
minutes	93.83	0.075	#200
1	70.32	0.043	
5	53.50	0.020	
15	43.22	0.012	
30	36.71	0.009	
60	31.13	0.006	
90	30.23	0.005	
120	29.32	0.004	
250	26.59	0.003	
1,440	23.33	0.001	

Site 9-2 Big Muddy River at Route 127 near Murphysboro Erosion Function Apparatus and Grain-Size Analysis Results Soil 2
(Elevation 330.6 – 332.6 feet) (Latitude: 37°45'29.5, Longitude: 89°19'39.5)

Water Mass Density (ρ) =	1,000	kg/m^3
Kinematic Viscosity (υ) =	0.000001	m^2/s
Flume Height (h_{rf}) =	0.0508	m
Flume Width (w_{rf}) =	0.1016	m
Flume Area (A) =	0.0052	m
Flume Perimeter (P) =	0.3048	m
Hydraulic Diameter (D) =	0.0677	m

Mean Particle Size (D_{50}) =	0.0171	mm
Surface Roughness (ε) =	0.0000086	m
Relative Roughness (ε/D) =	0.0001262	

Velocity v (m/s)	**Reynold's Number Re**	**Friction Factor f**	**Shear Stress τ (N/m^2)**	**Erosion Rate (mm/hr)**
2.0	135,467	0.0176	8.8	0.0
2.5	169,333	0.0170	13.3	1.0
3.0	203,200	0.0165	18.6	21.0
4.0	270,933	0.0159	31.8	21.0
5.0	338,667	0.0154	48.1	22.0
6.0	406,400	0.0151	68.0	17.0

% Smaller than		Diameter	
Size Shown		(mm)	Sieve
	100.00	75	3
	100.00	63	2.5
	100.00	50	2
	100.00	37.5	1.5
	100.00	25	1
	100.00	19	¾
	100.00	12.5	½
	100.00	9.5	3/8
	100.00	4.75	# 4
	100.00	2	# 10
	99.98	0.850	#20
	99.96	0.425	#40
T-88	98.67	0.150	#100
minutes	95.24	0.075	#200
1	73.54	0.043	
5	54.52	0.020	
15	42.14	0.012	
30	35.50	0.009	
60	31.72	0.006	
90	29.86	0.005	
120	27.97	0.004	
250	27.10	0.003	
1,440	22.82	0.001	

APPENDIX C – SRICOS INPUT VELOCITY AND DEPTH DATA

Site 1-1 Des Plaines River at Cermak upstream contracted velocity and depth data from HEC-RAS for input into SRICOS (U.S. Customary units (top) and SI units (bottom))

Reach	River Sta	Profile	Q Total	Vel Chnl	Hydr Depth C	Hydr Radius C
			(cfs)	(ft/s)	(ft)	(ft)
Reach-1	47.801	PF 1	10.00	0.03	2.39	2.38
Reach-1	47.801	PF 2	30.00	0.09	2.50	2.49
Reach-1	47.801	PF 3	100.00	0.24	2.84	2.83
Reach-1	47.801	PF 4	300.00	0.51	3.63	3.61
Reach-1	47.801	PF 5	1600.00	1.09	6.13	6.04
Reach-1	47.801	Q2	3613.00	1.53	9.72	9.32
Reach-1	47.801	Q5	4728.00	1.76	11.07	10.51
Reach-1	47.801	Q10	5286.00	1.85	11.74	11.08
Reach-1	47.801	Q25	5935.00	1.97	12.41	11.66
Reach-1	47.801	Q50	6425.00	2.06	12.86	12.04
Reach-1	47.801	Q100	6863.00	2.13	13.26	12.37
Reach-1	47.801	Q500	7767.00	2.26	14.15	13.11

Reach	River Sta	Profile	Q Total	Vel Chnl	Hydr Depth C	Hydr Radius C
			(m3/s)	(m/s)	(m)	(m)
Reach-1	47.801	PF 1	0.28	0.01	0.73	0.73
Reach-1	47.801	PF 2	0.85	0.03	0.76	0.76
Reach-1	47.801	PF 3	2.83	0.07	0.87	0.86
Reach-1	47.801	PF 4	8.50	0.16	1.10	1.10
Reach-1	47.801	PF 5	45.31	0.33	1.87	1.84
Reach-1	47.801	Q2	102.31	0.47	2.96	2.84
Reach-1	47.801	Q5	133.88	0.54	3.38	3.20
Reach-1	47.801	Q10	149.68	0.57	3.58	3.38
Reach-1	47.801	Q25	168.06	0.60	3.78	3.55
Reach-1	47.801	Q50	181.94	0.63	3.92	3.67
Reach-1	47.801	Q100	194.34	0.65	4.04	3.77
Reach-1	47.801	Q500	219.94	0.69	4.31	4.00

Site 1-4 Des Plaines River at Palatine Road (south bridge) upstream contracted velocity and depth data from HEC-RAS for input into SRICOS (U.S. Customary units (top) and SI units (bottom))

Reach	River Sta	Profile	Q Total	Vel Chnl	Hydr Depth C	Hydr Radius C
			(cfs)	(ft/s)	(ft)	(ft)
Reach-1	71.78	PF 1	10.00	0.06	1.22	1.21
Reach-1	71.78	PF 2	30.00	0.16	1.38	1.36
Reach-1	71.78	PF 3	100.00	0.37	2.00	1.96
Reach-1	71.78	PF 4	300.00	0.62	3.53	3.41
Reach-1	71.78	PF 5	1300.00	1.28	6.81	6.42
Reach-1	71.78	Q2	2632.00	1.79	9.81	9.09
Reach-1	71.78	Q5	3669.00	2.15	11.42	10.48
Reach-1	71.78	Q10	4393.00	2.39	12.29	11.22
Reach-1	71.78	Q25	5224.00	2.62	13.31	12.08
Reach-1	71.78	Q50	5839.00	2.78	14.01	12.67
Reach-1	71.78	Q100	6368.00	2.90	14.66	13.26
Reach-1	71.78	Q500	7407.00	3.14	15.73	14.22

Reach	River Sta	Profile	Q Total	Vel Chnl	Hydr Depth C	Hydr Radius C
			(m3/s)	(m/s)	(m)	(m)
Reach-1	71.78	PF 1	0.28	0.02	0.37	0.37
Reach-1	71.78	PF 2	0.85	0.05	0.42	0.41
Reach-1	71.78	PF 3	2.83	0.11	0.61	0.60
Reach-1	71.78	PF 4	8.50	0.19	1.07	1.04
Reach-1	71.78	PF 5	36.81	0.39	2.08	1.96
Reach-1	71.78	Q2	74.53	0.55	2.99	2.77
Reach-1	71.78	Q5	103.89	0.65	3.48	3.19
Reach-1	71.78	Q10	124.40	0.73	3.75	3.42
Reach-1	71.78	Q25	147.93	0.80	4.06	3.68
Reach-1	71.78	Q50	165.34	0.85	4.27	3.86
Reach-1	71.78	Q100	180.32	0.88	4.47	4.04
Reach-1	71.78	Q500	209.74	0.96	4.79	4.34

Site 1-6 Des Plaines River at Touhy upstream contracted velocity and depth data from HEC-RAS for input into SRICOS (U.S. Customary units (top) and SI units (bottom))

Reach	River Sta	Profile	Q Total	Vel Chnl	Hydr Depth C	Hydr Radius C
			(cfs)	(ft/s)	(ft)	(ft)
Reach-1	62.001	PF 1	10.00	0.07	1.17	1.15
Reach-1	62.001	PF 2	30.00	0.18	1.27	1.25
Reach-1	62.001	PF 3	100.00	0.45	1.61	1.58
Reach-1	62.001	PF 4	300.00	0.75	2.44	2.38
Reach-1	62.001	PF 5	1300.00	0.93	5.61	5.46
Reach-1	62.001	Q2	3053.00	1.27	9.20	8.77
Reach-1	62.001	Q5	4014.00	1.39	10.99	10.48
Reach-1	62.001	Q10	4575.00	1.47	11.87	11.32
Reach-1	62.001	Q25	5350.00	1.58	12.93	12.32
Reach-1	62.001	Q50	5908.00	1.64	13.71	13.07
Reach-1	62.001	Q100	6385.00	1.69	14.41	13.74
Reach-1	62.001	Q500	7339.00	1.78	15.76	15.03

Reach	River Sta	Profile	Q Total	Vel Chnl	Hydr Depth C	Hydr Radius C
			(m3/s)	(m/s)	(m)	(m)
Reach-1	62.001	PF 1	0.28	0.02	0.36	0.35
Reach-1	62.001	PF 2	0.85	0.06	0.39	0.38
Reach-1	62.001	PF 3	2.83	0.14	0.49	0.48
Reach-1	62.001	PF 4	8.50	0.23	0.74	0.73
Reach-1	62.001	PF 5	36.81	0.28	1.71	1.66
Reach-1	62.001	Q2	86.45	0.39	2.80	2.67
Reach-1	62.001	Q5	113.66	0.42	3.35	3.19
Reach-1	62.001	Q10	129.55	0.45	3.62	3.45
Reach-1	62.001	Q25	151.50	0.48	3.94	3.76
Reach-1	62.001	Q50	167.30	0.50	4.18	3.98
Reach-1	62.001	Q100	180.80	0.52	4.39	4.19
Reach-1	62.001	Q500	207.82	0.54	4.80	4.58

Site 1-7 Salt Creek at Route 83 upstream contracted velocity and depth data from HEC-RAS for input into SRICOS (U.S. Customary units (top) and SI units (bottom))

Reach	River Sta	Profile	Q Total	Vel Chnl	Hydr Depth C	Hydr Radius C
			(cfs)	(ft/s)	(ft)	(ft)
1	1055	PF 1	100.00	0.50	1.99	1.95
1	1055	PF 2	300.00	0.68	4.44	4.25
1	1055	PF 3	500.00	0.84	5.98	5.64
1	1055	PF 4	700.00	1.00	6.98	6.53
1	1055	PF 5	900.00	1.17	7.72	7.17
1	1055	Q2	1060.00	1.29	8.21	7.59
1	1055	Q10	1600.00	1.69	9.47	8.66
1	1055	Q50	2020.00	1.98	10.21	9.27
1	1055	Q100	2180.00	2.08	10.46	9.47
1	1055	Q500	2550.00	2.32	10.99	9.91

Reach	River Sta	Profile	Q Total	Vel Chnl	Hydr Depth C	Hydr Radius C
			(m3/s)	(m/s)	(m)	(m)
1	1055	PF 1	2.83	0.15	0.61	0.59
1	1055	PF 2	8.50	0.21	1.35	1.30
1	1055	PF 3	14.16	0.26	1.82	1.72
1	1055	PF 4	19.82	0.31	2.13	1.99
1	1055	PF 5	25.49	0.36	2.35	2.19
1	1055	Q2	30.02	0.39	2.50	2.31
1	1055	Q10	45.31	0.52	2.89	2.64
1	1055	Q50	57.20	0.60	3.11	2.82
1	1055	Q100	61.73	0.64	3.19	2.89
1	1055	Q500	72.21	0.71	3.35	3.02

Site 3-25 Indian Creek at Route 24 upstream contracted velocity and depth data from HEC-RAS for input into SRICOS (U.S. Customary units (top) and SI units (bottom))

Reach	River Sta	Profile	Q Total	Vel Chnl	Hydr Depth C	Hydr Radius C
			(cfs)	(ft/s)	(ft)	(ft)
1	5033	PF 1	10.00	0.26	0.81	0.76
1	5033	PF 2	200.00	1.22	2.17	2.06
1	5033	PF 3	800.00	2.39	4.02	3.78
1	5033	Q2	1770.00	3.35	6.00	5.63
1	5033	Q5	2850.00	4.09	7.81	7.34
1	5033	Q10	3590.00	4.51	8.83	8.29
1	5033	Q25	4480.00	4.95	9.92	9.32
1	5033	Q50	5170.00	5.26	10.68	10.04
1	5033	Q100	5780.00	5.52	11.31	10.63
1	5033	Q500	7240.00	6.08	12.66	11.90

Reach	River Sta	Profile	Q Total	Vel Chnl	Hydr Depth C	Hydr Radius C
			(m3/s)	(m/s)	(m)	(m)
1	5033	PF 1	0.28	0.08	0.25	0.23
1	5033	PF 2	5.66	0.37	0.66	0.63
1	5033	PF 3	22.65	0.73	1.22	1.15
1	5033	Q2	50.12	1.02	1.83	1.72
1	5033	Q5	80.70	1.25	2.38	2.24
1	5033	Q10	101.66	1.38	2.69	2.53
1	5033	Q25	126.86	1.51	3.02	2.84
1	5033	Q50	146.40	1.60	3.26	3.06
1	5033	Q100	163.67	1.68	3.45	3.24
1	5033	Q500	205.01	1.85	3.86	3.63

Site 4-5 LaMoine River at Route 61 upstream contracted velocity and depth data from HEC-RAS for input into SRICOS (U.S. Customary units (top) and SI units (bottom))

Reach	River Sta	Profile	Q Total	Vel Chnl	Hydr Depth C	Hydr Radius C
			(cfs)	(ft/s)	(ft)	(ft)
IL 61	1090.*	PF 1	10.00	0.11	1.83	1.81
IL 61	1090.*	PF 2	30.00	0.24	2.12	2.09
IL 61	1090.*	PF 3	300.00	0.96	4.32	4.19
IL 61	1090.*	PF 4	1000.00	1.82	6.87	6.50
IL 61	1090.*	PF 5	3000.00	3.15	10.49	9.62
IL 61	1090.*	Q2	8490.00	3.68	10.98	10.35
IL 61	1090.*	Q10	21300.00	4.81	15.84	14.93
IL 61	1090.*	Q50	35000.00	5.21	20.33	19.16
IL 61	1090.*	Q100	41300.00	5.21	22.58	21.28
IL 61	1090.*	Q500	57000.00	5.73	26.28	24.76

Reach	River Sta	Profile	Q Total	Vel Chnl	Hydr Depth C	Hydr Radius C
			(m3/s)	(m/s)	(m)	(m)
IL 61	1090.*	PF 1	0.28	0.03	0.56	0.55
IL 61	1090.*	PF 2	0.85	0.07	0.65	0.64
IL 61	1090.*	PF 3	8.50	0.29	1.32	1.28
IL 61	1090.*	PF 4	28.32	0.56	2.10	1.98
IL 61	1090.*	PF 5	84.95	0.96	3.20	2.93
IL 61	1090.*	Q2	240.41	1.12	3.35	3.15
IL 61	1090.*	Q10	603.15	1.47	4.83	4.55
IL 61	1090.*	Q50	991.09	1.59	6.20	5.84
IL 61	1090.*	Q100	1169.49	1.59	6.88	6.49
IL 61	1090.*	Q500	1614.06	1.75	8.01	7.55

Site 5-17 Kaskaskia River at County Road 1550N upstream contracted velocity and depth data from HEC-RAS for input into SRICOS (U.S. Customary units (top) and SI units (bottom))

Reach	River Sta	Profile	Q Total	Vel Chnl	Hydr Depth C	Hydr Radius C
			(cfs)	(ft/s)	(ft)	(ft)
1	1015	PF 1	100.00	1.03	1.85	1.82
1	1015	PF 2	175.00	1.33	2.40	2.35
1	1015	PF 3	300.00	1.68	3.10	3.01
1	1015	PF 4	500.00	2.06	3.99	3.83
1	1015	PF 5	1000.00	2.63	5.49	5.22
1	1015	PF 6	1500.00	2.83	6.52	6.19
1	1015	Q2	1810.00	2.92	7.02	6.66
1	1015	Q10	2860.00	3.12	8.17	7.79
1	1015	Q100	4080.00	3.38	9.12	8.72
1	1015	Q500	4900.00	3.58	10.34	9.89

Reach	River Sta	Profile	Q Total	Vel Chnl	Hydr Depth C	Hydr Radius C
			(m3/s)	(m/s)	(m)	(m)
1	1015	PF 1	2.83	0.31	0.56	0.55
1	1015	PF 2	4.96	0.41	0.73	0.72
1	1015	PF 3	8.50	0.51	0.95	0.92
1	1015	PF 4	14.16	0.63	1.22	1.17
1	1015	PF 5	28.32	0.80	1.67	1.59
1	1015	PF 6	42.48	0.86	1.99	1.89
1	1015	Q2	51.25	0.89	2.14	2.03
1	1015	Q10	80.99	0.95	2.49	2.37
1	1015	Q100	115.53	1.03	2.78	2.66
1	1015	Q500	138.75	1.09	3.15	3.02

Site 5-20 Lake Fork at County Road 100N upstream contracted velocity and depth data from HEC-RAS for input into SRICOS (U.S. Customary units (top) and SI units (bottom))

Reach	River Sta	Profile	Q Total	Vel Chnl	Hydr Depth C	Hydr Radius C
			(cfs)	(ft/s)	(ft)	(ft)
1	1020	PF 1	1.00	0.26	0.17	0.17
1	1020	PF 2	10.00	0.63	0.43	0.43
1	1020	PF 3	30.00	0.88	0.80	0.79
1	1020	PF 4	100.00	0.89	1.74	1.71
1	1020	PF 5	1000.00	1.35	6.51	6.25
1	1020	Q2	2230.00	1.79	10.11	9.70
1	1020	Q5	3010.00	2.06	11.59	11.12
1	1020	Q100	4650.00	2.58	13.89	13.33
1	1020	Q500	5320.00	2.77	14.68	14.09

Reach	River Sta	Profile	Q Total	Vel Chnl	Hydr Depth C	Hydr Radius C
			(m3/s)	(m/s)	(m)	(m)
1	1020	PF 1	0.03	0.08	0.05	0.05
1	1020	PF 2	0.28	0.19	0.13	0.13
1	1020	PF 3	0.85	0.27	0.24	0.24
1	1020	PF 4	2.83	0.27	0.53	0.52
1	1020	PF 5	28.32	0.41	1.99	1.91
1	1020	Q2	63.15	0.54	3.08	2.96
1	1020	Q5	85.23	0.63	3.53	3.39
1	1020	Q100	131.67	0.79	4.23	4.06
1	1020	Q500	150.65	0.84	4.47	4.29

Site 6-22 Spring Creek at Route 97 upstream contracted velocity and depth data from HEC-RAS for input into SRICOS (U.S. Customary units (top) and SI units (bottom))

Reach	River Sta	Profile	Q Total	Vel Right	Hydr Depth R	Hydr Radius R
			(cfs)	(ft/s)	(ft)	(ft)
1	835	PF 1	1.00			0.00
1	835	PF 2	10.00			0.00
1	835	PF 3	100.00			0.00
1	835	PF 4	300.00			0.00
1	835	Q2	1730.00	0.94	2.32	2.27
1	835	Q5	3760.00	1.71	4.58	4.45
1	835	Q25	8570.00	2.85	7.76	7.48
1	835	Q50	11200.00	3.29	9.02	8.66
1	835	Q100	14300.00	3.69	10.30	9.87
1	835	Q500	23100.00	4.39	12.62	11.95

Reach	River Sta	Profile	Q Total	Vel Right	Hydr Depth R	Hydr Radius R
			(m3/s)	(m/s)	(m)	(m)
1	835	PF 1	0.03			0.00
1	835	PF 2	0.28			0.00
1	835	PF 3	2.83			0.00
1	835	PF 4	8.50			0.00
1	835	Q2	48.99	0.29	0.71	0.69
1	835	Q5	106.47	0.52	1.40	1.36
1	835	Q25	242.68	0.87	2.37	2.28
1	835	Q50	317.15	1.00	2.75	2.64
1	835	Q100	404.93	1.12	3.14	3.01
1	835	Q500	654.12	1.34	3.85	3.64

Site 7-1 Little Wabash at Route 45 upstream contracted velocity and depth data from HEC-RAS for input into SRICOS (U.S. Customary units (top) and SI units (bottom))

Reach	River Sta	Profile	Q Total	Vel Chnl	Hydr Depth C	Hydr Radius C
			(cfs)	(ft/s)	(ft)	(ft)
1	1020	PF 1	10.00	1.05	0.36	0.36
1	1020	PF 2	30.00	1.64	0.57	0.57
1	1020	PF 3	100.00	2.53	0.92	0.91
1	1020	PF 4	300.00	2.11	1.94	1.92
1	1020	PF 5	1000.00	2.49	4.52	4.42
1	1020	Q2	11200.00	3.73	17.78	16.98
1	1020	Q10	24600.00	5.69	22.73	21.71
1	1020	Q50	41100.00	7.34	26.82	25.61
1	1020	Q100	49600.00	7.71	28.54	27.25
1	1020	Q500	73200.00	8.14	32.68	31.21

Reach	River Sta	Profile	Q Total	Vel Chnl	Hydr Depth C	Hydr Radius C
			(m3/s)	(m/s)	(m)	(m)
1	1020	PF 1	0.28	0.32	0.11	0.11
1	1020	PF 2	0.85	0.50	0.17	0.17
1	1020	PF 3	2.83	0.77	0.28	0.28
1	1020	PF 4	8.50	0.64	0.59	0.59
1	1020	PF 5	28.32	0.76	1.38	1.35
1	1020	Q2	317.15	1.14	5.42	5.17
1	1020	Q10	696.59	1.73	6.93	6.62
1	1020	Q50	1163.82	2.24	8.17	7.81
1	1020	Q100	1404.52	2.35	8.70	8.31
1	1020	Q500	2072.79	2.48	9.96	9.51

Site 7-18 Kaskakia River at Route 51 upstream contracted velocity and depth data from HEC-RAS for input into SRICOS (U.S. Customary units (top) and SI units (bottom))

Reach	River Sta	Profile	Q Total	Vel Chnl	Hydr Depth C	Hydr Radius C
			(cfs)	(ft/s)	(ft)	(ft)
US 40	2032	PF 1	10.00	0.05	2.57	2.55
US 40	2032	PF 2	500.00	0.91	5.81	5.65
US 40	2032	PF 3	2000.00	1.72	9.41	9.02
US 40	2032	PF 4	7000.00	1.74	13.49	12.89
US 40	2032	Q2	12700.00	2.25	15.60	14.90
US 40	2032	Q5	21800.00	3.27	16.67	15.91
US 40	2032	Q10	29200.00	5.03	17.37	16.57
US 40	2032	Q50	49800.00	4.44	18.79	17.92
US 40	2032	Q100	60500.00	4.32	19.33	18.43
US 40	2032	Q500	90400.00	4.10	20.63	19.65

Reach	River Sta	Profile	Q Total	Vel Chnl	Hydr Depth C	Hydr Radius C
			(m3/s)	(m/s)	(m)	(m)
US 40	2032	PF 1	0.28	0.02	0.78	0.78
US 40	2032	PF 2	14.16	0.28	1.77	1.72
US 40	2032	PF 3	56.63	0.52	2.87	2.75
US 40	2032	PF 4	198.22	0.53	4.11	3.93
US 40	2032	Q2	359.62	0.68	4.75	4.54
US 40	2032	Q5	617.31	1.00	5.08	4.85
US 40	2032	Q10	826.85	1.53	5.29	5.05
US 40	2032	Q50	1410.18	1.35	5.73	5.46
US 40	2032	Q100	1713.17	1.32	5.89	5.62
US 40	2032	Q500	2559.84	1.25	6.29	5.99

Site 8-3 Macoupin Creek at Route 67 upstream contracted velocity and depth data from HEC-RAS for input into SRICOS (U.S. Customary units (top) and SI units (bottom))

Reach	River Sta	Profile	Q Total	Vel Chnl	Hydr Depth C	Hydr Radius C
			(cfs)	(ft/s)	(ft)	(ft)
Reach-1	3.3	PF 1	10.00	0.67	0.49	0.49
Reach-1	3.3	PF 2	100.00	1.09	0.98	0.97
Reach-1	3.3	PF 3	1000.00	1.77	4.76	4.65
Reach-1	3.3	PF 4	5000.00	2.93	10.71	10.33
Reach-1	3.3	PF 5	12000.00	3.84	15.89	15.25
Reach-1	3.3	PF 6	26000.00	5.76	20.45	19.62
Reach-1	3.3	PF 7	31000.00	6.31	21.69	20.82
Reach-1	3.3	PF 8	36000.00	6.78	22.94	22.02
Reach-1	3.3	Q100	40700.00	7.16	24.09	23.12
Reach-1	3.3	Q500	52800.00	7.20	27.37	26.27

Reach	River Sta	Profile	Q Total	Vel Chnl	Hydr Depth C	Hydr Radius C
			(m3/s)	(m/s)	(m)	(m)
Reach-1	3.3	PF 1	0.28	0.20	0.15	0.15
Reach-1	3.3	PF 2	2.83	0.33	0.30	0.30
Reach-1	3.3	PF 3	28.32	0.54	1.45	1.42
Reach-1	3.3	PF 4	141.58	0.89	3.26	3.15
Reach-1	3.3	PF 5	339.80	1.17	4.84	4.65
Reach-1	3.3	PF 6	736.24	1.76	6.23	5.98
Reach-1	3.3	PF 7	877.82	1.92	6.61	6.34
Reach-1	3.3	PF 8	1019.41	2.07	6.99	6.71
Reach-1	3.3	Q100	1152.50	2.18	7.34	7.05
Reach-1	3.3	Q500	1495.13	2.20	8.34	8.01

Site 8-50 Little Crooked Creek at Route 177 upstream contracted velocity and depth data from HEC-RAS for input into SRICOS (U.S. Customary units (top) and SI units (bottom))

Reach	River Sta	Profile	Q Total	Vel Right	Hydr Depth R	Hydr Radius R
			(cfs)	(ft/s)	(ft)	(ft)
Reach-1	4	PF 1	1.00			0.00
Reach-1	4	PF 2	10.00			0.00
Reach-1	4	PF 3	100.00			0.03
Reach-1	4	PF 4	500.00	0.56	1.11	1.06
Reach-1	4	PF 5	1000.00	0.82	2.53	2.46
Reach-1	4	PF 6	3000.00	1.69	6.03	5.81
Reach-1	4	PF 7	7500.00	3.09	8.68	8.32
Reach-1	4	PF 8	17000.00	4.97	11.72	11.04
Reach-1	4	Q100	17600.00	5.02	11.87	11.18
Reach-1	4	Q500	23400.00	2.39	2.57	2.55

Reach	River Sta	Profile	Q Total	Vel Right	Hydr Depth R	Hydr Radius R
			(m3/s)	(m/s)	(m)	(m)
Reach-1	4	PF 1	0.03			0.00
Reach-1	4	PF 2	0.28			0.00
Reach-1	4	PF 3	2.83			0.01
Reach-1	4	PF 4	14.16	0.17	0.34	0.32
Reach-1	4	PF 5	28.32	0.25	0.77	0.75
Reach-1	4	PF 6	84.95	0.51	1.84	1.77
Reach-1	4	PF 7	212.38	0.94	2.65	2.54
Reach-1	4	PF 8	481.39	1.51	3.57	3.36
Reach-1	4	Q100	498.38	1.53	3.62	3.41
Reach-1	4	Q500	662.61	0.73	0.78	0.78

Site 9-1 Big Muddy River at Route 149 near Plumfield upstream contracted velocity and depth data from HEC-RAS for input into SRICOS (U.S. Customary units (top) and SI units (bottom))

Reach	River Sta	Profile	Q Total	Vel Chnl	Hydr Depth C	Hydr Radius C
			(cfs)	(ft/s)	(ft)	(ft)
1	1220	PF 1	30.00	0.39	1.05	1.05
1	1220	PF 2	100.00	0.44	2.40	2.39
1	1220	PF 3	300.00	0.61	3.62	3.59
1	1220	PF 4	1000.00	0.91	5.97	5.89
1	1220	PF 5	3000.00	1.26	11.49	11.33
1	1220	PF 6	7000.00	1.93	16.57	16.32
1	1220	PF 7	17000.00	3.36	22.31	21.98
1	1220	Q100	28100.00	4.86	25.96	25.58
1	1220	Q500	36100.00	4.97	28.26	27.85

Reach	River Sta	Profile	Q Total	Vel Chnl	Hydr Depth C	Hydr Radius C
			(m3/s)	(m/s)	(m)	(m)
1	1220	PF 1	0.85	0.12	0.32	0.32
1	1220	PF 2	2.83	0.13	0.73	0.73
1	1220	PF 3	8.50	0.18	1.10	1.09
1	1220	PF 4	28.32	0.28	1.82	1.80
1	1220	PF 5	84.95	0.38	3.50	3.45
1	1220	PF 6	198.22	0.59	5.05	4.98
1	1220	PF 7	481.39	1.02	6.80	6.70
1	1220	Q100	795.70	1.48	7.91	7.80
1	1220	Q500	1022.24	1.51	8.61	8.49

Site 9-2 Big Muddy River near Murphysboro upstream contracted velocity and depth data from HEC-RAS for input into SRICOS (U.S. Customary units (top) and SI units (bottom))

Reach	River Sta	Profile	Q Total	Vel Chnl	Hydr Depth C	Hydr Radius C
			(cfs)	(ft/s)	(ft)	(ft)
1	1030	PF 1	10.00	0.01	8.11	7.46
1	1030	PF 2	300.00	0.24	9.67	8.92
1	1030	PF 3	1000.00	0.60	11.26	10.42
1	1030	PF 4	3000.00	1.22	14.16	13.12
1	1030	PF 5	10000.00	2.22	20.47	19.11
1	1030	PF 6	20000.00	3.02	29.46	27.50
1	1030	Q25	32700.00	3.99	36.00	33.61
1	1030	Q50	37800.00	4.36	37.86	35.35
1	1030	Q100	42800.00	4.75	39.56	36.94
1	1030	Q500	54300.00	5.29	43.06	40.20

Reach	River Sta	Profile	Q Total	Vel Chnl	Hydr Depth C	Hydr Radius C
			(m3/s)	(m/s)	(m)	(m)
1	1030	PF 1	0.28	0.00	2.47	2.27
1	1030	PF 2	8.50	0.07	2.95	2.72
1	1030	PF 3	28.32	0.18	3.43	3.18
1	1030	PF 4	84.95	0.37	4.32	4.00
1	1030	PF 5	283.17	0.68	6.24	5.82
1	1030	PF 6	566.34	0.92	8.98	8.38
1	1030	Q25	925.96	1.22	10.97	10.24
1	1030	Q50	1070.38	1.33	11.54	10.77
1	1030	Q100	1211.96	1.45	12.06	11.26
1	1030	Q500	1537.61	1.61	13.13	12.25

APPENDIX D – HEC-18 REPORTS

Site 1-1 Des Plaines River at Cermak 100-year Flood HEC-18 Report

Contraction Scour				
		Left	Channel	Right
Input Data				
	Average Depth (ft):	3.67	11.30	2.00
	Approach Velocity (ft/s):	0.19	1.70	0.13
	Br Average Depth (ft):		13.19	
	BR Opening Flow (cfs):		6863.00	
	BR Top WD (ft):		232.42	
	Grain Size D50 (mm):		0.01	
	Approach Flow (cfs):	423.72	6428.25	11.03
	Approach Top WD (ft):	601.25	335.00	43.80
	K1 Coefficient:	0.590	0.690	0.590
Results				
	Scour Depth Ys (ft):		2.19	
	Critical Velocity (ft/s):		0.54	
	Equation:		Live	

Pier Scour		
	All piers have the same scour depth	
Input Data		
	Pier Shape:	Round nose
	Pier Width (ft):	3.50
	Grain Size D50 (mm):	0.01000
	Depth Upstream (ft):	13.26
	Velocity Upstream (ft/s):	2.13
	K1 Nose Shape:	1.00
	Pier Angle:	0.00
	Pier Length (ft):	130.00
	K2 Angle Coef:	1.00
	K3 Bed Cond Coef:	1.10
	Grain Size D90 (mm):	
	K4 Armouring Coef:	1.00
Results		
	Scour Depth Ys (ft):	4.62
	Froude #:	0.10
	Equation:	CSU equation

Site 1-1 Des Plaines River at Cermak 500-year Flood HEC-18 Report

Contraction Scour				
		Left	Channel	Right
Input Data				
	Average Depth (ft):	3.93	12.20	1.97
	Approach Velocity (ft/s):	0.20	1.76	0.12
	Br Average Depth (ft):		13.44	
	BR Opening Flow (cfs):		7767.00	
	BR Top WD (ft):		232.42	
	Grain Size D50 (mm):		0.01	
	Approach Flow (cfs):	553.79	7195.99	17.22
	Approach Top WD (ft):	715.31	335.00	70.69
	K1 Coefficient:	0.590	0.690	0.590
Results				
	Scour Depth Ys (ft):		3.32	
	Critical Velocity (ft/s):		0.54	
	Equation:		Live	

Pier Scour		
	All piers have the same scour depth	
Input Data		
	Pier Shape:	Round nose
	Pier Width (ft):	3.50
	Grain Size D50 (mm):	0.01000
	Depth Upstream (ft):	14.15
	Velocity Upstream (ft/s):	2.26
	K1 Nose Shape:	1.00
	Pier Angle:	0.00
	Pier Length (ft):	130.00
	K2 Angle Coef:	1.00
	K3 Bed Cond Coef:	1.10
	Grain Size D90 (mm):	
	K4 Armouring Coef:	1.00
Results		
	Scour Depth Ys (ft):	4.78
	Froude #:	0.11
	Equation:	CSU equation

Site 1-4 Des Plaines River at Palatine Road (south bridge) 100-year Flood HEC-18 Report

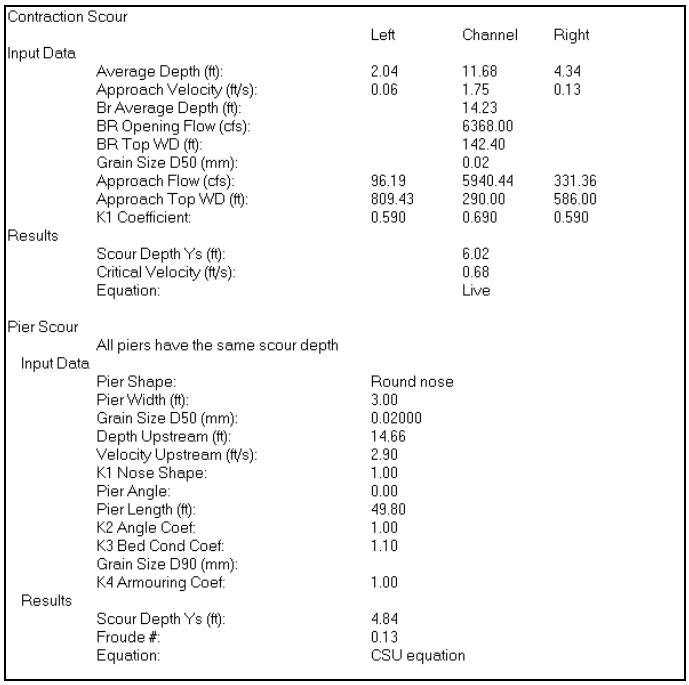

Contraction Scour				
		Left	Channel	Right
Input Data				
	Average Depth (ft):	2.04	11.68	4.34
	Approach Velocity (ft/s):	0.06	1.75	0.13
	Br Average Depth (ft):		14.23	
	BR Opening Flow (cfs):		6368.00	
	BR Top WD (ft):		142.40	
	Grain Size D50 (mm):		0.02	
	Approach Flow (cfs):	96.19	5940.44	331.36
	Approach Top WD (ft):	809.43	290.00	586.00
	K1 Coefficient:	0.590	0.690	0.590
Results				
	Scour Depth Ys (ft):		6.02	
	Critical Velocity (ft/s):		0.68	
	Equation:		Live	

Pier Scour		
	All piers have the same scour depth	
Input Data		
	Pier Shape:	Round nose
	Pier Width (ft):	3.00
	Grain Size D50 (mm):	0.02000
	Depth Upstream (ft):	14.66
	Velocity Upstream (ft/s):	2.90
	K1 Nose Shape:	1.00
	Pier Angle:	0.00
	Pier Length (ft):	49.80
	K2 Angle Coef:	1.00
	K3 Bed Cond Coef:	1.10
	Grain Size D90 (mm):	
	K4 Armouring Coef:	1.00
Results		
	Scour Depth Ys (ft):	4.84
	Froude #:	0.13
	Equation:	CSU equation

Site 1-4 Des Plaines River at Palatine Road (south bridge) 500-year Flood HEC-18 Report

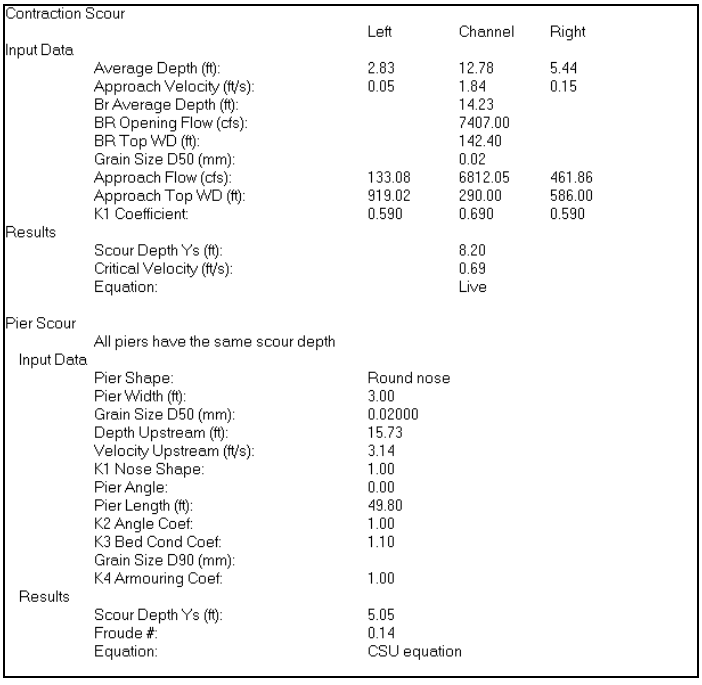

Contraction Scour				
		Left	Channel	Right
Input Data				
	Average Depth (ft):	2.83	12.78	5.44
	Approach Velocity (ft/s):	0.05	1.84	0.15
	Br Average Depth (ft):		14.23	
	BR Opening Flow (cfs):		7407.00	
	BR Top WD (ft):		142.40	
	Grain Size D50 (mm):		0.02	
	Approach Flow (cfs):	133.08	6812.05	461.86
	Approach Top WD (ft):	919.02	290.00	586.00
	K1 Coefficient:	0.590	0.690	0.590
Results				
	Scour Depth Ys (ft):		8.20	
	Critical Velocity (ft/s):		0.69	
	Equation:		Live	

Pier Scour		
	All piers have the same scour depth	
Input Data		
	Pier Shape:	Round nose
	Pier Width (ft):	3.00
	Grain Size D50 (mm):	0.02000
	Depth Upstream (ft):	15.73
	Velocity Upstream (ft/s):	3.14
	K1 Nose Shape:	1.00
	Pier Angle:	0.00
	Pier Length (ft):	49.80
	K2 Angle Coef:	1.00
	K3 Bed Cond Coef:	1.10
	Grain Size D90 (mm):	
	K4 Armouring Coef:	1.00
Results		
	Scour Depth Ys (ft):	5.05
	Froude #:	0.14
	Equation:	CSU equation

Site 1-6 Des Plaines River at Touhy 100-year Flood HEC-18 Report

Contraction Scour				
		Left	Channel	Right
Input Data				
	Average Depth (ft):	2.65	12.28	3.43
	Approach Velocity (ft/s):	0.15	1.72	0.18
	Br Average Depth (ft):		13.57	
	BR Opening Flow (cfs):		6385.00	
	BR Top WD (ft):		177.30	
	Grain Size D50 (mm):		0.01	
	Approach Flow (cfs):	20.66	6312.95	51.39
	Approach Top WD (ft):	53.04	298.50	85.60
	K1 Coefficient:	0.590	0.690	0.590
Results				
	Scour Depth Ys (ft):		4.19	
	Critical Velocity (ft/s):		0.55	
	Equation:		Live	

Pier Scour		
	All piers have the same scour depth	
Input Data		
	Pier Shape:	Round nose
	Pier Width (ft):	21.20
	Grain Size D50 (mm):	0.01000
	Depth Upstream (ft):	14.41
	Velocity Upstream (ft/s):	1.69
	K1 Nose Shape:	1.00
	Pier Angle:	0.00
	Pier Length (ft):	61.80
	K2 Angle Coef:	1.00
	K3 Bed Cond Coef:	1.10
	Grain Size D90 (mm):	
	K4 Armouring Coef:	1.00
Results		
	Scour Depth Ys (ft):	13.64
	Froude #:	0.08
	Equation:	CSU equation

Site 1-6 Des Plaines River at Touhy 500-year Flood HEC-18 Report

Contraction Scour				
		Left	Channel	Right
Input Data				
	Average Depth (ft):	3.08	13.63	3.14
	Approach Velocity (ft/s):	0.16	1.78	0.18
	Br Average Depth (ft):		13.57	
	BR Opening Flow (cfs):		7339.00	
	BR Top WD (ft):		177.30	
	Grain Size D50 (mm):		0.01	
	Approach Flow (cfs):	35.40	7227.64	75.96
	Approach Top WD (ft):	73.32	298.50	135.22
	K1 Coefficient:	0.590	0.690	0.590
Results				
	Scour Depth Ys (ft):		6.21	
	Critical Velocity (ft/s):		0.56	
	Equation:		Live	

Pier Scour		
	All piers have the same scour depth	
Input Data		
	Pier Shape:	Round nose
	Pier Width (ft):	21.20
	Grain Size D50 (mm):	0.01000
	Depth Upstream (ft):	15.76
	Velocity Upstream (ft/s):	1.78
	K1 Nose Shape:	1.00
	Pier Angle:	0.00
	Pier Length (ft):	61.80
	K2 Angle Coef:	1.00
	K3 Bed Cond Coef:	1.10
	Grain Size D90 (mm):	
	K4 Armouring Coef:	1.00
Results		
	Scour Depth Ys (ft):	14.10
	Froude #:	0.08
	Equation:	CSU equation

Site 1-7 Salt Creek at Route 83 100-year Flood HEC-18 Report

Contraction Scour				
		Left	Channel	Right
Input Data				
	Average Depth (ft):		8.14	1.42
	Approach Velocity (ft/s):		2.69	0.82
	Br Average Depth (ft):		10.40	
	BR Opening Flow (cfs):		2180.00	
	BR Top WD (ft):		95.91	
	Grain Size D50 (mm):		0.13	
	Approach Flow (cfs):		2172.42	7.58
	Approach Top WD (ft):		99.01	6.53
	K1 Coefficient:		0.690	0.590
Results				
	Scour Depth Ys (ft):		0.00	
	Critical Velocity (ft/s):		1.20	
	Equation:		Live	

Pier Scour		
	All piers have the same scour depth	
Input Data		
	Pier Shape:	Square nose
	Pier Width (ft):	2.44
	Grain Size D50 (mm):	0.13000
	Depth Upstream (ft):	10.46
	Velocity Upstream (ft/s):	2.08
	K1 Nose Shape:	1.10
	Pier Angle:	0.00
	Pier Length (ft):	109.80
	K2 Angle Coef:	1.00
	K3 Bed Cond Coef:	1.10
	Grain Size D90 (mm):	
	K4 Armouring Coef:	1.00
Results		
	Scour Depth Ys (ft):	3.86
	Froude #:	0.11
	Equation:	CSU equation

Site 1-7 Salt Creek at Route 83 500-year Flood HEC-18 Report

Contraction Scour				
		Left	Channel	Right
Input Data				
	Average Depth (ft):		8.67	1.69
	Approach Velocity (ft/s):		2.96	0.96
	Br Average Depth (ft):		10.92	
	BR Opening Flow (cfs):		2550.00	
	BR Top WD (ft):		95.96	
	Grain Size D50 (mm):		0.13	
	Approach Flow (cfs):		2537.44	12.56
	Approach Top WD (ft):		99.00	7.74
	K1 Coefficient:	0.590	0.690	
Results				
	Scour Depth Ys (ft):		0.00	
	Critical Velocity (ft/s):		1.21	
	Equation:		Live	

Pier Scour		
	All piers have the same scour depth	
Input Data		
	Pier Shape:	Square nose
	Pier Width (ft):	2.44
	Grain Size D50 (mm):	0.13000
	Depth Upstream (ft):	10.99
	Velocity Upstream (ft/s):	2.32
	K1 Nose Shape:	1.10
	Pier Angle:	0.00
	Pier Length (ft):	109.80
	K2 Angle Coef:	1.00
	K3 Bed Cond Coef:	1.10
	Grain Size D90 (mm):	
	K4 Armouring Coef:	1.00
Results		
	Scour Depth Ys (ft):	4.07
	Froude #:	0.12
	Equation:	CSU equation

Site 3-25 Indian Creek at Route 24 100-year Flood HEC-18 Report

Contraction Scour				
		Left	Channel	Right
Input Data				
	Average Depth (ft):	1.85	9.70	0.93
	Approach Velocity (ft/s):	1.39	6.50	0.75
	Br Average Depth (ft):	3.90	11.15	3.10
	BR Opening Flow (cfs):	275.17	5366.00	138.84
	BR Top WD (ft):	18.11	82.92	13.60
	Grain Size D50 (mm):	0.06	0.06	0.06
	Approach Flow (cfs):	60.10	5670.47	49.43
	Approach Top WD (ft):	23.33	90.00	71.23
	K1 Coefficient:	0.690	0.690	0.690
Results				
	Scour Depth Ys (ft):	4.22	0.00	3.96
	Critical Velocity (ft/s):	0.72	0.95	0.64
	Equation:	Live	Live	Live

Pier Scour		
	All piers have the same scour depth	
Input Data		
	Pier Shape:	Round nose
	Pier Width (ft):	2.50
	Grain Size D50 (mm):	0.06000
	Depth Upstream (ft):	11.31
	Velocity Upstream (ft/s):	5.52
	K1 Nose Shape:	1.00
	Pier Angle:	0.00
	Pier Length (ft):	46.00
	K2 Angle Coef:	1.00
	K3 Bed Cond Coef:	1.10
	Grain Size D90 (mm):	
	K4 Armouring Coef:	1.00
Results		
	Scour Depth Ys (ft):	5.47
	Froude #:	0.29
	Equation:	CSU equation

Site 3-25 Indian Creek at Route 24 500-year Flood HEC-18 Report

Contraction Scour				
		Left	Channel	Right
Input Data				
	Average Depth (ft):	2.53	11.06	1.45
	Approach Velocity (ft/s):	1.68	6.93	0.99
	Br Average Depth (ft):	4.64	12.50	3.78
	BR Opening Flow (cfs):	438.41	6558.30	243.30
	BR Top WD (ft):	20.87	82.92	16.57
	Grain Size D50 (mm):	0.06	0.06	0.06
	Approach Flow (cfs):	135.76	6899.08	205.16
	Approach Top WD (ft):	31.95	115.17	143.32
	K1 Coefficient:	0.690	0.690	0.690
Results				
	Scour Depth Ys (ft):	4.63	0.78	3.66
	Critical Velocity (ft/s):	0.76	0.97	0.69
	Equation:	Live	Live	Live

Pier Scour		
	All piers have the same scour depth	
Input Data		
	Pier Shape:	Round nose
	Pier Width (ft):	2.50
	Grain Size D50 (mm):	0.06000
	Depth Upstream (ft):	12.66
	Velocity Upstream (ft/s):	6.08
	K1 Nose Shape:	1.00
	Pier Angle:	0.00
	Pier Length (ft):	46.00
	K2 Angle Coef:	1.00
	K3 Bed Cond Coef:	1.10
	Grain Size D90 (mm):	
	K4 Armouring Coef:	1.00
Results		
	Scour Depth Ys (ft):	5.79
	Froude #:	0.30
	Equation:	CSU equation

Site 4-5 LaMoine River at Route 61 100-year Flood HEC-18 Report

Contraction Scour				
		Left	Channel	Right
Input Data				
	Average Depth (ft):	13.41	22.58	12.28
	Approach Velocity (ft/s):	4.46	5.21	2.93
	Br Average Depth (ft):		29.51	
	BR Opening Flow (cfs):	2438.35	38291.86	569.79
	BR Top WD (ft):		146.70	
	Grain Size D50 (mm):	0.00	.02	0.00
	Approach Flow (cfs):	11415.57	23234.43	6650.00
	Approach Top WD (ft):	191.00	197.50	184.83
	K1 Coefficient:	0.590	0.690	0.590
Results				
	Scour Depth Ys (ft):		13.03	
	Critical Velocity (ft/s):		0.76	
	Equation:		Live	

Pier Scour		
Pier: #4 (CL = 32.5)		
Input Data		
	Pier Shape:	Round nose
	Pier Width (ft):	3.99
	Grain Size D50 (mm):	0.02000
	Depth Upstream (ft):	29.30
	Velocity Upstream (ft/s):	4.34
	K1 Nose Shape:	1.00
	Pier Angle:	0.00
	Pier Length (ft):	42.00
	K2 Angle Coef:	1.00
	K3 Bed Cond Coef:	1.10
	Grain Size D90 (mm):	
	K4 Armouring Coef:	1.00
Results		
	Scour Depth Ys (ft):	7.60
	Froude #:	0.14
	Equation:	CSU equation

Site 4-5 LaMoine River at Route 61 500-year Flood HEC-18 Report

Contraction Scour				
		Left	Channel	Right
Input Data				
	Average Depth (ft):	17.10	26.28	15.98
	Approach Velocity (ft/s):	5.21	5.73	3.47
	Br Average Depth (ft):	5.72	23.85	6.35
	BR Opening Flow (cfs):	14203.53	36529.89	6266.58
	BR Top WD (ft):	1191.50	146.70	450.50
	Grain Size D50 (mm):	0.02	0.02	0.02
	Approach Flow (cfs):	17025.40	29728.51	10246.09
	Approach Top WD (ft):	191.00	197.50	184.83
	K1 Coefficient:	0.690	0.690	0.690
Results				
	Scour Depth Ys (ft):	0.00	14.65	0.00
	Critical Velocity (ft/s):	0.73	0.78	0.72
	Equation:	Live	Live	Live

Pier: #4 (CL = 32.5)		
Input Data		
	Pier Shape:	Round nose
	Pier Width (ft):	3.99
	Grain Size D50 (mm):	0.02000
	Depth Upstream (ft):	36.31
	Velocity Upstream (ft/s):	4.43
	K1 Nose Shape:	1.00
	Pier Angle:	0.00
	Pier Length (ft):	42.00
	K2 Angle Coef:	1.00
	K3 Bed Cond Coef:	1.10
	Grain Size D90 (mm):	
	K4 Armouring Coef:	1.00
Results		
	Scour Depth Ys (ft):	7.89
	Froude #:	0.13
	Equation:	CSU equation

Site 5-17 Kaskaskia River at County Road 1550N 100-year Flood HEC-18 Report

Contraction Scour				
		Left	Channel	Right
Input Data				
	Average Depth (ft):	0.26	8.69	0.27
	Approach Velocity (ft/s):	0.20	3.24	0.39
	Br Average Depth (ft):		9.66	
	BR Opening Flow (cfs):		4080.00	0.00
	BR Top WD (ft):		125.00	
	Grain Size D50 (mm):	0.02	0.02	0.02
	Approach Flow (cfs):	1.53	4078.33	0.14
	Approach Top WD (ft):	29.14	144.92	1.31
	K1 Coefficient:	0.690	0.690	0.690
Results				
	Scour Depth Ys (ft):		0.00	
	Critical Velocity (ft/s):		0.65	
	Equation:		Live	

Pier Scour		
	All piers have the same scour depth	
Input Data		
	Pier Shape:	Round nose
	Pier Width (ft):	1.00
	Grain Size D50 (mm):	0.02000
	Depth Upstream (ft):	9.12
	Velocity Upstream (ft/s):	3.38
	K1 Nose Shape:	1.00
	Pier Angle:	0.00
	Pier Length (ft):	29.80
	K2 Angle Coef:	1.00
	K3 Bed Cond Coef:	1.10
	Grain Size D90 (mm):	
	K4 Armouring Coef:	1.00
Results		
	Scour Depth Ys (ft):	2.37
	Froude #:	0.20
	Equation:	CSU equation

Site 5-17 Kaskaskia River at County Road 1550N 500-year Flood HEC-18 Report

Contraction Scour				
		Left	Channel	Right
Input Data				
	Average Depth (ft):	0.88	9.93	0.75
	Approach Velocity (ft/s):	0.43	3.38	0.76
	Br Average Depth (ft):		9.66	
	BR Opening Flow (cfs):		4900.00	0.00
	BR Top WD (ft):		125.00	
	Grain Size D50 (mm):	0.02	0.02	0.02
	Approach Flow (cfs):	36.77	4858.90	4.33
	Approach Top WD (ft):	97.69	144.92	7.64
	K1 Coefficient:	0.690	0.690	0.690
Results				
	Scour Depth Ys (ft):		1.42	
	Critical Velocity (ft/s):		0.66	
	Equation:		Live	

Pier Scour		
	All piers have the same scour depth	
Input Data		
	Pier Shape:	Round nose
	Pier Width (ft):	1.00
	Grain Size D50 (mm):	0.02000
	Depth Upstream (ft):	10.34
	Velocity Upstream (ft/s):	3.58
	K1 Nose Shape:	1.00
	Pier Angle:	0.00
	Pier Length (ft):	29.80
	K2 Angle Coef:	1.00
	K3 Bed Cond Coef:	1.10
	Grain Size D90 (mm):	
	K4 Armouring Coef:	1.00
Results		
	Scour Depth Ys (ft):	2.40
	Froude #:	0.20
	Equation:	CSU equation
	Pier Scour Limited to Maximum of Ys = 2.4 * a	

Site 5-20 Lake Fork at County Road 100N 100-year Flood HEC-18 Report

Contraction Scour				
		Left	Channel	Right
Input Data				
	Average Depth (ft):	3.69	12.07	2.92
	Approach Velocity (ft/s):	1.13	2.38	0.89
	Br Average Depth (ft):		11.50	
	BR Opening Flow (cfs):	20.46	3887.09	742.44
	BR Top WD (ft):		108.38	
	Grain Size D50 (mm):	0.01	0.01	0.01
	Approach Flow (cfs):	302.88	4202.05	145.07
	Approach Top WD (ft):	73.03	146.53	55.76
	K1 Coefficient:	0.690	0.690	0.690
Results				
	Scour Depth Ys (ft):		2.40	
	Critical Velocity (ft/s):		0.54	
	Equation:		Live	
Pier Scour				
	All piers have the same scour depth			
Input Data				
	Pier Shape:	Round nose		
	Pier Width (ft):	4.50		
	Grain Size D50 (mm):	0.01000		
	Depth Upstream (ft):	13.89		
	Velocity Upstream (ft/s):	2.58		
	K1 Nose Shape:	1.00		
	Pier Angle:	0.00		
	Pier Length (ft):	38.00		
	K2 Angle Coef:	1.00		
	K3 Bed Cond Coef:	1.10		
	Grain Size D90 (mm):			
	K4 Armouring Coef:	1.00		
Results				
	Scour Depth Ys (ft):	5.94		
	Froude #:	0.12		
	Equation:	CSU equation		

Site 5-20 Lake Fork at County Road 100N 500-year Flood HEC-18 Report

Contraction Scour				
		Left	Channel	Right
Input Data				
	Average Depth (ft):	4.05	12.87	3.30
	Approach Velocity (ft/s):	1.24	2.49	0.97
	Br Average Depth (ft):		11.50	
	BR Opening Flow (cfs):	23.41	4447.17	849.42
	BR Top WD (ft):		108.38	
	Grain Size D50 (mm):	0.02	0.02	0.02
	Approach Flow (cfs):	411.04	4703.75	205.20
	Approach Top WD (ft):	81.92	146.53	63.79
	K1 Coefficient:	0.690	0.690	0.690
Results				
	Scour Depth Ys (ft):		3.60	
	Critical Velocity (ft/s):		0.69	
	Equation:		Live	
Pier Scour				
	All piers have the same scour depth			
Input Data				
	Pier Shape:	Round nose		
	Pier Width (ft):	4.50		
	Grain Size D50 (mm):	0.02000		
	Depth Upstream (ft):	14.68		
	Velocity Upstream (ft/s):	2.77		
	K1 Nose Shape:	1.00		
	Pier Angle:	0.00		
	Pier Length (ft):	38.00		
	K2 Angle Coef:	1.00		
	K3 Bed Cond Coef:	1.10		
	Grain Size D90 (mm):			
	K4 Armouring Coef:	1.00		
Results				
	Scour Depth Ys (ft):	6.17		
	Froude #:	0.13		
	Equation:	CSU equation		

Site 6-22 Spring Creek at Route 97 100-year Flood HEC-18 Report

Contraction Scour				
		Left	Channel	Right
Input Data				
	Average Depth (ft):	11.09	15.18	9.51
	Approach Velocity (ft/s):	2.40	4.78	1.80
	Br Average Depth (ft):	13.10	17.66	10.19
	BR Opening Flow (cfs):	4872.77	6150.03	3277.20
	BR Top WD (ft):	68.14	54.48	84.34
	Grain Size D50 (mm):	0.02	0.02	0.02
	Approach Flow (cfs):	5565.82	3992.03	4742.14
	Approach Top WD (ft):	209.27	55.00	276.75
	K1 Coefficient:	0.690	0.690	0.690
Results				
	Scour Depth Ys (ft):	8.36	4.47	5.54
	Critical Velocity (ft/s):	0.68	0.71	0.66
	Equation:	Live	Live	Live

Pier Scour		
	All piers have the same scour depth	
Input Data		
	Pier Shape:	Round nose
	Pier Width (ft):	2.25
	Grain Size D50 (mm):	0.02000
	Depth Upstream (ft):	17.75
	Velocity Upstream (ft/s):	5.26
	K1 Nose Shape:	1.00
	Pier Angle:	0.00
	Pier Length (ft):	93.17
	K2 Angle Coef:	1.00
	K3 Bed Cond Coef:	1.10
	Grain Size D90 (mm):	
	K4 Armouring Coef:	1.00
Results		
	Scour Depth Ys (ft):	5.32
	Froude #:	0.22
	Equation:	CSU equation

Site 6-22 Spring Creek at Route 97 500-year Flood HEC-18 Report

Contraction Scour				
		Left	Channel	Right
Input Data				
	Average Depth (ft):	14.47	19.20	12.96
	Approach Velocity (ft/s):	2.79	5.56	2.20
	Br Average Depth (ft):	14.48	15.88	14.41
	BR Opening Flow (cfs):	8411.02	8329.37	6359.61
	BR Top WD (ft):	80.30	54.48	63.76
	Grain Size D50 (mm):	0.02	0.02	0.02
	Approach Flow (cfs):	8934.26	5866.98	8298.76
	Approach Top WD (ft):	221.00	55.00	290.87
	K1 Coefficient:	0.690	0.690	0.690
Results				
	Scour Depth Ys (ft):	13.15	10.22	14.99
	Critical Velocity (ft/s):	0.71	0.74	0.69
	Equation:	Live	Live	Live

Pier Scour		
	All piers have the same scour depth	
Input Data		
	Pier Shape:	Round nose
	Pier Width (ft):	2.25
	Grain Size D50 (mm):	0.02000
	Depth Upstream (ft):	21.76
	Velocity Upstream (ft/s):	6.00
	K1 Nose Shape:	1.00
	Pier Angle:	0.00
	Pier Length (ft):	93.17
	K2 Angle Coef:	1.00
	K3 Bed Cond Coef:	1.10
	Grain Size D90 (mm):	
	K4 Armouring Coef:	1.00
Results		
	Scour Depth Ys (ft):	5.40
	Froude #:	0.23
	Equation:	CSU equation
	Pier Scour Limited to Maximum of Ys = 2.4 * a	

Site 7-1 Little Wabash at Route 45 100-year Flood HEC-18 Report

Contraction Scour				
		Left	Channel	Right
Input Data				
	Average Depth (ft):	9.86	25.37	5.30
	Approach Velocity (ft/s):	0.88	5.02	0.58
	Br Average Depth (ft):	5.54	25.60	2.53
	BR Opening Flow (cfs):	12713.23	32354.57	4532.19
	BR Top WD (ft):	1614.69	153.80	1707.25
	Grain Size D50 (mm):	0.03	0.03	0.03
	Approach Flow (cfs):	19986.13	23685.61	5928.27
	Approach Top WD (ft):	2308.48	185.91	1930.30
	K1 Coefficient:	0.690	0.690	0.690
Results				
	Scour Depth Ys (ft):	3.02	12.18	1.24
	Critical Velocity (ft/s):	0.76	0.89	0.68
	Equation:	Live	Live	Clear

Pier: #9 (CL = 128318.8)		
Input Data		
	Pier Shape:	Round nose
	Pier Width (ft):	2.81
	Grain Size D50 (mm):	0.03000
	Depth Upstream (ft):	28.49
	Velocity Upstream (ft/s):	7.71
	K1 Nose Shape:	1.00
	Pier Angle:	0.00
	Pier Length (ft):	36.00
	K2 Angle Coef:	1.00
	K3 Bed Cond Coef:	1.10
	Grain Size D90 (mm):	
	K4 Armouring Coef:	1.00
Results		
	Scour Depth Ys (ft):	6.75
	Froude #:	0.25
	Equation:	CSU equation
	Pier Scour Limited to Maximum of Ys = 2.4 * a	

Site 7-1 Little Wabash at Route 45 500-year Flood HEC-18 Report

Contraction Scour				
		Left	Channel	Right
Input Data				
	Average Depth (ft):	13.43	29.50	9.42
	Approach Velocity (ft/s):	0.98	4.94	0.78
	Br Average Depth (ft):	7.52	25.60	6.68
	BR Opening Flow (cfs):	25871.60	25660.35	21668.04
	BR Top WD (ft):	2436.20	153.80	1946.20
	Grain Size D50 (mm):	0.03	0.03	0.03
	Approach Flow (cfs):	32012.01	27086.57	14101.42
	Approach Top WD (ft):	2424.33	185.91	1930.30
	K1 Coefficient:	0.690	0.690	0.690
Results				
	Scour Depth Ys (ft):	3.63	6.50	6.86
	Critical Velocity (ft/s):	0.80	0.91	0.75
	Equation:	Live	Live	Live

Pier: #9 (CL = 128318.8)		
Input Data		
	Pier Shape:	Round nose
	Pier Width (ft):	2.81
	Grain Size D50 (mm):	0.03000
	Depth Upstream (ft):	32.63
	Velocity Upstream (ft/s):	8.14
	K1 Nose Shape:	1.00
	Pier Angle:	0.00
	Pier Length (ft):	36.00
	K2 Angle Coef:	1.00
	K3 Bed Cond Coef:	1.10
	Grain Size D90 (mm):	
	K4 Armouring Coef:	1.00
Results		
	Scour Depth Ys (ft):	6.75
	Froude #:	0.25
	Equation:	CSU equation
	Pier Scour Limited to Maximum of Ys = 2.4 * a	

Site 7-18 Kaskaskia at Route 51 100-year Flood HEC-18 Report

Contraction Scour		
		Channel
Input Data		
	Average Depth (ft):	21.80
	Approach Velocity (ft/s):	1.72
	Br Average Depth (ft):	19.33
	BR Opening Flow (cfs):	16235.81
	BR Top WD (ft):	194.48
	Grain Size D50 (mm):	0.03
	Approach Flow (cfs):	7990.65
	Approach Top WD (ft):	212.73
	K1 Coefficient:	0.590
Results		
	Scour Depth Ys (ft):	22.87
	Critical Velocity (ft/s):	0.87
	Equation:	Live
Pier Scour		
	Input Data	
	Pier Shape:	Round nose
	Pier Width (ft):	2.75
	Grain Size D50 (mm):	0.03000
	Depth Upstream (ft):	19.33
	Velocity Upstream (ft/s):	4.32
	K1 Nose Shape:	1.00
	Pier Angle:	0.00
	Pier Length (ft):	
	K2 Angle Coef:	1.00
	K3 Bed Cond Coef:	1.10
	Grain Size D90 (mm):	
	K4 Armouring Coef:	1.00
Results		
	Scour Depth Ys (ft):	5.63
	Froude #:	0.17
	Equation:	CSU equation

Site 7-18 Kaskaskia at Route 51 500-year Flood HEC-18 Report

Contraction Scour		
		Channel
Input Data		
	Average Depth (ft):	23.15
	Approach Velocity (ft/s):	1.87
	Br Average Depth (ft):	20.63
	BR Opening Flow (cfs):	16808.17
	BR Top WD (ft):	198.82
	Grain Size D50 (mm):	0.03
	Approach Flow (cfs):	9366.20
	Approach Top WD (ft):	216.05
	K1 Coefficient:	0.590
Results		
	Scour Depth Ys (ft):	19.50
	Critical Velocity (ft/s):	0.87
	Equation:	Live
Pier Scour		
	Input Data	
	Pier Shape:	Round nose
	Pier Width (ft):	2.75
	Grain Size D50 (mm):	0.03000
	Depth Upstream (ft):	20.63
	Velocity Upstream (ft/s):	4.10
	K1 Nose Shape:	1.00
	Pier Angle:	0.00
	Pier Length (ft):	
	K2 Angle Coef:	1.00
	K3 Bed Cond Coef:	1.10
	Grain Size D90 (mm):	
	K4 Armouring Coef:	1.00
Results		
	Scour Depth Ys (ft):	5.56
	Froude #:	0.17
	Equation:	CSU equation

Site 8-3 Macoupin Creek at Route 67 100-year Flood HEC-18 Report

Contraction Scour				
		Left	Channel	Right
Input Data				
	Average Depth (ft):	12.65	20.91	12.31
	Approach Velocity (ft/s):	1.50	4.94	1.44
	Br Average Depth (ft):		22.44	
	BR Opening Flow (cfs):	3659.08	30534.63	6506.29
	BR Top WD (ft):		175.52	
	Grain Size D50 (mm):	0.01	0.01	0.01
	Approach Flow (cfs):	16021.71	19817.03	4861.27
	Approach Top WD (ft):	846.46	191.93	273.95
	K1 Coefficient:	0.690	0.690	0.690
Results				
	Scour Depth Ys (ft):		9.77	
	Critical Velocity (ft/s):		0.60	
	Equation:		Live	
Pier: #2 (CL = 5077.92)				
Input Data				
	Pier Shape:	Round nose		
	Pier Width (ft):	3.00		
	Grain Size D50 (mm):	0.01000		
	Depth Upstream (ft):	24.09		
	Velocity Upstream (ft/s):	7.16		
	K1 Nose Shape:	1.00		
	Pier Angle:	0.00		
	Pier Length (ft):	26.25		
	K2 Angle Coef:	1.00		
	K3 Bed Cond Coef:	1.10		
	Grain Size D90 (mm):	0.08000		
	K4 Armouring Coef:	1.00		
Results				
	Scour Depth Ys (ft):	7.20		
	Froude #:	0.26		
	Equation:	CSU equation		
	Pier Scour Limited to Maximum of Ys = 2.4 * a			

Site 8-3 Macoupin Creek at Route 67 500-year Flood HEC-18 Report

Contraction Scour				
		Left	Channel	Right
Input Data				
	Average Depth (ft):	4.36	24.09	3.33
	Approach Velocity (ft/s):	1.23	4.97	0.91
	Br Average Depth (ft):	1.90	23.15	2.70
	BR Opening Flow (cfs):	10671.86	30938.80	11189.34
	BR Top WD (ft):	3617.11	175.52	2180.61
	Grain Size D50 (mm):	0.01	0.01	0.01
	Approach Flow (cfs):	23175.13	22973.84	6651.03
	Approach Top WD (ft):	4325.90	191.93	2195.13
	K1 Coefficient:	0.690	0.690	0.690
Results				
	Scour Depth Ys (ft):	0.64	9.92	2.52
	Critical Velocity (ft/s):	0.46	0.61	0.44
	Equation:	Live	Live	Live
Pier: #2 (CL = 5077.92)				
Input Data				
	Pier Shape:	Sharp nose		
	Pier Width (ft):	3.00		
	Grain Size D50 (mm):	0.01000		
	Depth Upstream (ft):	32.65		
	Velocity Upstream (ft/s):	7.20		
	K1 Nose Shape:	0.90		
	Pier Angle:	0.00		
	Pier Length (ft):	26.25		
	K2 Angle Coef:	1.00		
	K3 Bed Cond Coef:	1.10		
	Grain Size D90 (mm):	0.08000		
	K4 Armouring Coef:	1.00		
Results				
	Scour Depth Ys (ft):	7.17		
	Froude #:	0.22		
	Equation:	CSU equation		

Site 8-50 Little Crooked Creek 100-year Flood HEC-18 Report

Contraction Scour				
		Left	Channel	Right
Input Data				
	Average Depth (ft):	12.33	18.84	10.53
	Approach Velocity (ft/s):	2.06	5.28	1.84
	Br Average Depth (ft):	8.07	16.45	8.15
	BR Opening Flow (cfs):	2792.13	10283.30	4524.57
	BR Top WD (ft):	46.06	59.88	73.32
	Grain Size D50 (mm):	0.01	0.01	0.01
	Approach Flow (cfs):	7911.27	5972.42	3716.31
	Approach Top WD (ft):	312.00	60.00	191.36
	K1 Coefficient:	0.690	0.690	0.690
Results				
	Scour Depth Ys (ft):	10.84	13.61	16.01
	Critical Velocity (ft/s):	0.55	0.59	0.53
	Equation:	Live	Live	Live

Pier Scour		
	All piers have the same scour depth	
Input Data		
	Pier Shape:	Round nose
	Pier Width (ft):	3.00
	Grain Size D50 (mm):	0.01000
	Depth Upstream (ft):	20.62
	Velocity Upstream (ft/s):	7.35
	K1 Nose Shape:	1.00
	Pier Angle:	0.00
	Pier Length (ft):	35.30
	K2 Angle Coef:	1.00
	K3 Bed Cond Coef:	1.10
	Grain Size D90 (mm):	0.25000
	K4 Armouring Coef:	1.00
Results		
	Scour Depth Ys (ft):	7.20
	Froude #:	0.29
	Equation:	CSU equation
	Pier Scour Limited to Maximum of Ys = 2.4 * a	

Site 8-50 Little Crooked Creek 500-year Flood HEC-18 Report

Contraction Scour				
		Left	Channel	Right
Input Data				
	Average Depth (ft):	14.69	21.20	12.33
	Approach Velocity (ft/s):	2.37	5.79	2.10
	Br Average Depth (ft):	2.11	15.91	2.41
	BR Opening Flow (cfs):	5977.83	9628.83	7793.34
	BR Top WD (ft):	796.87	59.88	813.57
	Grain Size D50 (mm):	0.01	0.01	0.01
	Approach Flow (cfs):	10847.39	7358.74	5193.86
	Approach Top WD (ft):	312.00	60.00	201.03
	K1 Coefficient:	0.690	0.690	0.690
Results				
	Scour Depth Ys (ft):	2.51	10.82	4.24
	Critical Velocity (ft/s):	0.56	0.60	0.55
	Equation:	Live	Live	Live

Pier Scour		
	All piers have the same scour depth	
Input Data		
	Pier Shape:	Round nose
	Pier Width (ft):	3.00
	Grain Size D50 (mm):	0.01000
	Depth Upstream (ft):	22.59
	Velocity Upstream (ft/s):	9.97
	K1 Nose Shape:	1.00
	Pier Angle:	0.00
	Pier Length (ft):	35.30
	K2 Angle Coef:	1.00
	K3 Bed Cond Coef:	1.10
	Grain Size D90 (mm):	0.25000
	K4 Armouring Coef:	1.00
Results		
	Scour Depth Ys (ft):	7.20
	Froude #:	0.37
	Equation:	CSU equation
	Pier Scour Limited to Maximum of Ys = 2.4 * a	

Site 9-1 Big Muddy River near Plumfield 100-year Flood HEC-18 Report

Contraction Scour				
		Left	Channel	Right
Input Data				
	Average Depth (ft):	5.64	26.73	11.71
	Approach Velocity (ft/s):	0.29	2.44	0.86
	Br Average Depth (ft):		23.46	3.41
	BR Opening Flow (cfs):	260.53	20762.72	7076.75
	BR Top WD (ft):		180.00	1620.30
	Grain Size D50 (mm):	0.02	0.02	0.02
	Approach Flow (cfs):	280.24	9847.80	17971.96
	Approach Top WD (ft):	170.06	151.00	1778.00
	K1 Coefficient:	0.690	0.690	0.690
Results				
	Scour Depth Ys (ft):		21.41	2.21
	Critical Velocity (ft/s):		0.78	0.68
	Equation:		Live	Live
Pier: #2 (CL = 22.15)				
Input Data				
	Pier Shape:	Round nose		
	Pier Width (ft):	2.50		
	Grain Size D50 (mm):	0.02000		
	Depth Upstream (ft):	25.96		
	Velocity Upstream (ft/s):	4.86		
	K1 Nose Shape:	1.00		
	Pier Angle:	0.00		
	Pier Length (ft):	35.00		
	K2 Angle Coef:	1.00		
	K3 Bed Cond Coef:	1.10		
	Grain Size D90 (mm):	0.25000		
	K4 Armouring Coef:	1.00		
Results				
	Scour Depth Ys (ft):	5.79		
	Froude #:	0.17		
	Equation:	CSU equation		

Site 9-1 Big Muddy River near Plumfield 500-year Flood HEC-18 Report

Contraction Scour				
		Left	Channel	Right
Input Data				
	Average Depth (ft):	7.87	28.99	13.97
	Approach Velocity (ft/s):	0.36	2.57	0.98
	Br Average Depth (ft):	2.73	23.46	5.44
	BR Opening Flow (cfs):	250.42	18573.58	17275.99
	BR Top WD (ft):	121.10	180.00	1780.00
	Grain Size D50 (mm):	0.02	0.02	0.02
	Approach Flow (cfs):	485.17	11232.38	24382.46
	Approach Top WD (ft):	170.63	151.00	1778.00
	K1 Coefficient:	0.690	0.690	0.690
Results				
	Scour Depth Ys (ft):	0.68	16.06	4.95
	Critical Velocity (ft/s):	0.64	0.79	0.70
	Equation:	Clear	Live	Live
Pier: #2 (CL = 22.15)				
Input Data				
	Pier Shape:	Round nose		
	Pier Width (ft):	2.50		
	Grain Size D50 (mm):	0.02000		
	Depth Upstream (ft):	30.78		
	Velocity Upstream (ft/s):	4.97		
	K1 Nose Shape:	1.00		
	Pier Angle:	0.00		
	Pier Length (ft):	35.00		
	K2 Angle Coef:	1.00		
	K3 Bed Cond Coef:	1.10		
	Grain Size D90 (mm):			
	K4 Armouring Coef:	1.00		
Results				
	Scour Depth Ys (ft):	5.99		
	Froude #:	0.16		
	Equation:	CSU equation		

Site 9-2 Big Muddy River near Murphysboro 100-year Flood HEC-18 Report

Contraction Scour				
		Left	Channel	Right
Input Data				
	Average Depth (ft):	15.54	38.47	17.42
	Approach Velocity (ft/s):	0.50	3.32	0.71
	Br Average Depth (ft):		35.09	3.47
	BR Opening Flow (cfs):	630.63	39748.31	2421.07
	BR Top WD (ft):		219	850.31
	Grain Size D50 (mm):	0.02	0.02	0.02
	Approach Flow (cfs):	364.91	29982.30	12452.79
	Approach Top WD (ft):	46.83	235.00	1012.58
	K1 Coefficient:	0.690	0.690	0.690
Results				
	Scour Depth Ys (ft):		16.34	1.02
	Critical Velocity (ft/s):		0.83	0.73
	Equation:		Live	Clear

Pier: #3 (CL = 144.62)		
Input Data		
	Pier Shape:	Round nose
	Pier Width (ft):	4.78
	Grain Size D50 (mm):	0.02000
	Depth Upstream (ft):	39.56
	Velocity Upstream (ft/s):	4.75
	K1 Nose Shape:	1.00
	Pier Angle:	0.00
	Pier Length (ft):	39.00
	K2 Angle Coef:	1.00
	K3 Bed Cond Coef:	1.10
	Grain Size D90 (mm):	0.10000
	K4 Armouring Coef:	1.00
Results		
	Scour Depth Ys (ft):	9.26
	Froude #:	0.13
	Equation:	CSU equation

Site 9-2 Big Muddy River near Murphysboro 500-year Flood HEC-18 Report

Contraction Scour				
		Left	Channel	Right
Input Data				
	Average Depth (ft):	18.64	42.02	20.93
	Approach Velocity (ft/s):	0.57	3.67	0.83
	Br Average Depth (ft):	9.51	35.09	6.43
	BR Opening Flow (cfs):	936.48	44966.92	8396.60
	BR Top WD (ft):	88.00	219.00	1029.00
	Grain Size D50 (mm):	0.02	0.02	0.02
	Approach Flow (cfs):	514.98	36227.85	17557.17
	Approach Top WD (ft):	48.08	235.00	1014.48
	K1 Coefficient:	0.690	0.690	0.690
Results				
	Scour Depth Ys (ft):	4.41	18.00	4.58
	Critical Velocity (ft/s):	0.74	0.84	0.75
	Equation:	Clear	Live	Live

Pier: #3 (CL = 144.62)		
Input Data		
	Pier Shape:	Round nose
	Pier Width (ft):	4.78
	Grain Size D50 (mm):	0.02000
	Depth Upstream (ft):	49.42
	Velocity Upstream (ft/s):	5.29
	K1 Nose Shape:	1.00
	Pier Angle:	0.00
	Pier Length (ft):	39.00
	K2 Angle Coef:	1.00
	K3 Bed Cond Coef:	1.10
	Grain Size D90 (mm):	0.10000
	K4 Armouring Coef:	1.00
Results		
	Scour Depth Ys (ft):	10.00
	Froude #:	0.13
	Equation:	CSU equation

APPENDIX E – HEC-18 AND SRICOS-EFA RESULTS SUMMARY

Scour results for various recurrence interval storms or hydrograph using Hydraulic Engineering Circular No. 18 (HEC-18) and Scour Rate In Cohesive Soils-Erosion Function Apparatus (SRICOS-EFA) for each sample. (ft, feet; Z_{max} , maximum contraction and pier scour; ---, observed scour not used to compare with corresponding soil layer)

	Pier Scour (ft)							Pier and Contraction Scour (ft)							
	HEC-18		SRICOS (no safety factor applied)					HEC-18		SRICOS (no safety factor applied)					
Sample	100 year	500 year	Risk Analysis	500 year - 5 days	Hydro-graph	Z_{max} 100 year	Z_{max} 500 year	100 year	500 year	Risk Analysis	500 year - 5 days	Hydro-graph	Z_{max} 100 year	Z_{max} 500 year	Observed Scour (ft)
1-1 Soil 1	4.62	4.78	0.03	0.00	0.00	3.12	3.25	6.81	8.10	0.03	0.00	0.00	4.53	4.83	2.56
1-4 Soil 1	4.84	5.05	0.03	0.00	0.00	5.96	6.29	16.52	17.83	0.03	0.00	0.00	4.83	5.36	---
1-4 Soil 2	4.84	5.05	3.31	2.49	3.54	5.96	6.29	16.52	17.83	2.95	2.56	3.28	5.95	6.61	2.20
1-4 Soil 3	4.84	5.05	0.03	0.00	0.00	5.96	6.29	16.52	17.83	0.03	0.00	0.00	4.61	5.12	---
1-4 Soil 4	4.84	5.05	0.03	0.00	0.00	5.96	6.29	16.52	17.83	0.03	0.00	0.00	4.83	5.36	---
1-6 Soil 1	13.64	14.10	0.25	0.30	0.75	2.98	3.05	17.83	20.31	0.25	0.52	0.79	4.13	4.35	1.59
1-7 Soil 1	3.86	4.07	0.03	0.00	0.00	2.80	2.99	3.86	4.07	0.03	0.00	0.00	3.91	4.32	2.33
1-7 Soil 2	3.86	4.07	0.03	0.00	0.00	2.80	2.99	3.86	4.07	0.03	0.00	0.00	4.06	4.50	---
3-25 Soil 1	5.47	5.79	0.33	0.89	0.52	4.72	5.45	9.69	10.42	0.49	0.98	0.56	8.96	10.21	1.90
4-5 Soil 1	7.60	7.89	4.43	4.19	4.59	4.97	5.28	20.63	22.54	7.87	8.56	9.12	12.60	14.79	---
4-5 Soil 2	7.60	7.89	0.82	0.36	1.97	4.97	5.28	20.63	22.54	0.61	0.36	2.03	11.22	13.09	---
4-5 Soil 1, 2	7.60	7.89	2.30	2.17	2.72	4.97	5.28	20.63	22.54	2.46	2.29	3.67	11.22	14.79	6.39
5-17 Soil 1	2.37	2.40	0.03	0.00	0.00	1.83	1.90	2.37	3.82	0.03	0.00	0.00	2.49	2.77	1.16
5-20 Soil 1	5.94	6.17	0.03	0.00	0.00	3.89	4.45	8.37	9.77	0.03	0.00	0.00	3.90	4.48	0.22
6-22 Soil 1	5.32	5.40	0.13	0.36	0.00	3.24	3.63	13.68	18.55	0.03	0.36	0.00	5.08	6.46	1.42
7-1 Soil 1	6.75	6.75	3.61	4.76	4.00	5.66	5.86	18.93	13.25	6.89	11.45	8.86	18.96	21.23	---
7-1 Soil 2	6.75	6.75	4.76	5.58	4.27	5.66	5.86	18.93	13.25	10.17	18.27	10.47	19.41	21.74	---
7-1 Soil 1,2	6.75	6.75	4.75	5.44	4.26	5.66	5.86	18.93	13.25	10.00	16.83	10.20	18.96	21.23	10.80
7-18 Soil 1	5.63	5.56	0.03	0.00	0.00	4.18	4.04	28.50	25.06	0.03	0.00	0.00	7.86	8.25	2.62
8-3 Soil 1	7.20	7.17	1.74	2.72	3.22	6.08	6.12	16.97	17.09	2.17	3.84	4.99	16.52	17.49	5.43
8-50 Soil 1	7.20	7.20	1.67	0.33	0.56	4.86	2.47	23.21	18.02	1.67	0.36	0.00	9.04	3.50	3.00
9-1 Soil 1	5.79	5.99	1.71	1.67	3.22	4.41	4.47	27.20	22.05	2.30	2.20	5.81	11.63	12.29	3.46
9-2 Soil 1	9.26	10.00	0.18	0.56	1.74	7.08	7.68	25.60	28.00	0.20	0.56	1.94	13.19	15.65	5.11
9-2 Soil 2	9.26	10.00	0.13	1.61	0.03	7.08	7.68	25.60	28.00	0.13	1.80	0.03	11.94	14.23	---
Average	6.33	6.53	1.27	1.39	1.47	4.78	4.95	16.60	16.50	2.02	2.96	2.57	9.16	10.11	
Average[1]	6.33	6.53	2.40	2.55	2.68	4.78	4.95	16.60	16.50	3.53	4.88	4.36	9.16	10.11	

[1]SRICOS runs with a 1.5 safety factor or 1 ft minimum scour depth. The Z_{max} does not have a safety factor because it is treated like the HEC-18 results where a safety factor is not used.

Scour results for peak flow of record using Hydraulic Engineering Circular No. 18 (HEC-18) and Scour Rate In Cohesive Soils-Erosion Function Apparatus (SRICOS-EFA) for each sample. (ft, feet; Z_{max} , maximum contraction and pier scour)

	Pier Scour for Peak Flow		Pier and Contraction Scour for Peak Flow		Observed
Sample	HEC-18 (ft)	SRICOS Z_{max} (ft)	HEC-18 (ft)	SRICOS Z_{max} (ft)	Scour (ft)
1-1 Soil 1	5.13	3.76	9.31	6.27	2.56
1-4 Soil 2	4.50	5.54	8.27	5.15	2.20
1-6 Soil 1	12.10	2.79	17.29	3.69	1.59
1-7 Soil 1	4.53	3.42	4.53	5.59	2.33
3-25 Soil 1	6.00	5.77	12.46	13.51	1.90
4-5 Soil 1, 2	7.75	4.97	17.21	12.41	6.39
5-17 Soil 1	2.30	1.78	2.46	1.79	1.16
5-20 Soil 1	5.71	4.06	6.95	4.09	0.22
6-22 Soil 1	4.99	2.97	8.62	4.27	1.42
7-1 Soil 1,2	6.75	5.61	18.49	18.53	10.80
7-18 Soil 1	5.60	4.17	28.18	8.23	2.62
8-3 Soil 1	7.20	6.06	16.63	16.37	5.43
8-50 Soil 1	6.85	4.17	15.02	6.92	3.00
9-1 Soil 1	5.96	4.47	17.77	12.57	3.46
9-2 Soil 1	9.90	6.43	20.75	10.93	5.11
Average	6.35	4.40	13.60	8.69	3.35


Illinois Department
of Transportation


ILLINOIS
UNIVERSITY OF ILLINOIS AT URBANA-CHAMPAIGN